Compound and Pre-Compound Emission in some Reactions Induced by Neutrons of 10 - 20 MeV

THESIS SUBMITTED FOR THE DEGREE OF

DOCTOR OF PHILOSOPHY

IN

PHYSICS

Jagdish Prasad Gupta

M. Sc., M. Phil. (Alig.)

DEPARTMENT OF PHYSICS

ALIGARH MUSLIM UNIVERSITY

ALIGARH-202001 (India)

1983

Compound and Pre-Compound Emission in some Reactions Induced by Neutrons of 10 - 20 MeV

THESIS SUBMITTED FOR THE DEGREE OF

DOCTOR OF PHILOSOPHY

IN

PHYSICS

Jagdish Prasad Gupta

M. Sc., M. Phil. (Alig.)

DEPARTMENT OF PHYSICS

ALIGARH MUSLIM UNIVERSITY

ALIGARH-202001 (India)

1983

Certified that the work presented in this thesis is the original work of Mr. Jagdish Prasad Gupta, done under my supervision. Due to some unavoidable circumstances the submission of the thesis has been considerably delayed.

(R. PRASAD)

Physics Department
Aligarh Muslim University
ALIGARH - 202 001 (India)

It is regretted that the submission of the thesis has been considerably delayed due to some unavoidable circumstances.

Jagdish Prasad Gupta

A C K N O W L E D G E M E N T S

I have no words to express my deep sense of gratitude to my supervisor, Dr. J. Prasad, for his inspiring guidence, constant encouragement, valuable suggestions and stimulating discussions throughout the course of the present work.

I am highly grateful to Professor M.Z.A. Khan, Chairman, Department of Physics, for providing me with all the research facilities for conducting this work in the department.

I am very much thankful to all my colleagues and friends in the Department of Physics, Aligarh Muslim University, Aligarh, for their timely help and co-operation in pursuing this work. Specially I wish to thank Mr. M.D. Bhardwaj, Doctor fellow, for his sincere help.

Thanks are also due to computer centre personnel of this University for their assistance.

I express my thanks to the Council of Scientific and Industrial Research (CSIR) New Delhi and Department of Atomic Energy (DAE), Government of India for granting financial assistance in the form of research fellowship.

Finally, I wish to express my indebtedness to my parents and specially to my wife for her constant and continuous help in innumerable ways.

(Jagdish Prasad Gupta)

Accelerator Laboratory,
Physics Department,
Aligarh Muslim University,
Aligarh (INDIA)

A B S T R A C T

This thesis reports on the study of some (n, p) reactions induced by neutrons of 10 to 20 MeV energy. The work reported in the thesis has been divided into five Chapters.

Chapter - I gives a brief qualitative description of reactions induced by neutrons. A historical survey of the development of work done with neutrons of about 14 MeV is also given in this Chapter. The study of trends in reaction cross sections is not possible unless reliable cross-section values determined with the same technique and the standard reaction are available for a large number of target nuclei. With this view, a programme of cross-section measurements at 14.8 MeV neutron energy by the activation technique has been under taken.

Chapter - II deals with the experimental set-up and technique employed in cross-section measurements. The various factors causing errors and uncertainties in the experimental results have been discussed in the section (2.1). In section (2.2) details of cross-section measurements are given. To measure cross-sections for those reactions which leave short lived residual nuclei electronic circuits have been developed. Cross-sections for some 19 cases of (n, p) reactions have been measured.

The experimental cross-section values are compared with the cross-section values calculated by the statistical theory. Pre-compound emission of particles has also been taken into account. Details of the statistical model and of pre-compound emission theories are given in Chapter - III. Four different models for including the pre-compound emission of particles in nuclear reactions are given in section (3.2).

Chapter - IV describes the method of calculations. A computer code ACT has been developed for these calculations.

In this code pre-compound emission from the first step of de-excitation has been included. Hybrid model frame work has been used for treating the pre-compound emission.

Results of the present investigation are given in Chapter - V. In the first section of this Chapter trends in (n, p) reactions have been studied and a comparison of the experimental and calculated values for (n, p) reaction cross-sections at 14.8 MeV neutron energy has been made. Section (5.2) deals with the excitation functions for (n, p) reaction in the energy range 10 - 20 MeV. In this section compilation of experimental values has been done and calculated excitation functions with and without pre-equilibrium emission have been compared with the experimental ones. It shows that pre-equilibrium process plays an important role in neutron induced reactions, its contribution increases with increasing excitation energy of the composite system. The results of calculations depend on quantities like level densities, level schemes and gamma ray strength functions. An attempt has been made to find the best values of these parameters of the pre-compound theory.

****

LIST OF PUBLICATIONS

1. " On the shell effect in (n, 2n) reaction cross-sections at 14.8 MeV "

   Nuclear Physics and Solid State Physics Symposium BARC Bombay (1972).

2. " A study of pre-compound emission in (n, p) reactions induced by neutrons of 10-20 MeV"

   7th Conference on the Application of Accelerators in Research and Industry, North Texas State University Denton, Texas U.S.A. (1982).

3. " A study of pre-equilibrium emission in (n, p) reactions between 10-20 MeV"

   Progress report on Nuclear data, Government of India Publication, Atomic Energy Commission BARC 1183 (1982) 33.

****

C O N T E N T S

****

CHAPTER - I

I N T R O D U C T I O N

The study of nuclear reactions holds a prominent place in the low energy nuclear physics. Soon after the existence of the neutron was established / 1-4 /, Physicists became aware of its importance as an ideal probe for nuclear research. Since the discovery of neutron in 1932, the scope and importance of neutron physics has grown remarkably and there is now a wide interest in the ideas, methods and applications which have been developed in this field. Many nuclear reactions induced by neutrons are valuable sources of information about the nucleus.

A nuclear reaction is a process that occurs when a nuclear particle (nucleon or nucleus) gets into close contact with another. Most of the nuclear reactions are produced by exposing different materials to a beam of nuclear particles. Usually a strong energy and momentum exchange take place and the final products of the reaction are one, two or more nuclear particles leaving the point of close contact in various directions. The products are mostly of species different from the particles in the original pair. The relative probabilities of different nuclear reactions give information about the mechanism of reaction and offers a testing ground for ideas about nuclear structure. Any nuclear transmutation process may lead to the excited states of the product nucleus, and the decay of the excited states then gives information about the energy levels and decay schemes. The process may be caused by different kinds of incident particles and may result in the emission of the various types of particles like protons, neutrons, deuterons, alphas and other heavy nuclei or gamma rays. The

great number of nuclear reactions which are possible provides, therefore, a wealth of experimental data for nuclear spectroscopic studies and for the study of nuclear reaction mechanism.

Neutrons are uncharged particles and, therefore, they interact with the nucleus with relative ease. The measure of the strength of the interaction of neutrons with matter is the neutron cross-section. The total neutron cross-section is defined as the fraction of the initial target nuclei which under go interaction of some kind when irradiated for a unit time with a unit neutron flux density. There are various types of cross-sections, depending on the type of nuclear interaction. For example σs may denote the cross-section for scattering of a given kind of particles and may consist of two parts, σe, the cross-section for elastic scattering and σi, the cross-section for inelastic scattering. There are also cross-sections for threshold reactions such as $\sigma(n,p)$, $\sigma(n,\alpha)$, $\sigma(n,t)$ etc., and for secondary reactions like $\sigma(n, 2n)$, $\sigma(n, 3n)$ etc. Cross-sections for nuclear reactions are often measured in unit of 10^{-24} cm^2 and this unit is called the barn. It follows from the definition that cross-section is a quantity which can be calculated theoretically for a given nuclear model and can also be measured experimentally. The validity of proposed model can be judged by comparing the measured cross-sections with theoretical values.

Neutron cross-section measurements in the region of low energy have helped in the development of the nuclear models. The appearance of sharp resonances in measured cross sections and the monotonic decrease of the total neutron cross-section with energy, supported the theory of the " Strongly absorbing nucleus " / 5 - 7 /. However, the variation of the strength function with the atomic weight of

the target nucleus, as deduced from the resonance parameters, and the maxima and minima observed in the experimental total cross-section values when plotted against the energy and atomic weight of the target nucleus, suggested an optical behaviour for the nucleus. These facts were explained by Weisskopf et al. / R - 9 / assuming the nucleus to be a weakly absorbing medium and led to the " Cloudy crystal ball model " of the nucleus. The cloudy crystal ball model, though very useful in predicting and explaining the total cross-sections, is however, not able to explain the partial reaction cross-sections, as for example the cross-sections for the (n, p), (n, α) and (n, 2n) reactions etc. For intermediate energies of incident particles where these partial cross-sections are important, the statistical theory / 10 / of the compound nucleus is normally employed. The main features of this theory are the formation of the compound nucluee and its subsequent decay into various channels, which correspond to different partial reactions. The statistical theory of nuclear reactions deals with average cross-sections. The model depicts the nuclear reaction as proceeding in two stages, in the first stage a compound nucleus is formed by the collision of the projectile with a target nucleus. In the second stage the compound nucleus decays into one of the possible pairs of reaction products. The evaporation model assumes that the compound nucleus, in its decay, losses all memory of the way in which it was formed, the decay treats all possible decay products in the democratic fashion realized in evaporation from a classical liquid drop model. The model further assumes a statistical distribution of energy levels in the excited nucleus. These assumptions put restrictions on the energy of the incoming particle and the size of the target nucleus. The statistical theory is, therefore, valid for a particular target and only in a certain energy interval of the incident particle. One way

of testing the theory is to compare the experimental excitation function (cross section vs projectile energy) of a certain reaction for a given nucleus with the one calculated theoretically. If the nuclear reaction produces a radio active residual nucleus, one can measure the excitation function using activation technique. Excitation functions upto several MeV have been measured using this method / 11 - 26 / for neutron induced reactions.

At higher excitation energies a nuclear reaction is more likely to proceed through direct interaction. Direct interactions are processes which involve few nucleons. The most important features of such interactions are the diffraction structure in the angular distributions, usually forward peaked, and the high selectivity which manifests itself in the excitation of particular levels of residual nucleus / 27 /.

In between these two extreme processes, intermediate processes are likely to occur. A series of complicated collisions inside the nucleus can follow the initial interaction and there is a certain probability that a particle be emitted after each one of these collisions. Emission of nuclear particles from this intermediate process is generally called ' Pre-equilibrium emission '. The experimental data / 28-35 / accumulated during the last few years have shown considerable contributions from pre-equilibrium emission.

Many workers / 36 - 81 / have measured the cross sections for neutron induced reactions in 10-20 MeV region. The experimental results of the cross-section measurements for (n, p) and (n, α) reactions show that the statistical theory of compound nucleus formation cannot fully account for the observed values / 82 / . The calculated cross-sections are smaller than experimental ones by a factor varying from

10 to 10^3 at the increase of target nucleus mass / 83 - 84 /. Attempts have also been made to see how a particular reaction cross-section changes with atomic number. Such a study is of considerable value in understanding the reaction mechanism. The problem with such an investigation is the existence of large discrépancies between the cross-section values of same reaction reported by different groups of workers. These discrepancies may be partly due to the different techniques and experimental set-ups employed by different workers/36-81/.

A small difference in the mean energy of the incident neutrons can change the cross-section values by a large amount in those cases where the excitation functions are very sensitive to the neutron energy. Cross-sections for those reactions in which charged particles are emitted, can be found by recording to emitted particles. In such cases the particular position of the detecting unit sometime puts a bias in the experiment by favouring the detection of those particles which are emitted by a special mechanism. Another problem is the absolute calibration of incident neutron flux, which is common to all the methods employed in cross section measurements. Most of the measurements have been done by the activation technique. In this method, the neutron flux is generally calibrated through some other standard reaction. Since the use of different standard reactions for flux calibration changes the systematic errors of the experiment, it is likely that cross-section values determined with different standards may diverge.

For the study of trends in nuclear reactions it is, therefore, necessary to measure the cross-sections for a large number of target nuclei using the same technique and the same standard reaction. A programme of cross-section measurements at 14.8 MeV neutron energy by the activation technique has

been undertaken with this view. Cockcroft-Walton accelerator of this laboratory supplied the fast neutrons. 130 keV deuteron beam of the accelerator has been made to fall on thin tritium target for this purpose. Cross-section for some selected (n, p) reactions have been measured at 14.8 ± 0.5 MeV. Literature values / 11-26 / of the cross-sections at other energies have been compiled. The experimental cross-section values have been compared with the cross-section values calculated by the statistical theory. Pre-compound emission of particles has also been taken into account using the Hybrid model / 35 / . A computer code ACT has been developed for this purpose that takes into account the particles which are emitted during the equilibration of the excited composite system alongwith the usually statistically emitted particles. Pre-compound emission is considered only in the first emission step where the excitation energy is sufficiently large. Further details of the measurements, the analysis and the computer programme organisation are given in the subsequent chapters of this thesis.

****

REFERENCES

/ 1/ W. Bothe and H. Becker; Zeit. f. Phys. 66 (1930) 289.
Nature Mac 12 (1931) 753.

/ 2/ I. Curie and F. Joliot; Compt. Rendus 194 (1931) 708.

/ 3/ W.C. Webster ; Proc. Roy. Soc. A 136 (1932) 428.

/ 4/ J. Chadwick; Nature 129 (1932) 312.

/ 5/ N. Bohr ; Nature 137 (1936) 344.

/ 6/ Feshbach, Peaslee and Weisskopf ; Phys. Rev. 71 (1947) 145.

/ 7/ Feshbach and Weisskopf ; Phys. Rev. 76 (1949) 1550.

/ 8/ Feshbach, Porter and Weisskopf ; Phys. Rev. 90 (1953) 166.

/ 9/ Feshbach, Porter and Weisskopf ; Phys. Rev. 96 (1954) 448.

/10/ J.M. Blatt and V.F. Weisskopf ; Theoretical Nuclear Physics
John Wiley & Sons, New York (1952) 340.

/11/ I. Hartje and H.H. Hyman Jr ; Physica 28 (1962) 661.

/12/ D.W. Fong, W.W. Thompson and J.M. Ferguson; Nucl. Phys.
12 (1959) 226.

/13/ H.L. Pal; Can. J. Phys. 44 (1966) 2337.

/14/ D.C. Arthur and I.L. Morgan; Nucl. Phys. 75 (1966) 561.

/15/ H. Jormann and J. Lerners; Nucl. Phys. A 130 (1969) 193.

/16/ V.N. Levkovskii, G.E. Vinitskaya and V.F. Suganov;
Sov. J. Nucl. Phys. 10 (1969) 25.

/17/ H. Jormann et al.; E A . D C (E) 66 "U" (1966) 42.

/18/ C.L. Hanni, G.J. Mecarillum and A.L.G. Ferguson; Nucl. Phys.
12 (1960) 535.

/19/ N. Paulsen and H. Liskien ; J. Nucl. En. A819 (1965) 107.

/20/ H. Jormann et al., Z. Physik 174 (1963) 1.

/21/ C.H. Haynurst and J.J. Kreewood ; J. Inorg. Nucl. Chem.
21 (1961) 173.

/22/ H. Jormann, F. Herbert, W. Scheibe, G. Krege, F. Ottmer,
A. Lindner and H. Feldner ; Nucl. Phys. 61 (1965)
438.

/23/ A.V. Cohen and R.H. White; Nucl. Phys. 1 (1956) 73.

/24/ H. Liskien and A. Paulsen; J. Nucl. En. 19 (1965) 73.

/25/ H. Jormann, I. Riehle and F. Prayer; Nucl. Data for Reactor,
I A E A, 225 (1967) Wien.

/26/ D.C. Santry and J.P. Butler ; Can. J. Phys. 42 (1964) 1030.

/27/ E. Gadioli and E. Gadioli erba; Proceeding Nuclear Theory for application (1980) 3.

/28/ L. Glowacka et al. ; Nucl.Phys A262 (1976) 205.

/29/ Hideo Kitasawa ; Nucl. Phys. A162 (1970) 513.

/30/ V.V. Verbinski and W.R. Burrus; Phys.Rev. 177 (1969) 1671.

/31/ R. Serber; Phys.Rev. 72 (1947) 1114.

/32/ G.D. Harp, J.M. Miller and B.J. Berne; Phys. Rev.165 (1968) 1166

/33/ J.J. Griffin ; Phys.Rev. Lett. 17 (1966) 478.

/34/ R. Hofstadter, Ann. Rev. Nucl.Sc. 7 (1957) 295.

/35/ M. Blann and A. Mignerey; Nucl.Phys. A 186 (1972) 245.

/36/ E.O. Salant and N.F. Ramsay; Phys.Rev. 57 (1940) 1047.

/37/ S.G. Forbes; Phys. Rev. 88 (1952) 1309.

/38/ H.C. Martin and B.C. Diven; Phys.Rev. 86 (1952) 965.

/39/ E.B. Paul and R.L. Clarke ; Can. J. Phys. 31 (1953) 267.

/40/ M.E. Saltat and F.L. Ribe; Phys. Rev 89 (1953) 80.

/41/ G.M. Frye Jr ; Phys.Rev 93 (1953) 1086.

/42/ H.C. Martin ; Phys.Rev 93 (1954) 498.

/43/ J.B. Marion and R.M. Brugger; Phys.Rev. 102 (1955) 69 .

/44/ F.L. Ribe ; Phys. Rev. 103 (1956) 741.

/45/ A.H. Armstrong and G.M. Frye Jr. ; Phys.Rev.103 (1956) 335.

/46/ J.B. Marion, R.M.Brugger and R.A.Chapman; Phys.Rev.101 (1956) 247.

/47/ D.L. Allan; Proc. Phys. Soc. A70 (1957) 195.

/48/ J.A. Grundle, R.L. Hankel and B.L. Perkins; Phys.Rev. 102 (1958) 425.

/49/ H.G. Blokrar, C.D. Goodman and T.H. Handley; Phys.Rev. 110 (1958) 531.

/50/ R.F. Colman, B.E. Kowkar, L.P.O. Conner and J.L.Perkins; Proc. Phys. Soc. 73 (1950) 215.

/51/ A. Polarikas and R.W. Fink; Phys.Rev.115 (1959) 989.

/52/ R.G. Wille and R.W. Fink ; Phys.Rev. 112 (1958) 1950.

/53/ R.S. Scelan and R.W. Fink; Nucl.Phys. 9 (1958) 334.

/54/ M. Cevolani and S. Petralia ; Nuovo.Cim. 26 (1962)1328.

/55/ L.A. Rayburn; Bull.Am. Phys.Soc. 3 (1958) 365

/56/ D.M. Chiltenden II, D.G. Gardner and R.W. Fink; Phys. Rev. 122 (1961) 860.

/57/ L.A. Rayburn ; Phys. Rev. 122 (1961) 168.

/58/ C.S. Khurana and H.S. Hans; Nucl.Phys. 28 (1961) 560.

/59/ K.W. Seeman and W.E. Moore ; Bull.Am.Phys.Soc. 6 (1961)237.

/60/ M. Bormann etal. ;Z.Nature forsch 15a (1960) 200.

/61/ D.L. Allan ; Nucl.Phys. 24 (1961) 274.

/62/ S.K. Mukherjee et al. ; Proc.Phys.Soc. 77A (1961)508.

/63/ I.L. Preiss and R.W. Fink ; Nucl.Phys. 15 (1960) 326.

/64/ J.Picard and C.F. Williamson ; Nucl.Phys. 63 (1965)673.

/65/ H. Jeremie ; Nucl.Phys. 47 (1963) 225.

/66/ G. Brown and H. Muirhead ; Phil.Mag. 2 (1957) 473.

/67/ V. Facchini et al.; Nucl.Phys. 51 (1964) 460.

/68/ D.G. Gardner et al. ; Nucl.Phys. 60 (1964) 49.
; Nucl.Phys. 72 (1965) 373.
; Nucl.Phys. 96A (1967) 121.

/69/ A. Chatterjee ; Nucl.Phys. 47 (1963) 511.
; Nucl.Phys. 60 (1964) 273.

/70/ M. Bormann ; Nucl.Phys. 65 (1965) 257.

/71/ V.N. Levkovskii ; J E T P (Sov.Phys.) 18 (1964)213.

/72/ R. Prasad, D.C. Sarkar and C.S. Khurana ; Nucl.Phys. 85 (1966)476.
89 (1966)349.

/73/ R. Prasad and D.C. Sarkar ; Il Nuovo Cim. 3A (1971)467.

/74/ A. Abboud et al.; Nucl. Phys. A139 (1969) 42.

/75/ J.C. Robertson, B.Audric et al.;J.Nucl.Energy(G.B.) 27 (1973) 531.

/76/ V.N. Levkovskii ; Sov. J. Nucl.Phys. USA 18 (1973)708.

/77/ A. Adam, L. Hrasko, G. Palla, P. Quittner; Nucl. Phys. 42 (1963) 489.

/78/ A. Adam, D. Horvath, A. Kiss and E. Mayr; Nucl. Phys. A186 (1972) 577.

/79/ L. Hormann ; Z. Naturef. 17a (1962) 479.

/80/ D.C. Gauntry & J.P. Butler; Can. J. Phys. 44 (1966) 1153.

/81/ P.I. Molla and M.L. Main, Nucl. Phys. A283 (1977) 269.

/82/ A. Millazzo Colli and G.M. Braga Marcazzan ; Phys. Lett. 236 (1971) 447.

/83/ G.M. Braga Marcazzan, L. Gadioli Erba, L. Millazzo Colli and P.G. Sona; Phys. Rev. C6 (1972) 1390.

/84/ J.M. Akkermans ; Phys. Lett. B82 (1979) 20.
Z. Physik A292 (1979) 57.

****

CHAPTER - II

(2.1) EXPERIMENTAL TECHNIQUE

Reaction cross-sections for (n, p) reactions have been measured using the activation technique. By following activities induced in samples due to the neutron bombardment, cross-sections of reactions responsible for these activities can be determined. This method of cross-section measurement is called the activation technique.

Neutron irradiation of a sample initiates many nuclear reactions in it. As a result of these reactions various isotopes present in the sample are transformed into different isotopes of the same or of different elements. The rate of formation ' R ' of a particular activation product, the incident neutron flux 'ϕ', the initial concentration 'N_0' of the target nuclei and the cross-section 'σ_r' of the reaction responsible for this transformation are related by:-

$$R = \sigma_r \cdot \phi \cdot N_0 \quad \ldots\ldots \quad (2.1)$$

If some of the isotopes so formed are radioactive, they will start decaying. For such cases eqn. (2.1) should be modified so as to take into account the simultaneous formation and decay of the reaction product. Feidlander and Kennedy / 1 / have shown that the disintegration rate $(dN / dt)_t$ of the radio-active nuclide in the specimen, after an arbitrary irradiation of duration ' t_0 ' and after it has decayed through a time 't' is given by :-

$$(dN/dt)_t = \phi \cdot N_0 \cdot \sigma_r \cdot \frac{1 - e^{-\lambda t_0}}{e^{\lambda t}} \quad \ldots\ldots \quad (2.2)$$

Here ' N_0 ' is the number of target nuclei present in the

sample before activation and 'λ' is the decay constant of the induced activity.

The decay rate $(dN / dt)_t$ of the activity can be found by following it with some suitable detector. If 'C_t' is the counting rate observed by the detector, 't' time after the stop of irradiation, then :-

$$(dN/ dt)_t = \frac{C_t}{G \cdot \epsilon} \quad .. .. \quad .. (2.3)$$

Where 'G' is the geometrical efficiency of detection and 'ϵ' is the efficiency of the detector system. From equs. (2.2) and (2.3) one gets :-

$$\sigma_r = \frac{C_t \cdot e^{\lambda t}}{G \cdot \phi \cdot \epsilon \cdot N_0 \cdot (1 - e^{-\lambda t_e})} \quad .. (2.4)$$

Quantities appearing on the right hand side of equ. (2.4) can be found from experiments and as such, cross section can be determined.

In actual irradiation various activities due to different reactions were induced in samples. The residual nuclei of different reactions generally decay with different half-lives. The decay of the irradiated samples were, therefore, followed for sufficiently long time to obtain the complete decay curves. Analysis of these curves gave rise to curves of different half lives corresponding to different reactions. Separated decay curves have been extrapolated to get the counting rates $C_{t=0}$ at zero time after the irradiation. From the observed counting rates at zero time, cross-sections for different reactions have been calculated using the equation (2.5) after substituting $t = 0$ in equ. (2.4) :-

$$\sigma_r = \frac{C_{t=0}}{G \cdot \phi \cdot \epsilon \cdot N_0 \cdot (1 - e^{-\lambda t_e})} \quad .. (2.5)$$

The number 'N_0' of the target nuclei of a particular isotope present in the sample can be calculated if the weight of the sample and the abundance of that isotope are known.

T (d, n)α reaction has been used as a source of 14.8 $\pm$ 0.5 MeV neutrons. The main advantage of the T (d, n)α reaction is its high cross-section at low deuteron energy of the order of 130 keV. Moreover, the reaction yield is almost isotropic (within about 3 %) and neutron energy only weakly depends on the emission angle. Cockcroft-Walton accelerator of this laboratory has been used to get 130 keV deuteron beam / 2 /. The deuteron beam has been made to fall on thin tritium target / 3 /. Neutron, being the lighter particle in T (d, n)α reaction, takes most of the available energy. From the analysis of the reaction done by Fowler et al. / 4 / and Manson et al. / 5 /, the maximum spread in the neutron energy, for the geometry used in irradiation, has been calculated to be less than $\pm$ 0.5 MeV.

The deuteron beam has been first allowed to fall on a quartz glass, placed at a distance of 3 cm. from the tritium target. The focusing and anode voltage have been adjusted so as to focus the ions in an area of 1 $cm.^2$ on the quartz / 6 /. The tritium has been placed in a brass cup of thickness .001 cm. Neutron irradiations have been carried out at the outer side of the brass backing. Beam current has been directly measured by a microammeter. A zinc sulphide lucide crystal mounted on a 6292 photo multiplier tube and placed at 90^0 to the incident deuteron beam has been used as a fast neutron monitor. Neutron flux of the order of 10^6 to 10^9 neutrons per second have been used in the present measurements.

Samples for irradiation have been prepared with spectroscopically pure substances of chemical purity better

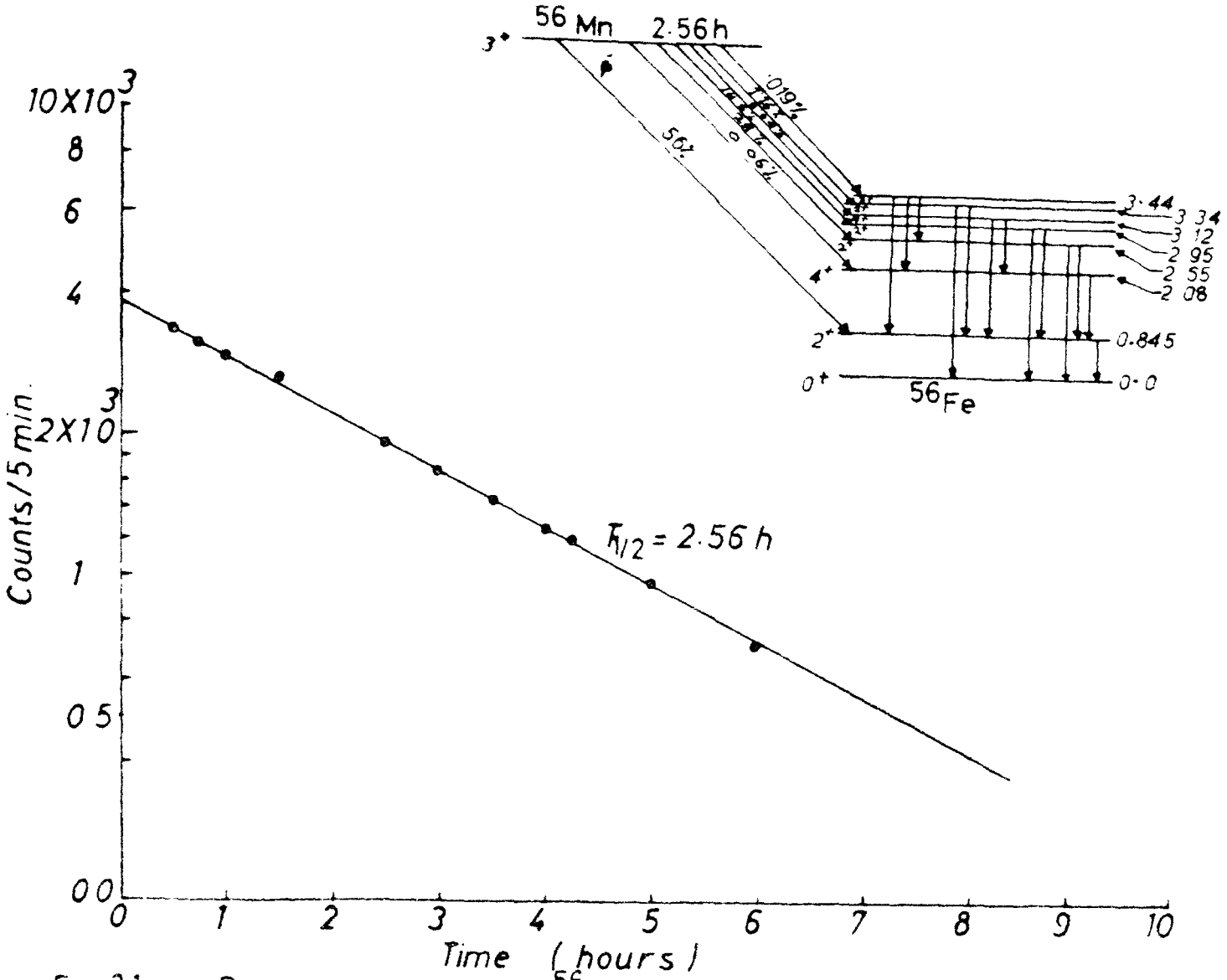

Fig. 2·1 Decay curve of ^{56}Mn

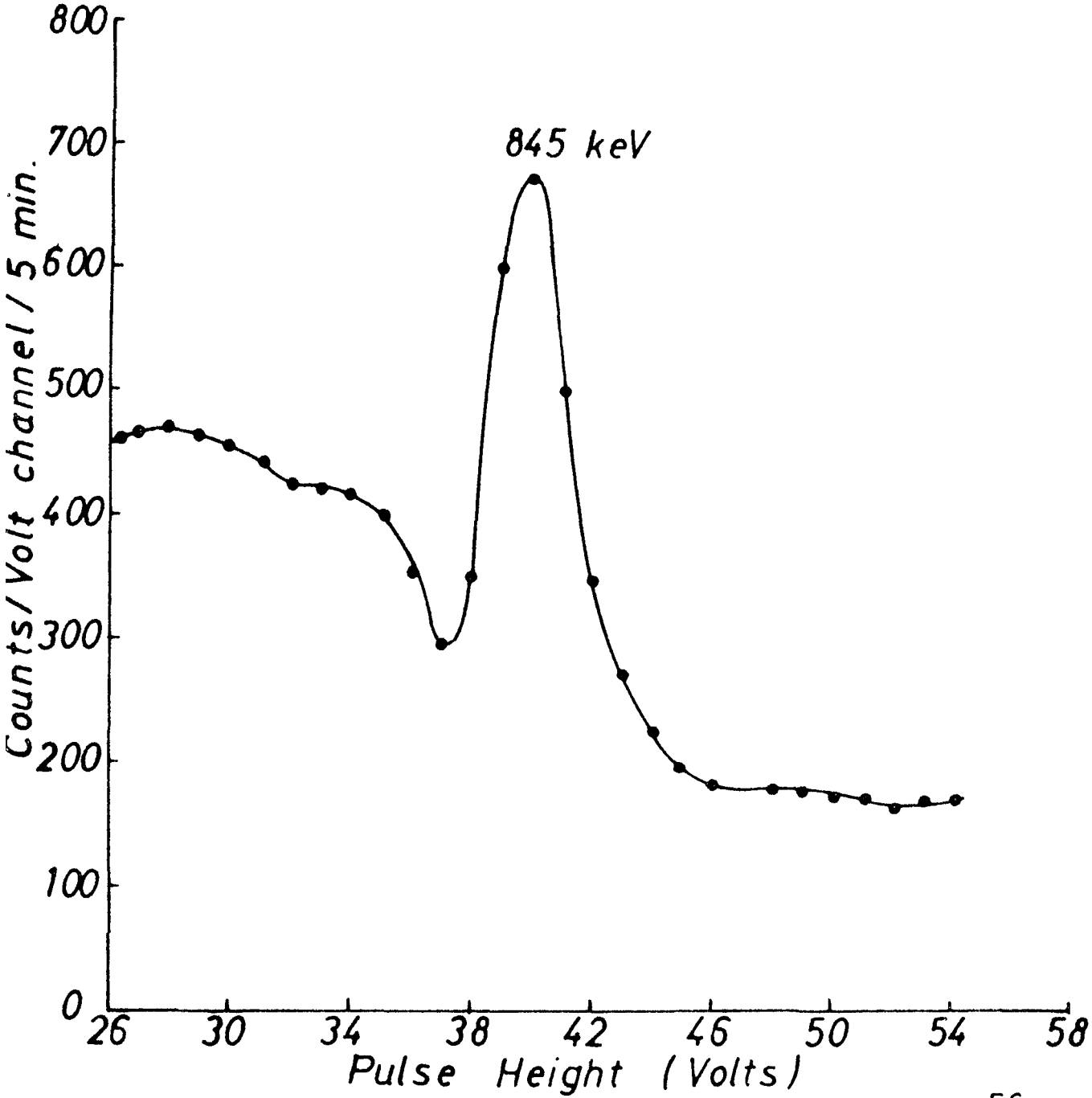

Fig. 22 Spectrum of 845keV Photo Peak of ^{56}Fe.

than 99.9 %. Samples have been made by uniformly spreading the powdered substances or their thin foils in a thin perspex ring of inner diameter 1.3 cm., which has been covered by the cellulose tapes on both the sides. The amount of the substance varied from case to case. In those cases where the activities have been recorded by β - counter, the sample thickness has been kept between 20 and 30 mg/cm^2, while in cases which have been studied by following γ-rays, a larger amount of the substance ($\gtrsim$ 100 mgs.) has been used depending on the energy of the γ-rays / 7 /.

Cross-sections have been measured relative to ^{56}Fe (n, p)^{56} Mn reaction. A cross-section value of 102 mb. has been used for this standard reaction, which is the weighted average of the various reported measurements / 8 - 17 /. The values of the " effective neutron flux " (neutron flux x geometrical efficiency) in each case has been found from the intensity of the activity induced in the standard iron sample. Iron as a standard has many advantages. The excitation function / 12 - 18 / has a flat shape around 14 MeV. The value of cross-section at 14.8 MeV is quite high and so it gives strong activity even for irradiation of short duration. ^{56}Fe (n, p)^{56} Mn reaction produces a nearly pure activity of 2.56 hours, which could be studied both by the β-counter and the γ-ray scintillation spectrometer. In this way measurements have been done for all the cases in which the product nuclei of reactions decay by either the beta and (or) the gamma-emission using the same standard sample. Figures (2.1) and (2.2) respectively show the typical decay curve obtained by β-counting of the irradiated 56 $_{Fe}$ standard sample and the spectrum of 0.845 MeV photo-peak of the standard iron sample taken by the γ- ray spectrometer.

Since the measurements have been made relative to the $^{56}Fe\ (n, p)^{56}Mn$ reaction, neutron flux has not been found directly. But instead, the value of the effective neutron flux i.e., $(\phi . G)$ has been determined in each case from the intensity of the activity induced in the standard iron sample. If N_0 is the number of ^{56}Fe nuclei present in an iron sample and if this sample is irradiated for a time 't_e' then it follows from equ. (2.5) that the effective neutron flux '$(\phi . G)$' can be given as :-

$$(\phi . G) = \frac{C_{t=0}}{\sigma(n,p) . \epsilon . N_0 . (1-e^{-\lambda t_e})} \quad .. \ (2.6)$$

Where

$C_{t=0}$ = observed counting rate (of the activity due to $^{56}Fe\ (n, p)$ reaction) at zero time after irradiation.

$(1-e^{-\lambda t_e})$ = saturation correction.

ϵ = efficiency of the detector.

$\sigma(n,p)$ = the (n,p) cross section in ^{56}Fe (=102 mb).

This equ. (2.6) has been used in calculation of the effective neutron flux.

In those cases where the irradiation times have been longer than five minutes, two standard iron samples one on each side of the unknown sample have been irradiated simultaneously. All the three samples have been then studied by the same detector in identical geometries to keep the geometrical efficiency of counting same for all cases including those of standard iron. In cases where the half-lives of the product nuclei have been short, small irradiation times have

been employed to avoid the build-up of back ground activities. Such small irradiations have not produced appreciable activities in standard samples. The effective neutron flux for such cases has been found from the counting rate of the fast neutron monitor which has been previously calibrated /7/ through standard iron samples. The position of the neutron monitor has been kept fixed.

Activities induced in different samples have been followed by the end-window β-counter and or the γ-ray scintillation spectrometer.

An end window β-counter of window thickness 2.5 mg/cm^2 has been used to count the β-particles. It is shielded by 12 cm. of lead from all sides to reduce the back ground and a hole is drilled in front of the counter window. Activated samples have been kept in contact with the window of the beta-counter. Attenuation of beta particles, in this condition, took place in half-thickness of the sample, in the cellulose tape and in the window of the counter. In cases where the radio active nucleus decay through beta particles of different energies, the detection efficiency ϵ of the counter can be calculated by the following relation :-

$$\epsilon = a\, e^{-\mu_1 d} + b\, e^{-\mu_2 d} + c\, e^{-\mu_3 d} \quad \ldots\ldots \quad (2.7)$$

where a, b, c ---- are the fraction of the total radiations which are decaying through beta particles of end point energies E_1, E_2, E_3 ---- , μ_1 , μ_2, μ_3 .... are their respective mass absorption coefficients and 'd' is the average thickness (in gm/cm)^2 which a β-particle has to traverse before entering the counter.

A NaI (Tl) crystal, in the form of right circular

cylindrical NaI(Tl) crystal mounted in an aluminium container has been used for the detection of γ-rays. In a γ-ray spectrum, each pulse height corresponds to the energy lost by the incident γ-ray in the scintillating crystal. In order to determine a relationship between the pulse height and the energy of the incident γ-ray, a spectrum of standard γ-ray sources have been taken. From the location of the photo-peaks in these spectra, the pulse height has been calibrated in terms of the γ-ray energies. By measuring the photo-peak intensity of a particular γ-ray emitted by a decaying source as a function of time it is possible to determine the half-life of the nuclide responsible for the peak. The efficiency of the γ-ray spectrometer can be written as :

$$\epsilon = \text{photo-peak efficiency} \times \text{detection efficiency} \times \text{absorption correction.}$$

In most of the cases studied with the γ-ray spectrometer, the end-point energy of the β rays, if present in the decay, has not been sufficient to reach the crystal. However, in some cases aluminium sheets have been used to remove the high energy β-particles and corrections for the attenuation of γ-rays in the absorbers have been applied. Decay of the induced activities have been followed till the counting rate falls to the background level.

The following factors can introduce errors in the measurements of the cross sections :

(i) <u>Uncertainties of neutron flux</u> :

The accuracy in the measurement of effective neutron flux depends on the reproducibility of the positioning of the standard sample and the sample to be studied, at the time of

irradiation and activity measurement . Fixed sample holders reduced the possibility of errors on this account to less than 1 %.

Variation of neutron flux during the period of irradiation can also produce errors. To avoid it, experimental data of those accelerator runs have been rejected in which the neutron flux (Fast neutron monitor counting rate) changed by more than 2 %.

(ii) Presence of Low Energy Neutrons :

The (D, D) reaction produces low energy ($\lesssim$ 3 MeV) neutrons at the place of irradiation. However, the ratio of 3 MeV neutrons to 14 MeV neutrons is estimated / 7 / to be less than 1 : 300 , so their presence is expected to introduce errors of negligible amount. Low energy neutrons can also be produced by in-elastic scattering of neutrons. Since in our case the target has been mounted on a thin backing of .001 cm. thickness and no bulky material was present near it, the possibility of in-elastic scattering has been reduced considerably.

The presence of thermal neutrons, even in a small number, can cause serious errors, due to the high values of cross-sections at these energies. The thermal neutrons can be produced by scattering from the walls of the laboratory and other heavy materials specially hydrogenious material around the target. To check the effects of thermal neutrons, some samples have been separately irradiated with and without a cadmium cover. The two cross-section values so determined have been found to be in agreement within the experimental errors.

(iii) Inaccurate Estimate of Target Nuclei in the Sample :

Inaccurate weighing and chemical impurities in the

sample can introduced errors in the estimation of target nuclei. This has been reduced to negligible value by weighing the samples accurately by a micro-balance and using spectroscopically pure substances of chemical purities better than 99.9%.

(iv) Statistical error :

Statistical errors vary from case to case depending on the intensity of induced activity. Statistical errors in some cases have been as large as 10%. They have been reduced in particular cases by repeating them many times.

(v) Interfering reactions :

The three reactions leading from different nuclides give the same end product. For instance, the (n, p) reaction from the nucleus with mass number A and (n, d) reaction from a nucleus with mass number (A + 1) led to the same residual nucleus. Other isotopes usually present in natural substances, also lead to interfering reactions. Errors due to the secondary reactions have been neglected because at 14 MeV energy these cross sections i.e. $\sigma(n, d)$ are expected to be very small in comparison to cross section for (n, p) reactions, if the abundance of (A + 1) isotope is very small.

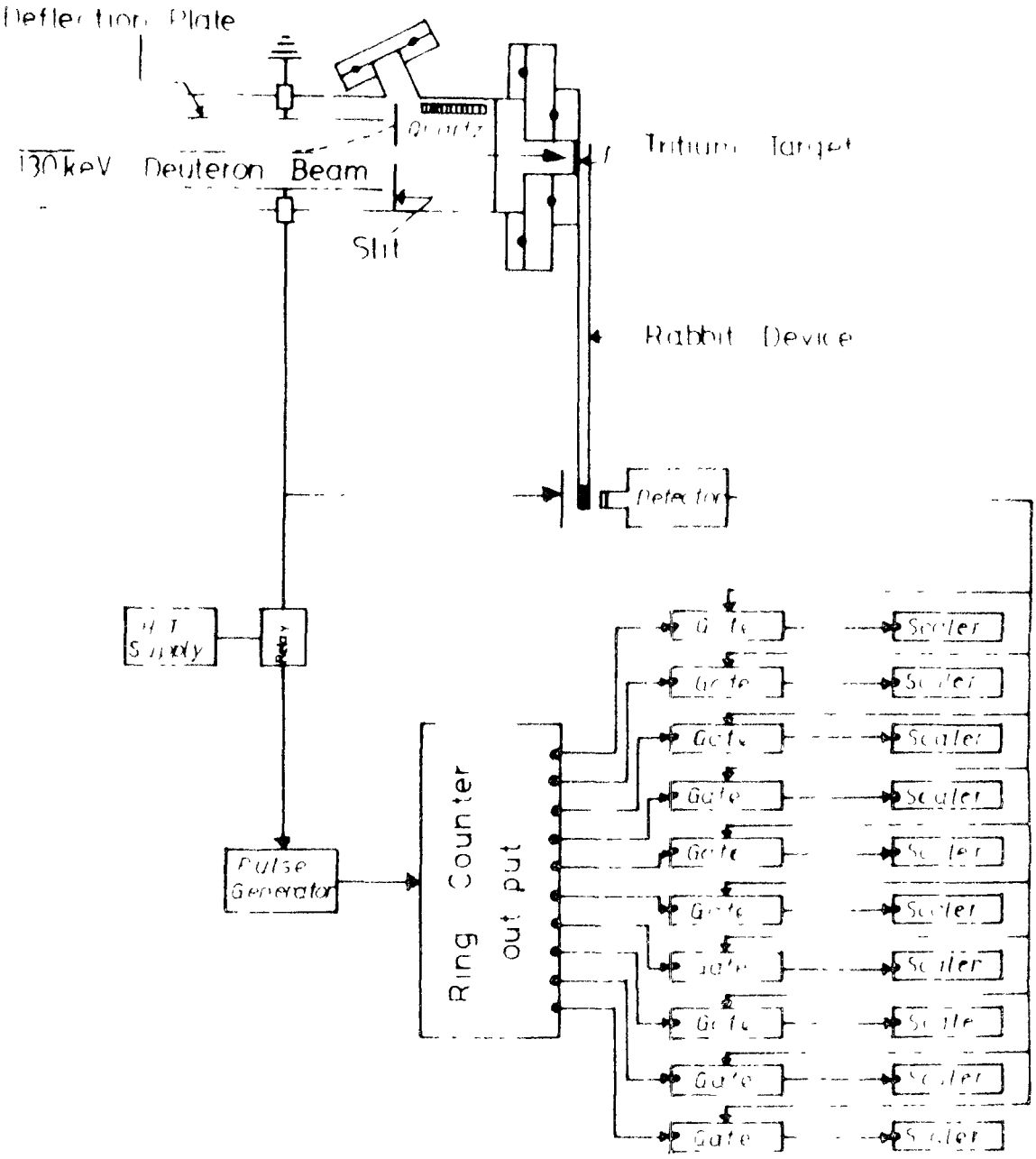

Fig 2.3 Electronic circuits and irradiation assembly.

(2.2) MEASUREMENT :

Reactions for which cross-sections have been measured can be divided into two categories according to the half lives of their residual nuclei. The length of neutron irradiations have been decided by the half life of activity of interest. In cases of short half lives ($T_{1/2} < 10^2$ Sec.) samples have been irradiated for short durations to avoid the build up of back ground activities. The shortest irradiation time has been of 5 seconds duration and the longest has been of 10 hours. In cases of long lived activities the decay of samples have been studied manually with the help of a stop watch, while for the cases of short half lives, the decay of the samples have been followed by the electronic circuits specially developed / 19 / in this laboratory.

A block diagram of the electronic arrangement alongwith the irradiation assembly is shown in fig. (2.3). The electronic circuit consists of a pulse generator capable of giving sharp negative pulses of variable frequency from one pulse per 10 seconds to 100 pulses per second. These pulses have been used to trigger a ten stage ring-counter. The pulses from the output stages of the ring counter are shown in fig. (2.4). The gating pulses from the outputs of the ring counter have been used to open ten cathode-follower transmission gates, which in turn allowed the detector pulses to be counted by scalers in succession for a certain duration of time depending on the frequency of the pulse generator.

Cross-sections have been calculated by applying the usual corrections for the decay of the sample, for

counting efficiency, for geometry, absorption, etc. The decay data employed have been taken from the literature / 20- 21 /. Reactions for which cross-sections have been measured are given in Table - I. The observed half-lives of the residual nuclei, radiation detected and the measured values of cross-sections are also listed in this table.

Table - 1

Measured (n, p) Cross - sections

Reaction	Observed half life	Natural abundance	Substance irradiated	Radiation detected	Measured cross-section (mb)
$^{24}Mg(n,p)^{24}Na$	15.0 h	79. 6	MgO	β^-	190 ± 20
$^{25}Mg(n,p)^{25}Na$	1.0 m	10. 1	MgO	β^-	45 ± 8
$^{27}Al(n,n)^{27}Mg$	9.1 m	100.0	Al-foil	β^-	76 ± 12
$^{34}S(n,p)^{34}P$	12.8 s	4. 18	element	β^-	75 ± 8
$^{37}Cl(n,p)^{37}S$	5.0 m	24. 6	C_2Cl_6	β^-	28 ± 5
$^{41}K(n,p)^{41}Ar$	1.83 h	6. 9	KI	β^-	53 ± 4
$^{48}Ti(n,p)^{48}Sc$	43.7 h	73. 45	Metal foils	β^-	60 ± 5
$^{49}Ti(n,p)^{49}Sc$	57.2 m	5. 51	-do-	β^-	40 ± 7
$^{50}Cr(n,p)^{50}V$	1.7 m	5. 34	-do-	β^-	20 ± 5

Table - 1 (contd..)

Reaction	Observed half life	Natural abundance	Substance irradiated	Radiation detected	Measured cross-section (mb)
$^{51}V\ (n,p)\ ^{51}Ti$	5. 2 m	99.75	Metal Pellets	β^-	38 ± 4
$^{52}Cr\ (n,p)\ ^{52}V$	4. 0 m	83.46	-do-	β^-	88 ± 6
$^{56}Fe\ (n,p)\ ^{56}Mn$	2.56 h	91.52	-do-	β^- & γ	100 ± 6
$^{65}Cu\ (n,p)\ ^{65}Ni$	2.5 h	30.91	Metal foil	β^-	21 ± 2
$^{64}Zn\ (n,p)\ ^{64}Cu$	11.8 h	48.87	element	β^+, β^-	171 ± 13
$^{66}Zn\ (n,p)\ ^{66}Cu$	5.0 m	27.62	element	β^-	74 ± 6
$^{75}As\ (n,p)\ ^{75}Ge$	1.38 h	100.0	element	β^-	35 ± 3
$^{88}Sr\ (n,p)\ ^{88}Rb$	17.5 m	82.74	element	β^-	15 ± 2
$^{109}Ag\ (n,p)\ ^{109}Pd$	13.0 h	48.65	Metal foil	β^-	14 ± 2
$^{197}Au\ (n,p)\ ^{197}Pt$	18.0 h	100.0	Metal foil	β^-	2 ± 1

References

/ 1/ G. Feidlander and J.M. Kennedy ; Introduction to Radio Chemistry, John Wiley & Sons Inc., New York.

/ 2/ C. S. Khurana ; Ph.D. Thesis, Aligarh Muslim University, Aligarh (1960).

/ 3/ H.N. Barocell ; Physics Today 22 (1969) 54.

/ 4/ J.L. Fowler and J.E. Strolley ; Revs. Mod. Phys. 28 (1956) 103.

/ 5/ A.O. Hanson, R.F. Taschek and J.H. Williams ; Revs. Mod. Phys. 21 (1949) 635.

/ 6/ J.P. Gupta; M. Phil. Thesis, Physics Department, Aligarh Muslim University, Aligarh (1974).

/ 7/ R. Prasad ; Ph.D. Thesis, Aligarh Muslim University, Aligarh (1967).

/ 8/ M.I. Molla and S.M. Qaim ; Nucl.Phys. A283 (1977) 269.

/ 9/ G.C. Panozzola, P. Krovetto, E. Chiavasse, R.Spinoglio and A. Pasquarelli ; Nucl. Phys. 51 (1964) 337.

/10/ P. Cuzzocrea, E. Perillo and S. Natorrigo; Nuvo.Cim., 4A (1971) 251.

/11/ R.C. Barrall, M. Silbergeld and D.G. Gardner; Nucl.Phys. A138 (1969) 387.

/12/ H. Liskien and A. Paulsen; J. Nucl.En. AB19 (1965)73.

/13/ D.C. Santry & J.P. Butler; Can.J.Phys. 42 (1964)1030.

/14/ J. Terrel and D.M. Helmy Phys.Rev. 109 (1958) 2031.

/15/ J.D. Hemingway, R.H. James, E.B.M. Martin and G.K. Martin; Proc. Roy. Soc. A292 (1966) 180.

/16/ B.D. Kern et al. Nucl.Phys. 10 (1959) 226.

/17/ M. Bormann et al. ; Z. Physik 166 (1962) 477.

/18/ P. Strohal et al. ; Phys. Lett. 10 (1964) 104.

/19/ R. Prasad and D.C. Sarker; Proc. Ind.Div.Inst.Elect. and Rad.Engineers 4 (1966)126.

/20/ C.M. Lederer ; J.M. Hallander and I. Perlman; Table of Isotopes, New York (1980).

/21/ Nuclear Data Sheets O.R.N.L. USA (Academic Press, New York (1960-1982).

****

(3.1) [illegible]

The statistical theory of nuclear reactions has been developed as a rough tool to provide an order to a large body of nuclear data. Ericksopf / 1 / and Hauser / 2-3 / proposed this theory in 1940. For a certain class of reactions, such as (n, n'), (n,) and (n,), induced by low energy (< 30 MeV) neutrons in medium weight nuclei, a statistical theory retains the most complete and easily applicable description of the reactions. The statistical model avoids any description of resonance phenomenon and in fact is particularly aimed at situations in which the resonances are so closely spaced compared to their width that at any one incident neutron energy a statistical average of the levels is excited. The statistical theory is based on the following assumptions :-

(a) Compound nucleus formation : According to Bohr's / 4 / idea, when the incident nucleon collides with the target nucleus, it is absorbed by the target nucleus and the kinetic energy as well as the binding energy of the incident particle, represents an excitation energy of the compound nucleus. Because of collision between the incoming nucleon and the nucleons in the target nucleus, this energy is assumed to be shared by a few nucleons or large number of particles. In this case, none of them will have sufficient energy to escape immediately. The compound nucleus stays together for a very short time ($\approx 10^{-17}$ sec.) until, by chance, enough energy is concentrated on one particle or an assembly of particles for escape to occur through various reaction channels.

(b) Continuum of compound nucleus levels : There is a very large number of levels at the excitation energy where the [illegible]

nucleus is formed. Excitation of the compound nucleus due to the incoming nucleon is so high that a continuum of levels of given quantum numbers such as the excitation energy 'E' , angular momentum J , parity Π , etc., is formed and a statistical average is obtained over all possible quantum numbers among the states.

(c) Independence Hypothesis : The mode of decay of the compound nucleus depends on the quantum parameters E, J, Π , etc. of the compound system and is assumed to be independent of the mode of formation of the compound nucleus.

This independence assumption / 5 / enables the cross-section for a given mode of decay to be factored into the cross-section for formation of the compound nucleus times the probability for the compound nucleus to decay by the given channel. We can thus speak of the cross-section for a nuclear reaction A (a, b) B resulting in a final state as

$$\sigma(a, b) = \sigma_c(a) \times P_c(b) \qquad \ldots \quad (3.1)$$

Here σ_c (a) is the cross-section for the formation of the compound nucleus C, formed by the particle 'a' incident on the target nucleus 'A'. P_c (b) is the probability of decay of the compound nucleus C by the emission of a particle 'b' leaving a residual nucleus 'B'.

These three assumptions discussed above can be considered as sufficient foundation for a statistical model of nuclear reactions. However, some times two more assumptions are needed :

(d) Continuum of Final States : In each approachable mode of decay (inelastic scattering, charged particle reactions, fission etc.) it is assumed that the state of the residual system forms a continuum of levels, similar to that assumed for the compound nucleus. For each mode of decay there are

thus many channels available, corresponding to the various final states.

(e) Absence of Compound Elastic Scattering : The compound nucleus has so many open channels available, that the probability that it decays by emitting a single particle of the same type and energy as the incident particle is taken to be negligible. Thus the elastic scattering does not take place through the intermediary of a compound nucleus, but occurs in the statistical model only as the diffraction of the incident nucleon beam by the target nucleus.

(3.1 a) REACTION CROSS-SECTION

The statistical theory of nuclear reaction deals with average cross-sections. To a great extent the treatment of average cross-sections employs an evaporation model. The early forms of evaporation model were developed by Bethe / 6 /, Weisskopf / 7 / and Weiskopf et al./ 1 / soon after the compound nucleus was proposed / 4, 8 / to explain nuclear resonance cross-sections.

There were two major defects in the early evaporation theory. The first concerns the lack of conservation of total angular momentum and parity in the cross-section formulas. The second concerns the use of compound nucleus cross-sections which do not exhibit the giant resonances. The giant resonances are one of the dominent features of the interaction between a nucleon and a nucleus. A modern evaporation theory has been built along the same physical principles as the early evaporation theory except that conservations of total angular momentum and parity have been taken into account. The absorption cross-sections are also computed with the optical model. This is some times

referred as the Hauser-Feshbach model after the authors / 9 /.

In a nuclear reaction of the type,

$$A + a \longrightarrow B + b$$

when the light incident particle 'a' and emitted particle 'b' are both in their ground states, the initial and final quantum numbers are related to each other through the following conservation laws for energy, momentum and parity:

$$\left.\begin{aligned} E + \epsilon + S_a &= \epsilon' + E' + S_b = U \\ I + i + l &= I' + i' + l' = J \\ P\, p\, (-1)^l &= P'_p\, (-1)^{l'} = \Pi \end{aligned}\right\} \quad \ldots (3.2)$$

Here E, I and P are respectively the excitation energy, spin and the parity of the target A', while i and p are the spin and parity of the incident particle 'a', primed letters E', I', P', i' and p' refer to the corresponding quantities for the residual nucleus B' and the emitted particle ' b ', ϵ and ϵ' are the kinetic energies of the relative motions in the incident and outgoing channels with l (l = 0, 1, 2, 3...) as its orbital angular momentum. S_a and S_b are the seperation energies of the incident and emitted particles. According to the statistical theory the angle integrated reaction cross-section, averaged over a large number of resonances, is given by / 9 / :

$$\overline{\sigma_{a\,b}}\,(E, I, P, E', I', P') = \sum_{J,\Pi} \sigma_a\,(E, I, P; U, J, \Pi) \times \frac{\Gamma_b(U, J, \Pi; E', I' p')}{\Gamma(U, J, \Pi)} \quad \ldots. (3.3)$$

Where σ_a (E, I, P ; U, J, Π) is the cross-section for the formation of compound nucleus with quantum number (U, J , Π) by the incident particle a, Γ_b (U, J, Π; E', I', P') is the particle width of the compound nucleus corresponding

to its decay to the level (E', I', P') of the residual nucleus 'B' by the emission of the particle b, $\Gamma(U,J,\Pi)$ is the total width i.e. the sum of all the possible particle widths consistent with the conservation laws given by the set of equation (3.2). Thus :-

$$\Gamma(U, J, \Pi) = \sum_{b''} \sum_{E'', I'', P''} \Gamma_{b''}(U,J,\Pi ; E'', I'', P'') \quad .. \; .. \quad (3.4)$$

The summation in equ. (3.4) extends over all the possible particles whose emission is energetically possible and over all possible levels (E'', I'', P'') of the residual nucleus. Using the optical model potential to calculate the cross-section for the formation of compound nucleus, in terms of the transmission co-efficients $T_l^{(a)}(\epsilon)$ is given by / 10 /

$$\sigma_a (E, I, P ; U, J, \Pi) = \frac{\pi}{K^2} \frac{(2J + 1)}{(2I + 1) (2i + 1)} \times \sum_{s=|I-i|}^{I+i} \sum_{l=|J-s|}^{J+s} \cdot f (l, \Pi) \; T_l^{(a)} (\epsilon) \quad .. \quad (3.5)$$

Where 'K' is the wave number of the relative motion of the incident particle and f (l, Π) is the function that guarantees the parity conservation. $T_l^{(a)}(\epsilon)$ in equ. (3.5) stands for transmission coefficient for the appropriate orbital angular momentum and particle, evaluated for a particle kinetic energy consistent with conservation of energy. These have been assumed to be independent of the spin 'J' of the compound nucleus. Factor $\frac{(2J + 1)}{[(2I+1) (2i+1)]}$ is the statistical weight representing

a sum over projection of J and an averaging over projections of i and I. The decay width for particle b, can be calculated from the reciprocity theorem as :-

$$\Gamma_b (U,J,\Pi ; E',I',P') = \frac{\mu \cdot \epsilon (2I'+1) (2I'+1)}{(\pi\hbar)^2 (2 J+1) \rho(U,J,\Pi)} \times$$

$$\times \sigma_b^{inv} (E', I', P'; U,J,\Pi)$$

.. .. (3.6)

Here $\rho (U,J, \Pi)$ is the density of the levels having quantum numbers (U,J, Π), μ is the reduced mass, ϵ is the decay energy and $\sigma_b^{inv} (E', I', P' ; U,J, \Pi)$ is the inverse cross-section, i.e. the cross-section for the formation of the intermediate nuclei through the inverse reaction. Inverse cross-section can again be calculated from equ (3.5), therefore, equ. (3.6) can be written as :-

$$\Gamma_b (U,J,\Pi ; E', I', P') = \frac{\mu \cdot \epsilon}{\pi\hbar^2 \; k^2 \; \rho (U,J, \Pi)} \times$$

$$\times \sum_{s' = |I'-i'|}^{|I'+i'|} \sum_{l' = |J-s'|}^{|J+s'|} \cdot$$

$$\cdot f (l', \Pi) T_{l'}^{(b)} (\epsilon')$$

.. ... (3.7)

Similarly we can have the total particle width :-

$$\Gamma_{b''}(U, J, \Pi, E'', I'' P'') = \frac{\mu \cdot \epsilon}{\pi \hbar^2 K^2 \rho(U, J, \Pi)} \times$$

$$\times \sum_{s''=|I''-i''|}^{|I''+i''|} \sum_{l''=|J-s''|}^{|J+s''|} \cdot$$

$$\cdot f(l'', \Pi)\, T_{l''}^{(b'')}(\epsilon)$$

.. .. (3.8)

Finally with the help of the above equation the average cross section $\overline{\sigma_{ab}}$ can be written as :-

$$\overline{\sigma_{ab}}(E, I, P; E', I', P') = \frac{\pi}{K^2} \sum_{J,\Pi} \frac{(2J+1)}{(2I+1)(2i+1)} \times$$

$$\times \left[\sum_{sl} T_l^{(a)}(\epsilon) f(l, \Pi) \right] \times$$

$$\times \left[\frac{\sum_{s'l'} T_{l'}^{(b)}(\epsilon) f(l', \Pi)}{\sum_{b''s''l''} T_{l''}^{(b'')}(\epsilon) f(l'', \Pi)} \right]$$

.. .. .. (3.9)

The sums in Equ. (3.9) are not unrestricted. They are subject to the conservation laws, for example energy, parity

...of the momentum, the term $\frac{\pi}{k^2}\frac{\Gamma}{2s+1}\,T_l^{(a)}(\epsilon)$:

$x_{s,l}(\epsilon,\pi)$ has been derived from the cross section for formation of a compound nucleus by a particle 'a' with the quantum numbers J, i and l.

$$\frac{\sum_{s'l'} T_{l'}^{(b)}(\epsilon)\; x_{s'l'}(\epsilon,\pi)}{\sum_{b'',s'',l''} T_{l''}^{(b'')}(\epsilon)\; x_{s''l''}(\epsilon,\pi)}$$

represents the probability that the compound nucleus so formed will decay by emission of a particle 'b' with orbital angular momentum l' and channel spin i'.

If the excitation energy of the residual nucleus is such that detailed information about its levels is not available, i.e. the reaction leads to the continuum of the residual nucleus then the decay width $\Gamma_b(U, J, \pi)$ can be written as the sum of the two factors. One coming from the continuum and other from the discrete levels of the residual nucleus, that is

$$\Gamma_b(U,J,\pi) = \frac{1}{I_1 I_2}\int_{E_C}^{U-Q_b} d\epsilon\,\Gamma_b(U,J,\pi;\,\epsilon',I',\pi')\,x$$

$$x\,\rho(\epsilon',I',\pi') + \sum_{kd}\Gamma_b(U,J,\pi;\,E_k',I_k',\pi_k')$$

..... (3.10)

The integral in the above equation extends from the boundry of the continuum E_G upto the maximum excitation energy of the residual nucleus (U-Sb) and the second term is the summation over the known discrete levels kd.

One further assumption is implicit in the derivation of eqn. (3.9). The terms in the summation are ratios of products and sums of level widths. The widths are interpreted as average widths over statistical distribution of levels in the compound nucleus. Actually the averaging sign occurs over products and ratios of widths. However, it is generally assumed that these can be replaced by products and ratios of average widths. At higher excitation energies, where a large number of compound levels are excited, this averaging is valid, but in those cases where only a few levels of the compound system are excited, either because of the energy definition of the incident beam, or because of the lower excitation energy, the condition of statistical independence is not satisfied. In such cases the cross-section will then show fluctuations with the variation of the average incident energy, because of the fluctuations in the number, widths, interferences of the levels excited at any specific average energy of the compound levels. Thus, the cross-section predicted by eqn. (3.9) should therefore be a smooth averaged variation about which the observed cross-section fluctuates to a greater or lesser extent / 10 /. These fluctuations have been considered by Feshbach / 11 /.

(3.2) THE PRE-COMPOUND EMISSION OR THE PRE-EQUILIBRIUM EMISSION

The statistical theory of nuclear reactions has proved extremely useful to explain the average behaviour of excitation fuctions for nuclear reactions at intermediate energies. Some recent measurements / 9, 12 - 16 / for angular distribution of the emitted particles and of their energy distribution have, however, indicated failure of the statistical theory. As the excitation energy increases, both literature and the experimental measurements indicate that the assumption of the statistical equilibrium of the excited compound system before its decay will not remain valid. It is more likely that the excited system will decay before thermodynamic equilibrium has reached. In nuclear reactions at moderate energies, it is, therefore, necessary to consider the emission of particles during the equilibration of the compound system itself. The particles which are emitted during the equilibration are called' Pre-compound or Pre-equilibrium particles ' and this process as the 'Pre-compound emission'. Thus actual energy spectrum in this energy region is thought to be composed of an evaporation or an equilibrium spectrum plus a Pre-compound spectrum or Pre-equilibrium spectrum. The Pre-compound emission serves as a bridge between the two extremities, i.e. the direct and the compound processes. Following four models have been put forward to include the Pre-compound emission of particles in nuclear reactions :-

(a) Intranuclear Cascade Model.
(b) Harp-Miller and Berne Model (HMB).
(c) Exciton Model . and
(d) Hybrid Model and Geometry Dependent Hybrid Model.

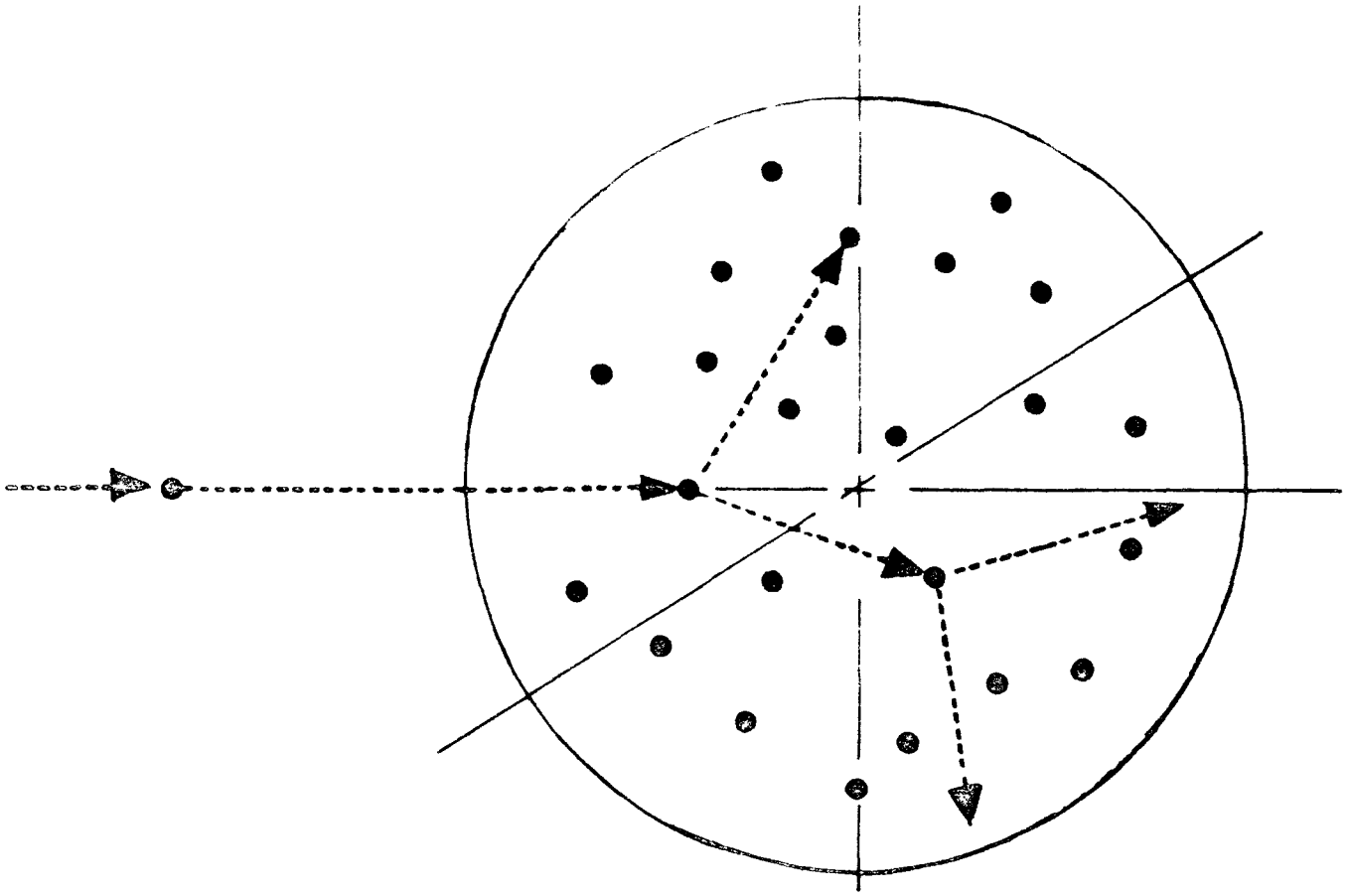

Fig.3.1 Pictorial representation of the Intranuclear Cascade Model.

(3.2 a) Intranuclear cascade model

The Intranuclear cascade model is the earliest model which can be applied to the question of equilibration in nuclear reactions / 17-20 /. The basic reaction mechanism of this model can be understood from figure (3.1). Here as may be seen from the figure the succession of two body interactions is followed in three dimensional geometry. In actual calculations the trajectories of the nucleons are followed one at a time during the cascade until some arbitrary energy, generally considerably above the average equilibrium value has been attained by the nucleon. The trajectories of the other struck nucleons are followed one at a time. Though simple in appearance, the cascade programmes have become more complex with respect to the physics going into the calculations. One such aspect is the treatment of the nuclear potential well and the nucleon density distributions /27/. Cascade model has two distinct features : (i) The time evolution of the reaction can be extracted from such an approach and (ii) It is the only model which can predict angular distributions.

(3.2 b) Harp-Miller and Berne Model

Nuclear reactions at medium and high energies have frequently been described in terms of two step process /15/. The first step in which the bombarding particles develops a cascade in the nucleus through a series of two body nucleon-nucleon collisions and some particles escape from the nucleus. The second step is slow step in which the still excited residual nucleus, de-excites by emission of nucleons, clusters of nucleons and gamma rays. This residual nucl

eus

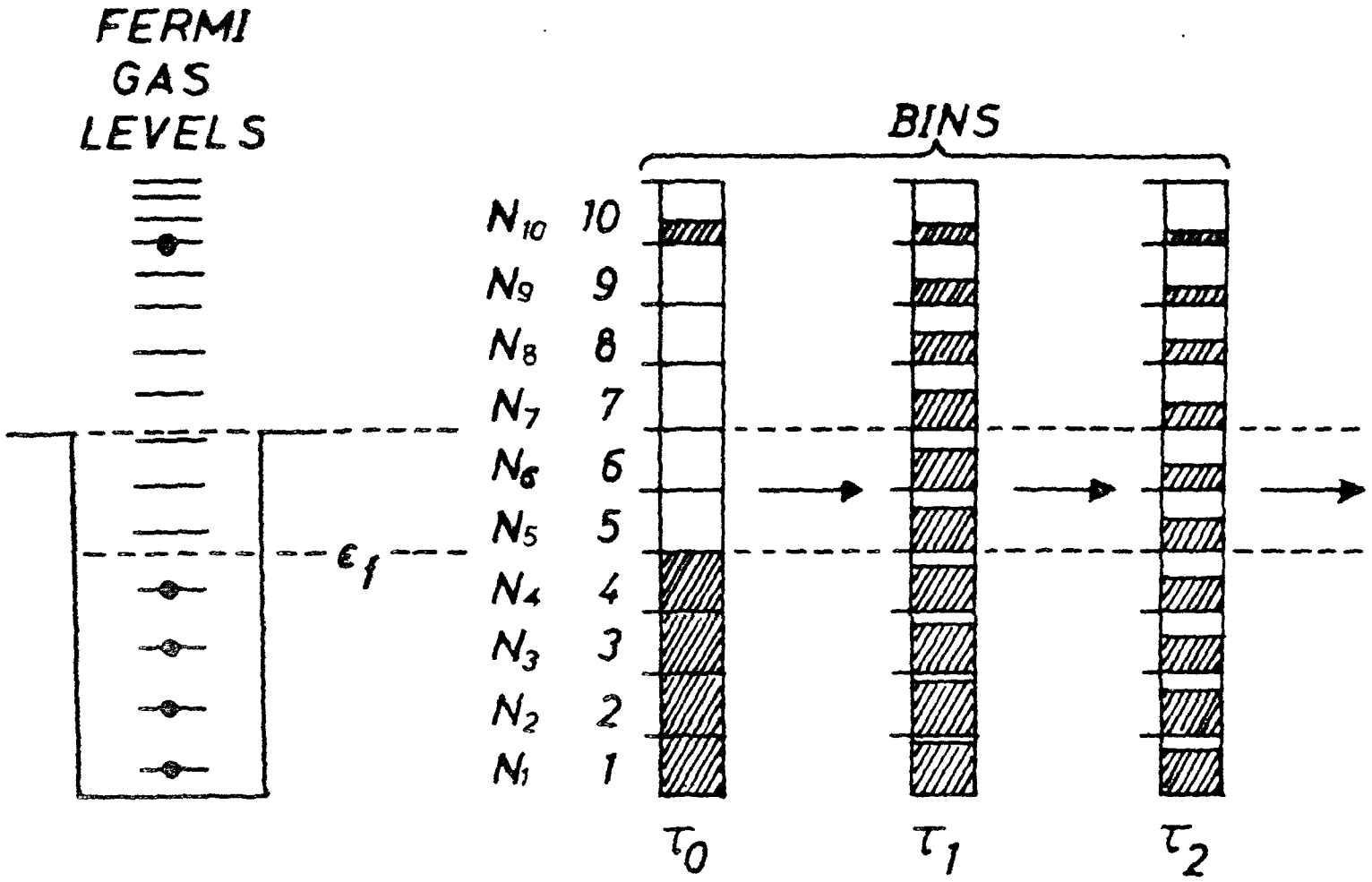

Fig. 3.2 Pictorial representation of the Harp-Miller-Berne Model.

after the first step, can be considered as a Fermi gas and its states can be described by the occupation numbers of the single particle nucleon states. Generally it is assumed that the residual excited nucleus left after the first step attains a thermodynamic equilibrium in such a small time that no nucleons are emitted during the relaxation time. It is further assumed that the emission of the nucleons from this relaxed nucleus takes place through evaporation like the thermodynamic emission of electron from metal. The equilibrium state of this relaxed excited nucleus is then characterised by its excitation energy and particle numbers. It is, however, likely that the relaxation time of a moderately excited nucleus is larger than the life time for nucleon emission. If it is so, it is possible that a considerable number of particles and hence the excitation energy loss may take place during the process of relaxation. Harp-Miller and Berne / 29 / have considered the problem of relaxation, i.e. the time in which a excited nucleus attains thermodynamic equilibrium and the emission of particles during this time. Their procedure is to solve a Boltzmann-like master equation for the time evolution of the occupation numbers of a Fermi gas system.

The physical ideas of the Harp-Miller and Berne (HMB) model / 29 -30 / are shown in figure (3.2). As in figure, the excitation energy is divided into bins of some convenience size, say 1 MeV, and the number of single particle states in each bin are then calculated and stored; a Fermi gas distribution has generally been used in calculations. The calculation has been done either beginning with some initial arbitrary population of excited particles and holes,

or with a nucleus in the ground state. Two body residual interaction is assumed to change the occupation number of each bin and hence occupation number varies with time. The fraction of occupation of each bin is then followed as a function of time. For a given incident nucleon the rate of allowed transitions with all nucleons in the nucleus is calculated against the rate of emission of excited particles into the continuum. Nucleon-nucleon scattering cross-sections are used for calculating the two body transition rates with each energy partition being assigned equal to a priori-probability. Transition rates in the continuum are calculated using the phase space factors and inverse cross-sections. Therefore, a statistical argument is applied, as to the number of ways the particle may be emitted vs the number of ways it may make an internal transition, and the cross-section is divided proportionately.

Actually, first the relative probabilities of scattering into and out of each bin and of emission from bins above the particle binding energies are calculated. After these calculations, occupation of each bin is changed, as shown in the central part of the figure (3.2). To calculate all possible ways of scattering into and out of each bin, the earlier calculation must be repeated for the particles occupying each bin, the population of each bin is again changed. The solution of the equilibration problem in this model depends on computer solution of a set of coupled differential equations. Harp and Miller / 30 / have extended this model for the two component Fermion gas. Following assumptions have been made in carrying out detailed

calculations : (1) Interactions within the nucleus take place from nucleon-nucleon scattering processes, thus two nucleons are always involved, going from two initial states to two final states. (2) The transition probabilities depend only on the energies of the particle involved. (3) These transition probabilites vary slowly with energy interval $\Delta\epsilon$.

The total number of states g_i^p (for proton) in ith group within the nucleus whose energies are lying between $\epsilon_i^p - \frac{\Delta\epsilon}{2}$ and $\epsilon_i^p + \frac{\Delta\epsilon}{2}$ may be written as :

$$g_i^p = \int_{\epsilon_i^p - \frac{\Delta\epsilon}{2}}^{\epsilon_i^p + \frac{\Delta\epsilon}{2}} \rho_p(\epsilon)\, d\epsilon \qquad \ldots \quad (3.11)$$

where $\rho(\epsilon) = 4\pi V (2M)^{3/2} \epsilon^{1/2} / h^3$ .. (3.12)

known as the density of nuclear transitional states for the gas inside the nucleus, V is the nuclear volume, M is the proton mass. This definition applies to all 'bins' whether the nuclear energy is less than or greater than the Fermi plus binding energies. Similarly the number of states for nucleon outside the nucleus is :-

$$g_{i'}^p = \int_{\epsilon_{i'}^p - \frac{\Delta\epsilon}{2}}^{\epsilon_{i'}^p + \frac{\Delta\epsilon}{2}} \rho_p'(\epsilon)\, d\epsilon \qquad \ldots \quad (3.13a)$$

Here

$$\rho'(\epsilon') = \left[\frac{4\pi\Omega(2M)^{3/2}}{h^3}\right]\epsilon'^{1/2} \qquad \ldots (3.13b)$$

is the density of the proton transitional states and Ω is the volume in which free particle phase space states are normalised.

For the nucleon states n_i , the occupation number of the ith group is defined as $n_i g_i = N_i$ = total number of occupied states within the ith group. The Boltzmann like master equationsthat describes the relaxation process of the proton Fermi gas in the two-gas model are given by :

$$\frac{dN_i^P}{dt} = \sum_{jkl}\Big[w^{PP}_{kl\to ij}\; g_k^P\; g_l^P\; g_j^P\; n_k^P n_l^P\; (1-n_i^P)\times$$

$$\times(1-n_j^P) - w^{PP}_{ij\to kl}\, g_j^P\; g_k^P\; g_l^P\; n_i^P\; n_j^P\times$$

$$\times(1-n_k^P)(1-n_l^P)\Big]\cdot\delta(\epsilon_i^P+\epsilon_j^P-\epsilon_l^P-\epsilon_k^P)+$$

$$+\sum_{jkl}\Big[w^{PN}_{kl\to ij}\; g_k^P\; g_l^N\; g_j^N\; n_l^N\; n_k^P\,(1-n_i^P)\times$$

$$\times(1-n_j^N) - w^{PN}_{ij\to kl}\; g_j^N\; g_l^N\; g_k^P\; n_i^P\; n_j^N\times$$

$$\times(1-n_k^P)(1-n_l^N)\Big]\times\delta(\epsilon_i^P+\epsilon_j^N-\epsilon_k^P-\epsilon_l^N)$$

$$-n_i^P\; w^P_{i\to i'}\; g_{i'}^P\times\delta(\epsilon_{i'}^P-\epsilon_i^P+\epsilon_f^P+BE_p)$$

$$\ldots\ldots\ldots (3.14)$$

Where

$$(i = 1 , \ldots \ldots \epsilon_g^P + E^* ; i' = 1, \ldots .. E^* - BE_p)$$

$\frac{dN_i^P}{dt}$ = time rate of change of number of protons in the ith sub-group.

g_i^P = number of levels in the ith sub-group.

$w_{ij \longrightarrow kl}^{XY}$ = probability per unit time that a nucleon of type X in a particular state of the ith group scatters with a nucleon of type Y in a particular state of the jth group with particle Y going to the lth group and particle X to the kth group.

$w_{i \longrightarrow i'}^P$ = probability per unit time that a proton in a particular state of the ith group escapes to the continuum.

n_i^P, = number of escaped protons with laboratory energy ϵ_i^P ,

n_i^P = is the group occupation number. The δ-function guarantees the conservation of energy in these transitions. The transition probabilities are defined as follows :

$$w_{ij \longrightarrow kl}^{PP} = \frac{\sigma_{pp} (\epsilon_i^P + \epsilon_j^P) \left[2 (\epsilon_i^P + \epsilon_j^P) / M \right]^{1/2}}{V \sum_{mn} g_m^P g_n^P \delta (\epsilon_i^P + \epsilon_j^P - \epsilon_m^P - \epsilon_n^P)}$$

.. .. (3.15)

Where $\sigma_{pp}(\epsilon)$ is the elementary P - P elastic scattering cross-section evaluated at an energy ϵ after the elimination of Coulomb effects; appropriate changes are made for P-N transitions, and σ_{pp} is taken equal to σ_{NN} . The summation in the denominator in equation (3.15) is taken only over those states which are allowed in P - P scattering process within the nucleus, and

$$w^{p}_{i \to i'} = \frac{\sigma^{p}_{inv}(\epsilon^{p}_{i'}) \left[2 \epsilon^{p}_{i'} / M\right]^{1/2}}{g^{p}_{i} \Omega} \quad .. (3.16)$$

Here $\sigma^{p}_{inv}(\epsilon^{p}_{i'})$ is the inverse cross-section for the absorption by nucleus of a proton of energy $\epsilon^{p}_{i'}$, and Ω is the laboratory volume.

This model is simple in approach and have fewer assumptions as compared to other models. However, this model is complicated by the problem of following the energy bin populations in time. Moreover angular information is not kept as it is in the intranuclear cascade model.

(3.2 e) EXCITON MODEL

In 1966 a simple model providing a quantitative description of the attainment of statistical equilibrium was proposed by Griffin / 31 - 33 / . In Griffin model the states of the system are classified according to the number of excited particles and holes they contain. The system is assumed to equilibrate through a series of two body interactions, which brings about transitions between these states.

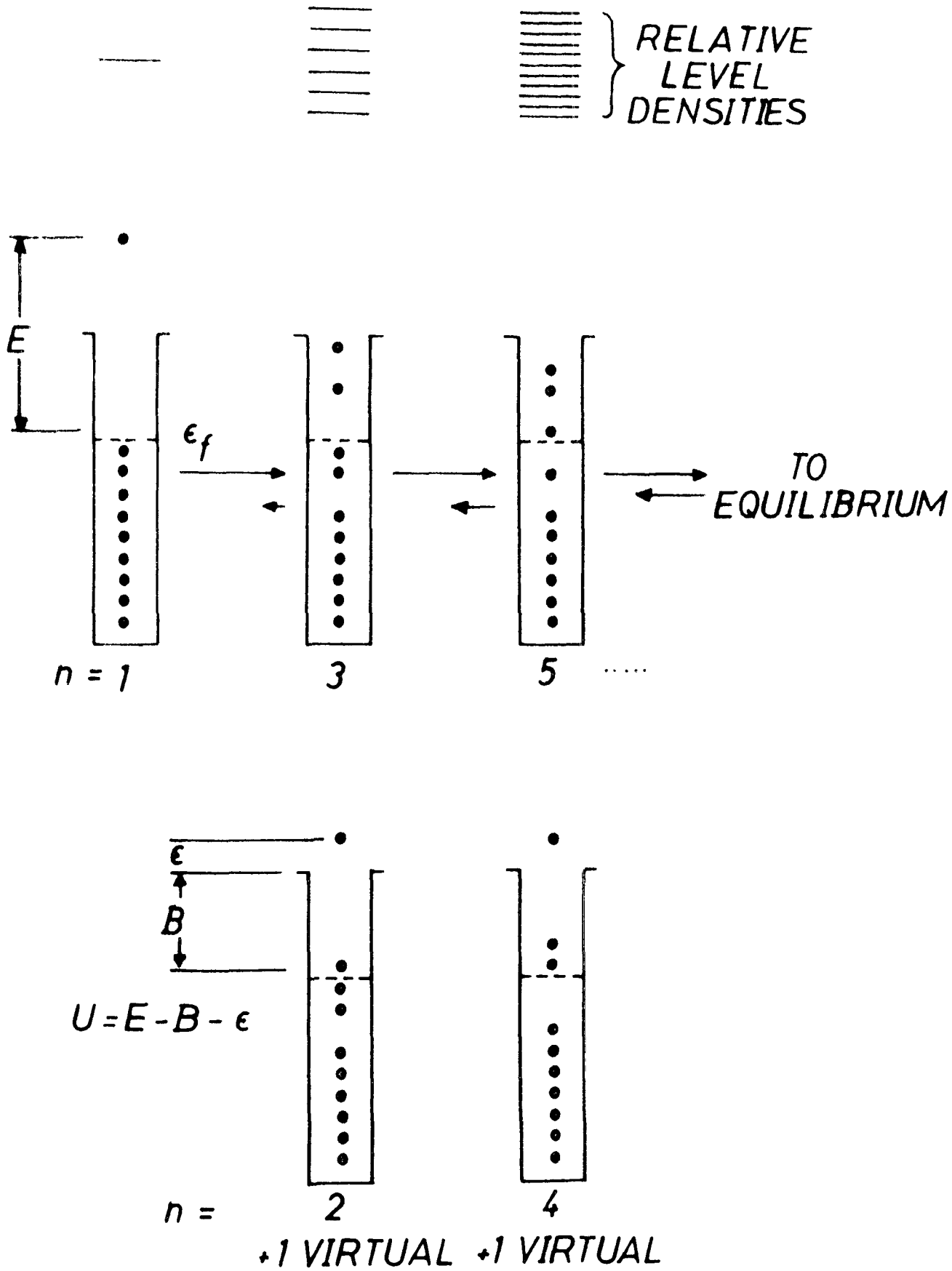

Fig. 3.3 Pictorial representation of the Exciton Model.

The physical concept of the exciton model is illustrated in figure (3.3). A nucleon is shown entering the nuclear potential. All the Fermions are in their ground states. It is assumed that a series of two body interactions occur. The first interaction would, therefore, lead to a 2p1h (two particles and 1 hole) state, and any configuration is equally likely. This could be followed by a transition between one of the two excited particles and a particle in the ground state, or with the other excited particle . This could lead either to a 3p2h state, back to the original configuration, or to a different 2p1h state. The probability of each occurance is assumed to be proportional to the density of the approachable final states. Since the initial simple configurations are far fewer than the equilibrium particle-hole numbers, the level densities are rapidly increasing functions of increasing p-h number, and the system then goes pre-dominantly in the direction of equilibrium as is indicated in this figure (3.3) by the larger arrows in that direction.

For a given configuration, specified by the particle-hole number , some fraction will have atleast one particle with energy in excess of its binding energy. The fraction of particles in a given exciton number state, which are at a given energy (ϵ + B) above the Fermi energy, where ϵ is the channel energy of the particle and B is the particle binding energy, can be computed and from this fraction relative probability of emission of a particle, having such a kinetic energy, can be calculated. The total spectrum emitted prior to equilibration can be calculated by summing over the contribution from each state. It is obvious that the simplest states have the largest probability of emitting particles of

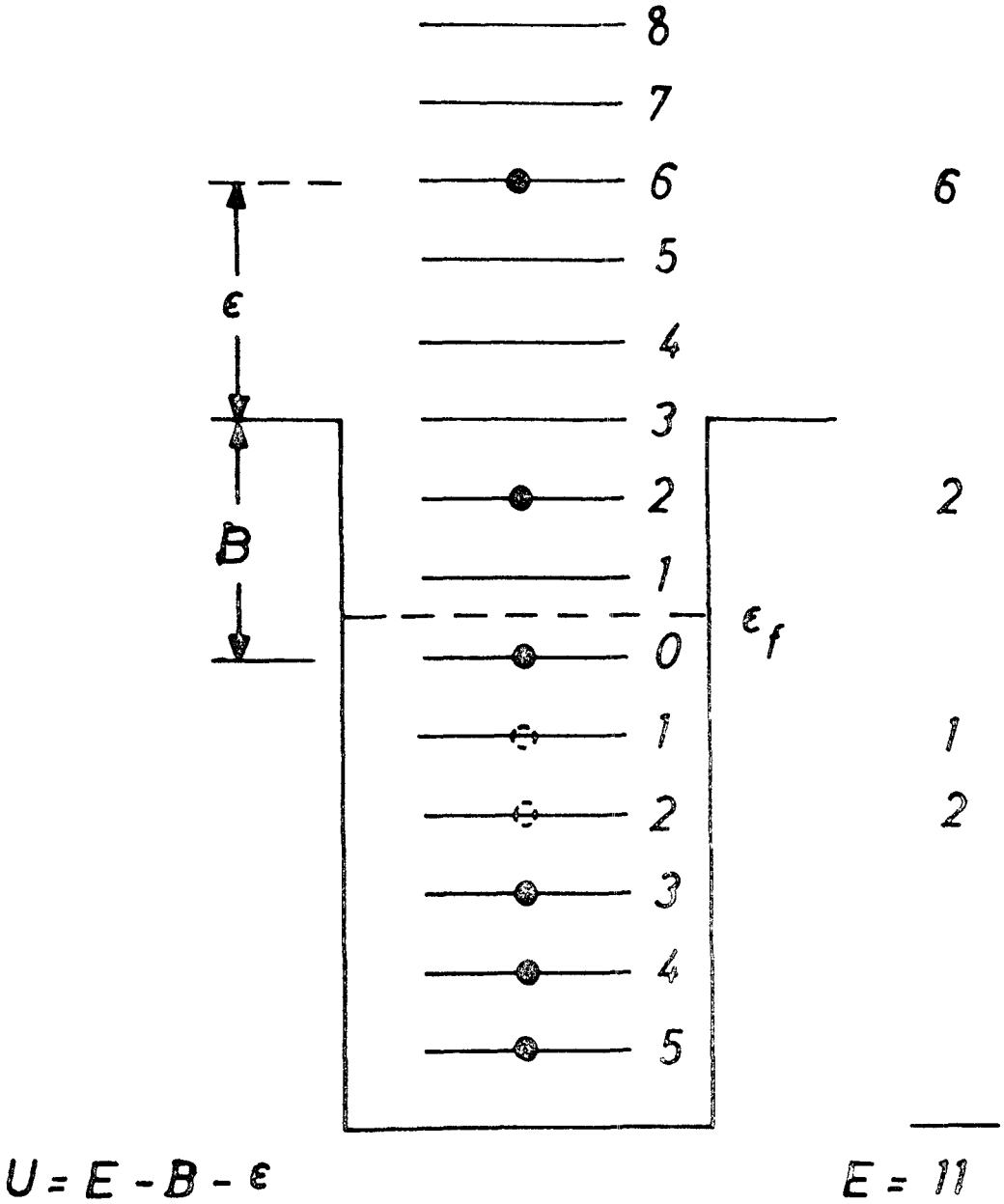

Fig. 3.4 Equidistant Fermi gas model. Excited 2p-2h states.

higher kinetic energy as the average excitation per particle is highest in these states. As the particle increases towards the equilibrium value and the total number of ways the energy may be partitioned between particles and holes increases exponentially, the probability, that any one particle has some high energy, exponentially decreases.

The main assumption in the exciton model is that every configuration of each intermediate state will occur with equal a priori-probability during the equilibration process. Intermediate state densities play an important role in exciton model. The first order approach to this density function is to assume that a nucleus behaves like a degenerate Fermi gas and all levels are equally spaced with a spacing equal to that at the Fermi energy. Let g be the single particle level density associated with such a spacing. Such a model is illustrated in Fig. (3.4). If E is the excitation energy then a natural unit for the excitation energy in the model may be defined as $\epsilon = gE$. It can be shown that the density of the states at excitation energy E is given by / 34 / as

$$\rho_{p,h}(E) = \frac{g(gE)^{n-1}}{p!\,h!\,(n-1)!} \quad \ldots\ldots\ldots (3.17)$$

where $n = p + h$, p be the number of particles and h be the number of holes. It is obvious that $\rho_n(E)$ is a rapidly increasing function of n when $n \ll \bar{n}$ where $\bar{n}$ is the equilibrium exciton number i.e. $\bar{n} = \sqrt{2gE}$. Considering this, Griffin / 32 / presented a model, for which only

transitions with $\Delta n = +2$ are considered and $\Delta n = 0, -2$ transitions are neglected. In this model it is also assumed that the fraction of n-exciton states in which one particle is at some energy $(\epsilon + B)$ above the Fermi energy is given by the ratio :-

$$\frac{\rho_n(U, \epsilon)}{\rho_n(E)} = \frac{\rho_{p,h}(U, \epsilon)}{\rho_{p,h}(E)} \quad \ldots (3.18)$$

Where U is the excitation energy of the residual nucleus, ϵ is the channel energy of the particle emission. Thus the probability of decay from an n -exciton state is given by /33, 35 / :-

$$P_n(\epsilon)\, d\epsilon = (2s+1)\left[\rho_n(U, \epsilon)/\rho_n(E)\right] \times \frac{\Omega 4\pi p^2\, dp\, \sigma_v}{h^3} \tau_n \quad \ldots (3.19)$$

Where τ_n is the mean life time of the n exciton state, Ω is the phase space and σ_v is penetrability factor. If s is the particle spin then the total decay expression is :

$$P(\epsilon)\, d\epsilon = \sum_{\substack{n=n_0 \\ \Delta n = +2}}^{\bar{n}} P_n(\epsilon)\, d\epsilon \propto \frac{(2s+1)}{(g.E)} \times \sigma\epsilon M \sum_{\substack{n=n_0 \\ \Delta n = +2}}^{\bar{n}} \left(\frac{U}{E}\right)^{n-2} P(n-1) \times \tau_n\, d\epsilon \quad \ldots (3.20)$$

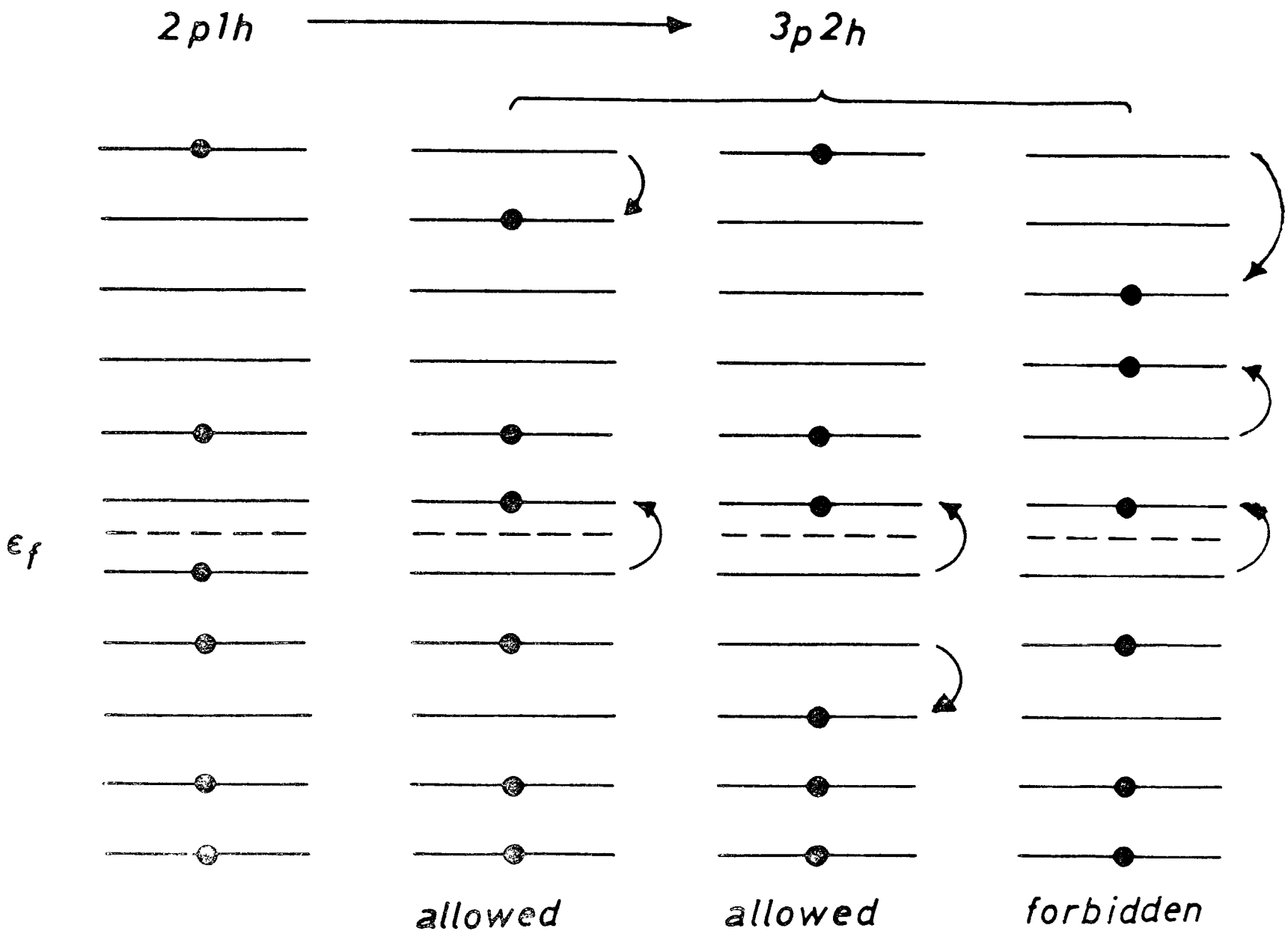

Fig. 3.5 Limitation on allowed transitions in the exciton model.

Here 'α' is a constant proportional to the fraction of compound decays, 'τ_n' can be evaluated, on a relative basis, by the Golden rule of Fermi / 31 / as :-

$$\lambda_{n,\,n'} = \frac{2\pi}{\hbar} \cdot |M|^2 \cdot \rho_{n'}(E) \quad \ldots\ldots \quad (3.21)$$

Here 'M' is the average matrix element for the interaction between the initial and final states and is taken to be independent of the exciton numbers of these states, '$\rho_{n'}(E)$' is the density of the accessible final states and '$\lambda_{n,\,n'}$' is the transition rate from a given initial n exciton state to any of the accessible n' exciton final states. There have been different types of transitions from 2p1h state but all transitions are not possible in calculating ρ_n, as shown in fig. (3.5)

Due to the fact that the two body interaction matrix M is not well known, the exciton model can give only the relative spectral yields. Williams / 36/ has given formulas for the average number of accessible states for each type of transition as follows :-

$$\lambda_+ = \frac{2\pi}{\hbar} \cdot |\bar{M}|^2 \cdot \frac{g^3\, U^2}{(p+h+1)}$$

$$\lambda_- = \frac{2\pi}{\hbar} \cdot |\bar{M}|^2 \cdot g\left[p,\, h,\, (p+h-2)\right]$$

$$\lambda_0 = \frac{2\pi}{\hbar} \cdot |\bar{M}|^2 \cdot g^2\, U \left[\frac{3(p+h)-2}{4}\right]$$

$$\ldots\ldots \quad (3.22)$$

Where λ_+ , λ_- and λ_0 are relative rates for transition, in which the exciton number changes by +2, -2 and 0. The exciton model provides within a single model a description of the reaction beginning with the target-projectile interaction, proceeding through the attainment of equilibrium, and then following the decay of the equilibrium compound nucleus. The model due to Griffin avoids the problem of following the bin population by substituting density of states characterized by exciton number.

(3.2 d) Hybrid Model and Geometry Dependent Hybrid Model

In both the HMB and the exciton models only the relative spectral shapes and reaction yields can be calculated. To facilitate the direct comparison of the measured cross-section, another approach to the exciton model has been suggested in which the average intermediate state life time has been replaced by an expression involving the transition time of individual excited nucleon and this quantity has been in turn related to nucleon-nucleon scattering data / 37 /. This approach combines the use of intermediate state densities as in the exciton model to give a simple closed form result. The transition times based on nucleon-nucleon scattering data are used to permit calculation of absolute cross-section, as in the Harp-Miller-Berne model. The model is called the 'Hybrid model' / 38 /.

In the Hybrid model the intranuclear transition rates for the intermediate states are calculated from the nucleon-nucleon scattering cross-sections. The average rate of transitions for the n - exciton excited state may be represented as / 38 / :-

$$\lambda_n (E) = 1.4 \times 10^{21} . E - 6 \times 10^{13} \text{ Sec}^{-1} \quad \ldots (3.23)$$

Where 'E' is the complex state excitation energy. As in high energy cascade calculations, it is assumed that a reaction proceeds through a series of particle-particle or particle-hole interactions, in which the total particle hole number characterising the nuclear state may either increase by two, decrease by two, or remain unchanged as a result of each interaction. It is assumed that the transitions in which the exciton number increases by two dominate in the early stage of the equilibration process. Like Griffin model / 31 / it is further assumed that the intermediate states are characterised by appropriate level density formulae, and that all levels may be populated with equal a priori-probability subject to the limitations of energy conservation and Pauli exclusion principle. As in the treatment of the exciton model, in Hybrid model also the total particle emission probability, in a given channel energy range, $P_x (\epsilon) \, d\epsilon$, is given as a sum over the contributions of the intermediate states. The sum is taken from some initial number of excitons n_0 to the equilibrium number $\bar{n}$, then decay probability is :

$$P_x (\epsilon) \, d\epsilon = \sum_{n = n_0}^{\bar{n}} {}^{n}P_x \left[\rho_n (U, \epsilon) / \rho_n (E) \right] \cdot \left[\lambda_c (\epsilon) / (\lambda_c (\epsilon) + \lambda_{n+2} (\epsilon)) \right] \cdot \left[\prod_{n' = n_0}^{n} (1 - P_{n'-2}) \right] =$$

$$= \sum_{n = n_0}^{\bar{n}} {}^{n}P_x (\epsilon) \, d\epsilon \quad \ldots (3.24)$$

In this equation the first bracket is the fraction of the n exciton state population which has one particle in a virtual level, which would have energy between ϵ and $\epsilon + d\epsilon$ in the continuum. The second bracket is the expression for the ratio of decay rate into the continuum to total decay rate.

The rates $\lambda_c (\epsilon)$ are calculated as :-

$$\lambda_c(\epsilon) = \sigma(\epsilon) \left(\frac{2\epsilon}{M} \right)^{1/2} \rho_c(\epsilon) / g\Omega \qquad \ldots\ldots (3.25)$$

The term in the third bracket of equation (3.24) is the depletion factor, which reduces the population of each state according to the amount of particle emission from the earlier simple states. With this definition $P_{n'}$ is given by :

$$P_{n'} = \sum_{X = n,p} \int_{\epsilon=0}^{\epsilon_{max}} n' P_X(\epsilon) \, d\epsilon \qquad \ldots\ldots (3.26)$$

Where $P_{n'}$ is zero for the first term in the summation of equation (3.24). The level densities used in the expression has been given by Williams / 34 / as :-

$$\rho_{p,h}(E) = g (gE - \theta)^{n-1} / (p! \, h! \, (n-1)!) \qquad \ldots\ldots (3.27)$$

Where $\theta = f (p, h)$ is a correction term for the Pauli-principle.

The Hybrid model has been further extended /39-40/ to include the effects of nuclear density distribution in the pre-equilibrium emission. This has been done by developing a geometric dependence of the impact parameter of the incident partial waves. The hybrid model has been reformulated as a sum of contributions over impact parameter :-

$$\sigma_x(\epsilon)\, d\epsilon = \pi \lambda^2 \sum_{l=0}^{\infty} (2l+1) \times$$

$$\times T_l\, P_x(\epsilon)\, d\epsilon \quad \ldots \quad (3.28)$$

Where 'T_l' are the optical model transmission coefficients for the projectile and 'P_x' is the pre-equilibrium probability, calculated as a function of nuclear density. Nuclear density is given by Fermi distribution / 41 / as :-

$$d(R) = \bar{d}\left(\exp(R-C)/Z+1\right)^{-1} \quad \ldots \quad \ldots (3.29)$$

Where d(R) is the density at radius R with $\bar{d}$ as the central nuclear density, $C = 1.07\ A^{1/3}$ fm, and Z=0.55 fm.

The nuclear density can influence the pre-equilibrium decay spectrum in two ways : (1) An increase in the mean free path for nucleon-nucleon collision, increasing the particle emission probability. (2) The Fermi energy will be lower in that region, so that the hole depth is limited. The transition rates and the Fermi energy have been modified in each region

$$E_g(R) = E_g \left[\frac{\langle d(R)\rangle}{\bar{d}}\right]^{2/3} \text{MeV} \quad \ldots \quad (3.30)$$

Where 'E_f' is the Fermi energy at central density and $\langle \delta (R) \rangle$ represents the average density for the impact parameter. The single particle level density is also taken to :-

$$g_{\nu} (R) = \left(\frac{E_f}{E_f (R)} \right) \cdot \left(\frac{A}{28} \right) \quad \ldots (3.31)$$

Here A is the mass number of the excited nucleus, E_f (R), is Fermi energy at R. In calculations, combinational probabilities have been used, considering the finite well depth for decay of the first excited state, which is the most important part of the application, with $g = g_n + g_p$, these values are calculated as given by Ericson's intermediate state density expressions [42] :-

$$\rho_{2p1h} (\epsilon, U) = 1/2\, g^2 (E_f (R)), \quad U > E_f (R)$$

and

$$\rho_{2p1h} (E) = 1/4\, g^3 E_f (R) \left[2E - E_f (R) \right], E > E_f (R)$$

$$\ldots \ldots \ldots (3.32)$$

****

References

/ 1/ V.F. Weisskopf and D.H. Ewing; Phys. Rev. 57 (1940)472.

/ 2/ H.Feshbach and V.F.Weisskopf; Phys.Rev. 76 (1949)1550.

/ 3/ J.M. Blatt and V.F. Weisskopf; "Theoretical Nuclear Physics "John Wiley & Sons,New York (1952).

/ 4/ N. Bohr ; Nature 137 (1936) 344.

/ 5/ A.C. Douglas and H. Macdonald; Nucl.Phys.13 (1959)382.

/ 6/ H.A. Bethe; Rev. Mod. Phys. 9 (1937) 69.

/ 7/ V.F. Weisskopf; Phys. Rev. 52 (1937) 295.

/ 8/ G. Breit and E.P. Wigner; Phys.Rev. 49 (1936) 519.

/ 9/ W. Hauser and H. Feshbach; Phys.Rev. 87 (1952) 366.

/10/ T.Ericson and T.M. Kuckuk ; Ann. Rev. Nucl.Sci.16(1966).

/11/ H. Feshbach, C.E. Porter and V.F.Weisskopf ; Phys.Rev. 96(1954)448.

/12/ M. Bormann, H.Schmidt, V.Schroder, W.Scobel and V.Seebeck; Nucl. Phys; A186 (1972)65.

/13/ L. Glowacka, M. Jaskola and J.Tarkiewicz ; Nucl.Phys. A244 (1975)117.

/14/ L.Glowacka, M.Jaskola and J.Tarkiewicz; Nucl. Phys. A262 (1976)205.

/15/ Hideo Yitazawa; Nucl.Phys. A149 (1970) 513.

/16/ V.V. Verbinski and W.R. Burrus ; Phys.Rev.177 (1969)1671.

/17/ R. Serber; Phys. Rev. 72 (1947) 1114.

/18/ M.L. Goldberger ; Phys. Rev. 74 (1948) 1268.

/19/ Bernardini, Booth and Lindenbaun ; Phys. Rev.88(1952)1017.

/20/ Morrison, Muirhead and Rosser; Phil.Mag.44 (1953)1326.

/21/ Mamamus, Sharp and Gellman; Phys. Rev. 93 (1954) 94A.

/22/ J.W. Meadows; Phys. Rev. 98 (1955) 744.

/23/ J. Combe; Nuovo.Cim. 3 (1956) 5182.

/24/ N. Metropolish et al. ; Phys.Rev. 110 (1958) 185.
; Phys.Rev. 110 (1958) 204.

/25/ H.W. Bertini; Phys. Rev. 131 (1963) 1801.

/26/ K. Chen et al.; Phys. Rev 166 (1968) 949.

/27/ K. Chen, G. Freidlander and J.M. Miller; Phys. Rev. 176 (1968) 1208.

/28/ K. Chen et al. ; Phys. Rev. C 4 (1971) 2234.

/29/ G.D. Harp, J.M. Miller and B.J. Berne; Phys.Rev. 165 (1968) 1166.

/30/ G.D. Harp and J.M. Miller ; Phys.Rev. C3 (1971) 1847.

/31/ J.J. Griffin; Phys.Rev.Lett. 17 (1966) 478.

/32/ J.J. Griffin; Phys.Lett. B24 (1967) 5.

/33/ M. Blann; Phys. Rev. Lett. 21 (1968) 1357.

/34/ F.C. Williams,Jr.; Nucl Phys. A166 (1971) 231.

/35/ M. Blann and F.M. Lanzafame; Nucl.Phys. A142 (1970) 559.

/36/ F.C. Williams, Jr. ; Phys.Lett. 31B (1970) 184.

/37/ M. Blann ; Phys. Rev. Lett. 27 (1971) 337.
; erratta 27 (1971) 1550.

/38/ M. Blann and A. Mignerey; Nucl.Phys. A186 (1972) 245.

/39/ M. Blann; Phys.Rev. Lett. 28 (1972) 757.

/40/ M. Blann; Nucl.Phys. A213 (1973) 570.

/41/ R. Hofstadter; Ann. Rev. Nucl. Sci. 7 (1957) 295.

/42/ T. Ericson ; Adv. in Phys. 9 (1960) 423.

****
****

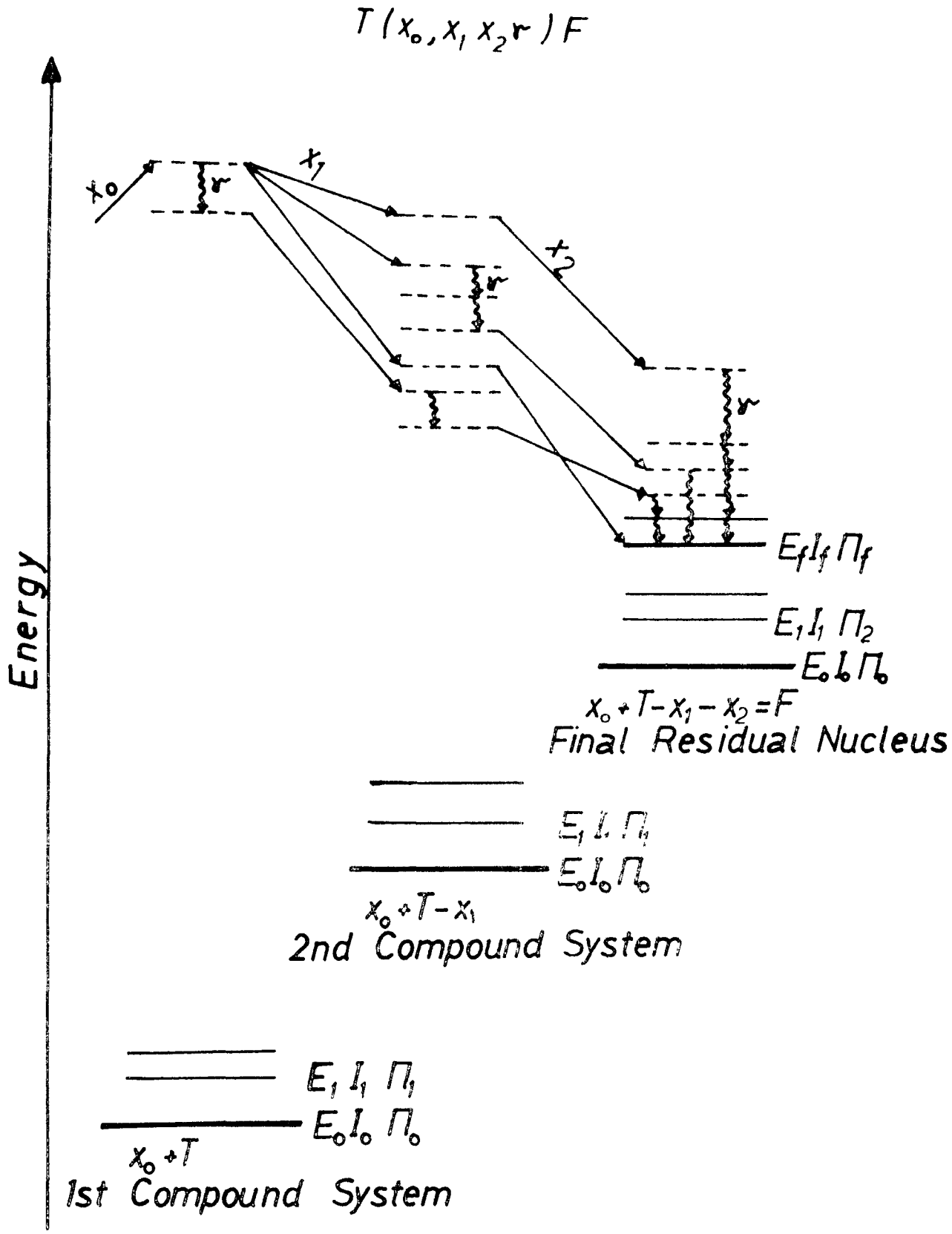

Fig. 4.1 The different ways of populating final states $(E_f I_f \Pi_f)$ for a reaction $T(x_0, x_1 x_2 \gamma)F$.

CHAPTER XV

COMPUTER CODE

Many computer codes for the calculation of excitation function for nucleon induced reactions have so far been developed / 1-6 /. Most of them, however, have not taken into account the conservation of parity, angular momentum and the pre-compound emission of particle. A computer code 'ACT ' has been developed on the lines of the code STAPRE by Uhl / 7 /, for the calculation of energy averaged cross-sections for nucleon induced reactions at moderate excitation energy. In this code upto four sequentially emitted particles have been considered. The code also takes into account γ-ray emission. The number of γ-rays have been limited only by the use of an energy grid for the calculations. In this code the pre-compound emission from the first step of de-excitation, using ' Hybrid model ' framework, has been included. After the first step of de-excitation the excitation energy of the still excited residual nucleus is considerably lowered, and hence the probability of pre-compound emission is negligible. The conservation of parity and angular momentum have been explicitly taken into account. The computer programme is quite versatile and is capable of calculating the activation cross-sections, isomeric cross-sections and cross-sections for the production of γ-rays from the lowly excited levels.

The different ways of populating a particular state of a final nucleus is shown in figure (4.1). Incident particle x_0 makes a composite system with the target T (E_0, I_0, Π_0),where E_0 , I_0 , and Π_0 are respectively the ground state energy, angular momentum and parity of the target nucleus. The residual nucleus F is reached by the subsequent emission of particles

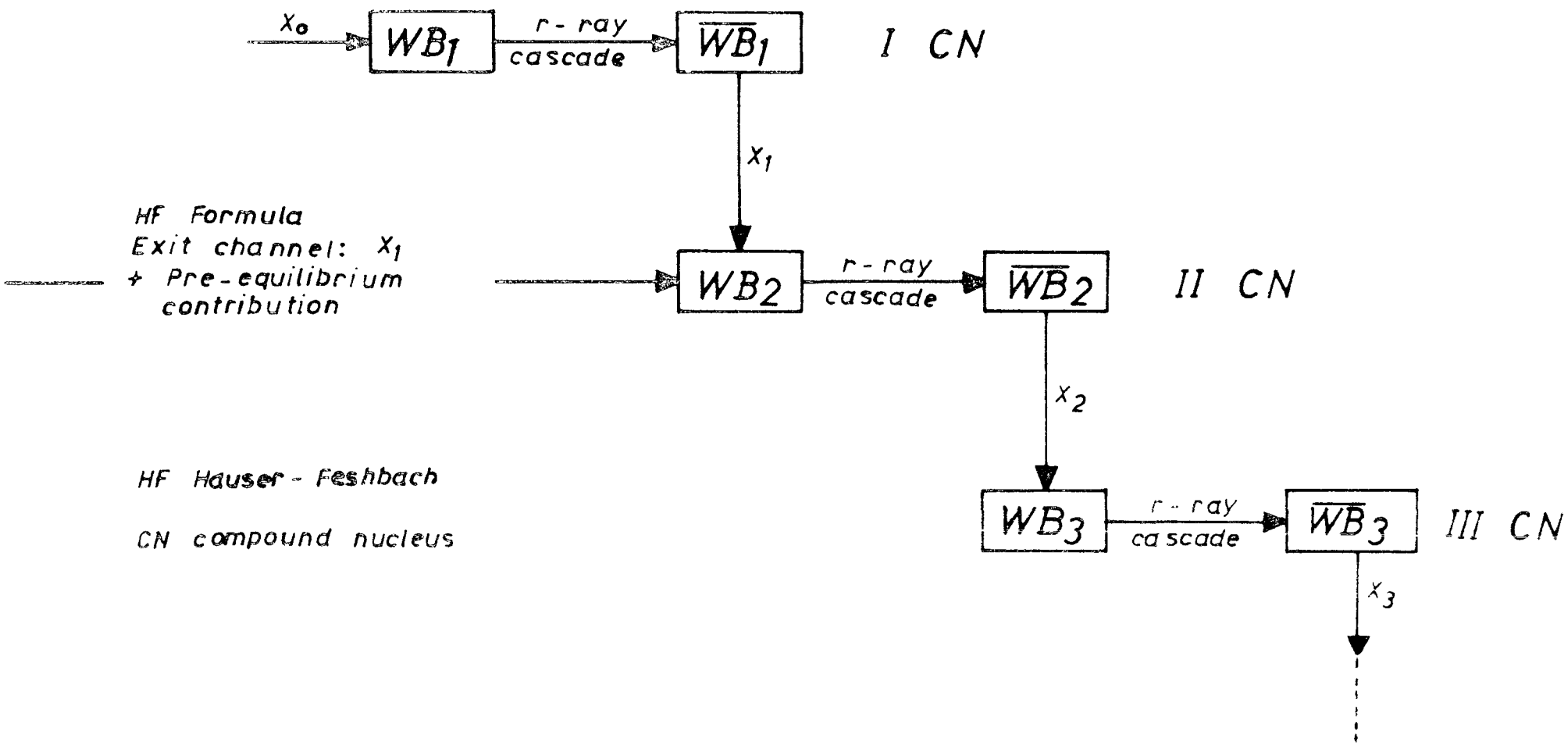

Fig. 4.2 Sequence of calculations

x_1 , x_2 , x_3, ... and γ-rays. Figure (4.2) schematically illustrates the sequence of calculations. The ith compound nucleus is defined as the nucleus that results from the emission of (i- 1) of a specified sequence of emitted particles (x_1 , x_2 , x_3 , ... x_i). The primary population of states with an excitation energy in an interval ΔE, with angular momentum I and parity Π is WB_i (E, I, Π).ΔE,

where the subscript denotes the number of the compound nucleus. Subsequent γ-ray cascades between the states of the ith compound nucleus lead to the population $\overline{WB_i}$ (E, I, Π) . Δ E.

The major part of the calculations is based on the statistical model. For particles emitted in the first step of the evaporation cascade a " pre-equilibrium decay " contribution of the cross-section is included. The fraction of the population of the composite system that is left over after the pre-compound emission is assumed to undergo statistical decay and for that Hauser - Feshbach formula has been used. If only the pre-compound (P R) and compound nucleus (C N) mechanism are assumed to be present, the total cross-section for the reaction T (x_0 , x_i) F can be written in the form :-

$$\sigma (x_0, x_i ; E) = \sigma_{PR} (x_0, x_i ; E) + R_{CN} (E) \sigma'_{CN} (x_0, x_i ; E) \quad .. .. \quad (4.1)$$

Where σ_{PR} (x_0 , x_i ; E) represents the pre-compound cross-section and R_{CN} (E) σ'_{CN} (x_0 , x_i ; E) the compound nucleus (evaporation) component of the cross-section (4.1) ; E is the excitation energy of the composite system . σ'_{CN} (x_0, x_i ; E) can be obtained assuming that the whole incoming flux forms a compound nucleus with the cross-section σ_R (x_0 , E_i).

$$\sigma'_{CN} (x_0 , x_i ; E) = \sigma_R (x_0 , E_i) \frac{\Gamma x_i}{\sum_{\nu} \Gamma \nu} \quad ... \quad (4.2)$$

Where Γx_i and $\sum_{\nu} \Gamma \nu$ are respectively the decay widths corresponding

to particle emission and the total decay width.

In the presence of pre-compound reaction mechanism, the compound-nucleus formation cross-section $\sigma_c (x_0 , E_i)$ is, however, reduced from $\sigma_R (x_0 , E_i)$ by the amount of the total non-compound cross-section $\sigma_{non} (x_0 , E_i)$. As the competition between pre-compound and compound nucleus processes is considered only, $\sigma_c (x_0 , E_i)$ has the form :-

$$\sigma_C (x_0 , E_i) = R_{CN} (E) \cdot \sigma_R (x_0 , E_i) \ldots\ldots (4.3)$$

Where

$$R_{CN} (E) = 1 - \frac{\sum_{x_i} \sigma_{PR} (x_0 , x_i , E)}{\sigma_R (x_0 , E_i)} \ldots\ldots (4.4)$$

Thus from Equs. (4.1), (4.2), (4.3) and (4.4) one gets :

$$\sigma (x_0, x_i , E) = \sigma_{PR} (x_0, x_i , E) + \left[1 - \frac{\sum_{x_i} \sigma_{PR} (x_0 , x_i , E)}{\sigma_R (x_0 , E_i)} \right] \times$$

$$\times \sigma_R (x_0 , E_i) \frac{\sqrt{x_i}}{\sum_{\nu} \sqrt{\nu}} \ldots\ldots (4.5)$$

In the present code the activation cross-section, population of isomeric states and related results for the ith compound nucleus can be obtained from the quantity $\overline{WB}_i \cdot \Delta E$. Further details of the calculations are given below :-

Hauser-Feshbach (H F) formula has been employed to calculate the population of states (E', I', π') resulting from the first equilibrium evaporation step. For particle

emission the (H F) formula / 8 / reads :-

$$\frac{\partial \sigma^{HF}_{x_0 x_1}}{\partial E'} (E', I', \Pi') \Delta E' = \frac{\pi}{k^2} \sum_{I \Pi} g_I \frac{\sum_{s_0 l_0} T_{x_0 l_0} \cdot}{N (E, I, \Pi)}$$

$$\cdot (\mathcal{E}_0) \frac{\sum_{s_1 l_1} T_{x_1 l_1} (\mathcal{E}_1)}{} \times$$

$$\times \sum_{x_0 l_0 s_0 ; x_1 l_1 s_1}^{I \Pi} (\mathcal{E}_0, \mathcal{E}_1) \rho_{x_1} (E', I', \Pi') \Delta E'$$

... ... (4.6)

and for the emission of γ-rays Hauser-Feshbach formula is given as :-

$$\frac{\partial \sigma^{H F}_{x_0 \gamma}}{\partial E'} (E', I', \Pi') \Delta E' = \frac{\pi}{k^2} \sum_{I \Pi} g_I \frac{\sum_{s_0 l_0} T_{x_0 l_0} (\mathcal{E}_0) \cdot}{}$$

$$\frac{\sum_{XL} T_{\gamma XL} (\mathcal{E}_\gamma)}{N (E, I, \Pi)} \times$$

$$\times \rho_\gamma (E', I', \Pi') \Delta E' \ldots (4.7)$$

Where the symbols have the following meanings :-

k	= the wave number of relative motion	for the entrance channel
$\mathcal{E}_0$	= energy of the relative motion	
l_0	= orbital angular momentum of relative motion	
s_0	= channel spin	
$T_{x_0 l_0} (\mathcal{E}_0)$	= transmission co-efficient	

g_I = statistical factor

E = excitation energy of the compound nucleus

$N(E, I, \Pi)$ = Hauser-Feshbach denominator.

$\mathcal{E}_1$ = energy of the relative motion.
l_1 = orbital angular momentum of relative motion
s_1 = channel spin
$T_{x_1 l_1}(\mathcal{E}_1)$ = transmission co-efficient
$\rho_{x_1}(E', I', \Pi')$ = level density of the residual nucleus

} for outgoing particle channels.

$W^{I\Pi}_{x_0 l_0 s_0, x_1 l_1 s_1}(\mathcal{E}_0, \mathcal{E}_1)$ = width fluctuation correction factor

$\mathcal{E}_\gamma$ = energy.
X L = multipole type.
$T_{\gamma XL}(\mathcal{E}_\gamma)$ = transmission co-efficient.
$\rho_\gamma(E', I', \Pi')$ = level density of the residual nucleus.

} for outgoing photon channels.

It may be noted that the summations in equs. (4.6) and (4.7) are restricted by angular momentum and parity conservation laws. The Hauser-Feshbach denominator N (E, I, Π) is the sum of the transmission co-efficients for all open channels consistent with angular momentum and parity selection rules and is given by :-

$$N(E, I, \Pi) = \sum_r \sum_{I'\Pi'} \sum_{s\,l} \int_0^{E - B_r} d\mathcal{E}_r \, T_{rl}(\mathcal{E}_r) \, \rho_r(E - B_r - \mathcal{E}_r, I', \Pi') + \sum_{I'\Pi'} \sum_{XL} \int_0^E d\mathcal{E}_\gamma \, T_{\gamma XL}(\mathcal{E}_\gamma) \, \rho_\gamma(E - \mathcal{E}_\gamma, I', \Pi') \quad \ldots\ldots\ (4.8)$$

Here 'B_r' is the seperation energy of the particle ' r '. In the present version of the programme upto four particles (n, p, α and d) can contribute to the Hauser-Feshbach denominator. Width fluctuation correction has been applied to take into account the probability distribution of the particle width. This correction factor has been calculated according to the following formula given by Moldauer / 9 /:-

$$\int_{x_0 l_0 s_0,\, x_1 l_1 s_1}^{I\,\Pi}(\varepsilon_0, \varepsilon_1) = \int_0^{\infty} dt \frac{\exp\left[-\frac{\Gamma_\gamma(E, I, \Pi)}{\Gamma(E, I, \Pi)} t\right]}{\left(1+\frac{2t\ T_{x_0 l_0}(\varepsilon_0)}{r_{x_0 l_0 s_0}\ N(E, I, \Pi)}\right)} \times$$

$$\times \frac{1}{\left(1+\frac{2t\ T_{x_1 l_1}(\varepsilon_1)}{r_{x_1 l_1 s_1}\ N(E, I, \Pi)}\right)} \times$$

$$\times \frac{1}{\prod_{r'' l'' s''}\left(1+\frac{2t\ T_{r'' l''}(\varepsilon'')}{r_{r'' l'' s''}\ N(E, I, \Pi)}\right)^{\frac{r_{r'' l'' s''}}{2}}} \times$$

$$\times \left(1+2\frac{\delta_{x_0 l_0 s_0\ ;\ x_1 l_1 s_1}}{\nu_{x_0 l_0 s_0}}\right) \quad \ldots (4.9)$$

The expression $\frac{\Gamma_\gamma(E, I, \Pi)}{\Gamma(E, I, \Pi)}$ represents the ratio of the total radiation width to the average total decay width and is given by :-

$$\frac{\Gamma_\gamma(E, I, \Pi)}{\Gamma(E, I, \Pi)} = \frac{1}{N(E, I, \Pi)} \sum_{I'\ \Pi'} \sum_{XL} \cdot$$

$$\cdot \int_0^E d\varepsilon_\gamma\, T_{\gamma XL}(\varepsilon_\gamma)\ \rho_\gamma(E - \varepsilon_\gamma, I', \Pi')$$

$$\ldots\ \ldots\ (4.10$$

The effect of the γ-ray cascades starting from the state (E, I, Π) of a given compound nucleus with an initial population $W_B^{(0)}$ (E, I, Π) ΔE has been treated in the following way :-

The population of levels (E', I', Π') reached by the emission of γ-rays from levels (E, I, Π) depends on the branching ratio of the partial decay width Γ_γ(E, I, Π ; E', I', Π') to the total decay width Γ(E, I, Π). This branching ratio is given as :

$$\frac{\Gamma_\gamma(E, I, \Pi ; E', I' \Pi')}{\Gamma(E, I, \Pi)} = \frac{1}{N(E, I, \Pi)} \times \times \sum_{XL} T_{\gamma XL}(E - E') \quad \ldots (4.11)$$

The population $W_B^{(n)}$ (E', I', Π') ΔE' of levels (E', I', Π') by n successive gamma transitions can be obtained by the following recursion relation :

$$W_B^{(n)}(E', I', \Pi')\Delta E' = \sum_{I\Pi} \int_{E'}^{E_{max}} dE\, W_B^{(n-1)}(E, I, \Pi) \times \times \frac{\Gamma_\gamma(E, I, \Pi ; E', I', \Pi')}{(E, I, \Pi)} \times \times \rho_\gamma(E', I', \Pi')\Delta E' \quad \ldots (4.12)$$

Where E_{max} is the maximum energy upto which the given compound nucleus has been populated. Then the cumulative population $\overline{W_B}$ (E', I', Π') Δ E' resulting from all γ-ray possible cascades can be given by :-

$$\overline{W_B}(E', I', \Pi')\Delta E' = \sum_{n=0}^{\infty} W_B^{(n)}(E', I', \Pi')\Delta E' \quad \ldots (4.13)$$

Thus finally using equs. (4.12) and (4.13) one gets :-

$$\overline{WB}\,(E', I', \Pi')\,\Delta E' = WB^{(0)}\,(E', I', \Pi')\,\Delta E' + \sum_{I\Pi}\int_{E'}^{E_{max}} dE\ \overline{WB}\,(E, I, \Pi) \times \frac{\Gamma_\gamma(E, I, \Pi; E', I', \Pi')}{\Gamma(E, I, \Pi)} \times \rho_\gamma(E', I', \Pi')\,\Delta E' \quad \ldots\ (4.14)$$

The emission of the ith particle from the ith compound nucleus with population $\overline{WB}_i\,(E, I, \Pi)\,\Delta E$ leads to a population $WB_{i+1}\,(E', I', \Pi')\,\Delta E'$ of the $(i+1)$th compound nucleus :

$$WB_{i+1}\,(E', I', \Pi')\,\Delta E' = \sum_{I\Pi}\int_{E'+B_{x_i}}^{E_{max}} dE\ \overline{WB}_i\,(E, I, \Pi) \times \frac{\Gamma_{x_i}(E, I, \Pi; E', I', \Pi')}{\Gamma_i(E, I, \Pi)} \times \rho_{x_i}(E', I', \Pi')\,\Delta E' \quad \ldots\ (4.15)$$

The branching ratio $\frac{\Gamma_{x_i}}{\Gamma_i}$ for the emission of particle x_i is given by :

$$\frac{\Gamma_{x_i}(E, I, \Pi; E', I', \Pi')}{\Gamma_i(E, I, \Pi)} = \frac{1}{N_i(E, I, \Pi)} \times \sum_{l_i s_i} T_{x_i l_i}(E - E' - B_{x_i}) \quad \ldots\ (4.16)$$

In the calculations with Hauser-Feshbach formula nuclear level densities $\rho(E, I, \Pi)$ are required. At low

excitation energy, where the experimental information on the quantum numbers E_i I_i and Π_i of the discrete levels is complete, the level density formula is given as :-

$$\rho(E, I, \Pi) = \sum_i \delta(E - E_i)\delta_{II_i}\delta_{\Pi\Pi_i} \quad \ldots (4.17)$$

At higher excitation energy , where the number of levels per MeV are rather large, $\rho(E, I, \Pi)$ has to be calculated by means of a suitable model. In the present code it is calculated within the frame work of the " back-shifted " Fermi gas model / 10 /. The level density is assumed to be independent of parity. For the energy and spin dependence of the level density, the expressions by Lang / 11 / have been used :-

$$\rho(E, I, \Pi) = \tfrac{1}{2}\rho(E, I)$$

$$\rho(E, I) = w(E, M = I) - w(E, M = I + 1)$$

$$w(E, M) = \frac{\exp\left[2\left\{a\left(E - \Delta - \hbar^2 M^2 / 2\Theta_{eff}\right)\right\}^{1/2}\right]}{12\sqrt{\frac{2\Theta_{eff}}{\hbar^2}}\left[E - \Delta - \hbar^2 M^2/2\Theta_{eff} + 3/2\ t\right]^{3/2}}$$

$$E = at^2 - 3/2\ t + \frac{\hbar^2 M^2}{2\Theta_{eff}}$$

$$\ldots\ldots (4.18)$$

The parameters for the model are the level density parameter ' a ', the effective moment of inertia 'Θ_{eff}' and fictive ground state position 'Δ'. These parameters have been taken from the work of Dilg et al. / 12 /.

The equilibration of the composite system formed by projectile 'x_0' and target ' T ' has been treated in the frame

work of the " Hybrid model " / 13 / . From a simple initial configuration the composite system is assumed to equilibrate through a series of two-body interactions. During this particles are emitted from all intermediate states. The intermediate states of the system are classified according to the number ' n ' of excitons or more specifically to the numbers ' p' and ' h ' of the excited particle and hole degrees of freedom (n = p + h). No distinction is made between neutrons and protons. The application of a two-body interaction to states of a (p , h) - configuration leads to states with (p + 1, h + 1) , (p, h) or (p - 1, h - 1) excited particles and holes. In competition with these internal transitions, particles can be emitted from each state. For all these processes transition rates averaged over all states of a configuration are employed .

If $b^{(k)}(n) = b^{(k)}(p, h)$ be the population probability of the states of a (p, h)-configuration resulting from ' k ' internal transitions, then the corresponding quantity $b^{(k+1)}(n)$ for (k + 1) internal transitions can be written as / 7 / :

$$b^{(k+1)}(n) = b^{(k)}(n+2)\frac{\lambda_-(n+2)}{\lambda(n+2)} + b^{(k)}(n)\frac{\lambda_0(n)}{\lambda(n)} + b^{(k)}(n-2)\frac{\lambda_+(n-2)}{\lambda(n-2)}$$

Where

$$\lambda(n) = \lambda_-(n) + \lambda_0(n) + \lambda_+(n) + \lambda^{\bullet}(n)$$

$$\lambda^{\bullet}(n) = \sum_r \int d\varepsilon_r \, \lambda_r^{\bullet}(n, \varepsilon_r)$$

.. .. .. (4. 19)

In this equation (4.19) $\lambda_+(n)$, $\lambda_0(n)$ and $\lambda_-(n)$ are the

average rates for internal transitions with a change of the exciton number by an amount of + 2, 0 and - 2 respectively, and $\lambda_r^e (n , \varepsilon_r) d\varepsilon_r$ is the average rate for emission of particle ' r ' with energy of relative motion ε_r. The quantity $\lambda^e (n)$, therefore, represents the total rate for emission of particles. Successive application of equation (4.19) gives the populations of the various (p, h)-configurations with an arbitrary number ' k ' of internal transitions. On increasing ' k ' the ratio $\frac{b^{(k-1)}(n)}{b^{(k)}(n)}$ becomes independent of 'n' and 'k'. Thus an upper limit 'K' for the number of internal transitions to be considered for pre-equilibrium decay is obtained from the following conditions-

$$\left| b^{(k-1)}(n) / b^{(k)}(n) - Q^{(k)} \right| < 0.01\, Q^{(k)} \quad \text{for all n and } k \geq K$$

$$Q^{(k)} = \left(\sum_n b^{(k-1)}(n) \right) / \left(\sum_n b^{(k)}(n) \right) \qquad \ldots\ldots\ldots (4.20)$$

The pre-equilibrium contribution $\frac{\partial \sigma^{pre}_{x_0 x_1}}{\partial \varepsilon_1} d\varepsilon_1$ to the differential cross-section is given by :-

$$\frac{\partial \sigma^{pre}_{x_0 x_1}}{\partial \varepsilon_1} d\varepsilon_1 = \sigma^{non}_{x_0} \sum_{k=0}^{K} \sum_n b^{(k)}(n) \times \frac{\lambda^e_{x_1}(n, \varepsilon_1)}{\lambda(n)} d\varepsilon_1 \quad \ldots (4.21)$$

Where $\sigma^{non}_{x_0}$ represents the optical model absorption cross-section for the projectile ' x_0 ' . The fraction q^{pre} of the

initial population surviving pre-equilibrium emission is given by :-

$$q^{pre} = 1 - \sum_{k=0}^{K} \sum_{n} b^{(k)}(n) \frac{\lambda^{(e)}(n)}{\lambda(n)} \quad .. (4.22)$$

The average rates $\lambda_+(n)$, $\lambda_0(n)$ and $\lambda_-(n)$ are related to the absolute square of the average effective matrix element $|\overline{M}|^2$ of residual interactions by the formulas of Williams / 14 / , corrected for the Pauli-principle by Cline / 15 / :-

$$\lambda_+(n) \equiv \lambda_+(p, h, E) = \frac{2\pi}{\hbar}|\overline{M}|^2 \frac{g(gE - C_{p+1,h+1})^2}{p+h+1}$$

$$\lambda_0(n) \equiv \lambda_0(p, h, E) = \frac{2\pi}{\hbar}|\overline{M}|^2 g(gE - C_{p,h})(p+h-1)$$

$$\lambda_-(n) \equiv \lambda_-(p, h, E) = \frac{2\pi}{\hbar}|\overline{M}|^2 gph(p+h-2)$$

$$C_{p,h} = \tfrac{1}{2}(p^2 + h^2) \quad .. .. (4.23)$$

Where E is the excitation energy of the composite system and 'g' the single particle state density. For the dependence of $|\overline{M}|^2$ on mass number 'A' and excitation energy 'E' the following expression is used / 16 / :-

$$|\overline{M}|^2 = FM \cdot A^{-3} \cdot E^{-1} \quad .. .. .. (4.24)$$

Where FM is a constant in MeV^3 units. The emission rates $\lambda_r^e(n, \varepsilon_r)$ for particle emission are given by the following equation / 3, 17 / :-

$$\lambda_r^e(n, \varepsilon_r)\, d\varepsilon_r \equiv \lambda_r^e(p, h, E, \varepsilon_r)\, d\varepsilon_r$$

$$\lambda_r^e(n, \varepsilon_r)\, d\varepsilon_r = \frac{2 S_r + 1}{\pi^2 \hbar^3} \mu_r \varepsilon_r \sigma_r(\varepsilon_r) \times \left\{\frac{Z}{A}\right\}^{Z_r} \cdot \left\{1 - \frac{Z}{A}\right\}^{P_r - Z_r} \times \left\{\begin{matrix} P_r \\ Z_r \end{matrix}\right\} \frac{w(p - p_r, h, E - B_r - \varepsilon_r)}{w(p, h, E)} d\varepsilon_r \quad \ldots\ldots \quad (4.25)$$

Where

S_r = spin
P_r = number of nucleons
Z_r = number of protons
B_r = seperation energy

} of particle 'r'

μ_r = reduced mass
ε_r = energy of relative motion
$\sigma_r(\varepsilon_r)$ = inverse cross-section

} in the exit channel

Z = charge number of the composite system

$w(p,h,E)$ = density of the states with excitation energy E, particles 'p' and holes 'h'.

The density $w(p, h, E)$ is given by / 14 / :-

$$w(p, h, E) = \frac{g\,(gE - A_{p,h})^{p+h-1}}{p!\;h!\;(p+h-1)!}$$

$$A_{p,h} = \frac{\lambda}{4}\,(p^2 + h^2 + p - 3h)$$

.. .. .. (4. 26)

The single particle state density 'g' has been obtained from the level density parameter 'a' by the relation :-

$$g = \frac{6}{\pi^2}\,a \qquad .. \;\; .. \;\; .. \qquad (4.27)$$

For the primary population by the first evaporation step, both the equilibrium and pre-equilbirium emission of particles have been taken into account. Pre-compound emission of particles causes a reduction of the population that reaches the equilibrium stage. Therefore, as far as γ -rays are concerned, the only effect of the pre-equilibrium particle emission is a loss of cross-section, accounted for by the factor q^{pre} :-

$$WB_1\,(E, I, \Pi)\,\Delta E = q^{pre} \cdot \frac{\partial \sigma^{HF}_{n\gamma}}{\partial E}\,(E, I, \Pi)\,\Delta E$$

.. .. (4.28)

While for particles a pre-equilibrium contribution has to be added to the reduced equilibrium portion. Hence, if the first step of an evaporation cascade populates levels (E, I, Π) in an interval ΔE around excitation energy 'E' the cross-section is given by :-

$$\frac{\partial \sigma_1}{\partial E}\,(E, I, \Pi)\,\Delta E = WB_2\,(E, I, \Pi)\,\Delta E \quad .... \quad (4.29)$$

Where

$$WB_2(E,I,\Pi)\,\Delta E = \left[q^{pre} \frac{\partial \sigma^{HF}_{x_0 x_1}(E,I,\Pi)}{\partial E} + \frac{\partial \sigma^{pre}_{x_0 x_1}}{\partial E} \times \frac{\frac{\partial \sigma^{HF}_{x_0 x_1}(E,I,\Pi)}{\partial E}}{\sum_{I'\Pi'} \frac{\partial \sigma^{HF}_{x_0 x_1}(E,I',\Pi')}{\partial E}} \right] \Delta E \quad \ldots (4.30)$$

The Hauser-Feshbach cross-section $\frac{\partial \sigma^{HF}}{\partial E}$ is given by equn. (4.6) and (4.7) and the pre-equilibrium cross-section $\frac{\partial \sigma^{pre}}{\partial E}$ by equ. (4.21). Since the pre-equilibrium model does not consider angular momentum and parity, it has been assumed in equ. (4.30) that the population $\frac{\partial \sigma^{pre}_{x_0 x_1}(E)}{\partial E} \Delta E$ is distributed among the levels with different spin and parity in the same proportion as the equilibrium contribution.

In order to perform the above described calculations additional information regarding the transmission co-efficients is required as the input data. Transmission co-efficients have been calculated by another computer code OPTIM / 18 / based on optical model.

The calculations have been performed at the DEC-VAX 11/780 computer of this University.

References

/ 1/ A.C. Douglas and N. Mac Donald, Nucl.Phys. 13(1959) 382.

/ 2/ J.J. Griffin, Phys. Lett. 17 (1966) 478.

/ 3/ C.K. Cline and M. Blann, Nucl. Phys. A172 (1971) 225.

/ 4/ M. Blann, Nucl Phys. 80 (1966) 223.

/ 5/ C.L. Dunford, AI -ABC-12931 (1970).

/ 6/ M. Uhl , Nucl. Phys. A184 (1972) 253.

/ 7/ M. Uhl and B. Strohmeier , Private communication.

/ 8/ W. Hauser and H. Feshbach , Phys. Rev. 87 (1952) 366.

/ 9/ P.A. Moldauer , Revs. of Mod. Phys. 36 (1964) 1079.

/10/ H.K. Vonach and M. Hille , Nucl. Phys. A127 (1969) 289.

/11/ D.W. Lang, Nucl. Phys. 77 (1966) 545.

/12/ W. Dilg, W. Schantl, H. Vonach and M. Uhl , Nucl. Phys. A217 (1973) 269.

/13/ M. Blann and A. Mignerey , Nucl. Phys. A186 (1972) 245.

/14/ F.C. Williams Jr. , Phys. Lett. 31B (1970) 184.

/15/ C.K. Cline, Nucl. Phys. A195 (1972) 353.

/16/ C.K. Cline, Nucl. Phys. A210 (1973) 590.

/17/ C.K. Cline, Nucl. Phys. A193 (1972) 273.

/18/ H.K. Vonach, Private communication.

"**********"

CHAPTER V

R E S U L T S AND D I S C U S S I O N S

(5.1) Measured and Calculated (n,p) Reaction Cross-Sections at 14.8 MeV -

The (n,p) reaction cross-sections for 19 nuclei ranging from A = 24 to A = 197 have been measured using activation technique at incident neutron energy of 14.8 ± 0.5 MeV. The investigated (n,p) reactions, their Q - values and the measured cross-sections are given in table-1. For each reaction the available literature values /1-77/ of cross-sections are also listed in column IV of table-1. Most of the reported measurements have been done by the activation technique. In cases where several measurements have been reported, our cross-section values, in general, agree with the more recent precise data. The litrature values showing largest deviation are mostly the results of earlier measurements.

Inspite of the simplicity of measuring activation cross-sections, there are considerable disagreements between published data as can be seen from table -1. In most cases the difference between the data relating to the same nuclei considerably exceeds the errors given in references. As can be seen, the spread is significant in the recent data too. The possible causes of these discrepancies may be :

Interferring reactions caused by impurities in the samples; half life data; abundance of the radiation detected; converting counting into disintegration rate; efficiency of the separation technique; absolute neutron flux and its variation in time; energy and energy spread of neutrons; cross-section of monitor reaction; escape of residual nuclei by

TABLE - 1

Results of the (n, p) Reaction Cross-Section Measurements :

Reaction	Q-Value (a) (MeV)	Cross - Section (mb)		
		Present work	Literature Values	
			σ (n,p)	ref.
I	II	III	IV	V
$^{24}Mg(n,p)^{24}Na$	-4.74	180 ± 20	132 ± 15	/ 1/
			191 ± 40	/17/
			210 ± 26	/19/
			110 ± 16	/18/
			180	/20/
$^{25}Mg(n,p)^{25}Na$	-3.023	45 ± 8	54 ± 10	/ 1/
			63 ± 10	/18/
			60 ± 10	/21/
			45 ± 10	/17/
			40 ± 4	/25/
			59 ± 6	/27-28/
$^{27}Al(n,p)^{27}Mg$	-1.798	76 ± 12	38 ± 5	/ 1/
			132 ± 10	/11/
			86 ± 8	/22/
			53 ± 5	/ 9/
			52 ± 10	/17/
			76 ± 11	/18/
			97 ± 10	/24/
			75 ± 7	/31-34,49, 50 /
$^{34}S(n,p)^{34}P$	-4.31	75 ± 8	32 ± 6	/ 1/
			85 ± 40	/17/
			73 ± 7	/25/
			32 ± 8	/28/

Table - I (contd..)

Reaction	Q-Value (a) (MeV)	Cross- Section (mb)		
		Present work	Literature Values σ (n,p)	ref.
I	II	III	IV	V
^{37}Cl (n,p) ^{37}S	-4.087	28 ± 5	42 ± 4	/ 1/
			39.8 ± 10	/11/
			25 ± 2	/36/
			33 ± 7	/17/
			21.3 ± 3	/24/
			41 ± 4	/16/
			39	/20/
^{41}K (n,p) ^{41}Ar	-1.74	53 ± 4	52 ± 4	/ 1/
			88 ± 18	/11/
			81 ± 32	/17/
			48 ± 10	/13,51 /
^{48}Ti (n,p) ^{48}Sc	-3.19	60 ± 5	70 ± 6	/ 1/
			53 ± 6	/ 3/
			55 ± 11	/ 4/
			80 ± 4	/ 5/
			61 ± 6	/6,53,54/
			93 ± 33	/17/
			57 ± 8	/ 7/
			63 ± 4	/ 8/
			58 ± 8	/ 9/
			55 ± 11	/10/

contd...

Table - 1 (contd..)

Reaction	Q-Value (MeV) (a)	Cross - section (mb)		
		Present work	Literature Values σ (n,p)	ref.
I	II	III	IV	V
^{49}Ti (n,p) ^{49}Sc	-1.23	40 ± 7	48 ± 8	/ 1/
			23 ± 5	/ 3/
			29 ± 5	/ 9/
			97 ± 16	/11/
			35 ± 3	/ 8/
			29 ± 8	/18/
			39 ± 6	/ 6/
^{50}Ti (n,p) ^{50}Sc	-5.65	20 ± 5	25 ± 6	/ 1/
			12 ± 2	/ 3/
			17.9± 2	/ 8/
			15 ± 7	/12/
			9 ± 3	/ 4/
			147 ± 13	/11/
			28 ± 12	/13/
			27 ± 6	/ 9/
			24 ± 5	/6, 23/
^{51}V (n,p) ^{51}Ti	-1.68	38 ± 4	37 ± 4	/ 1/
			33 ± 3	/ 3/
			35 ± 1.6	/ 5/
			27 ± 4	/17/
			20 ± 7	/18/
			55 ± 12	/13/
			25 ± 3	/16/
			25 ± 2	/24/
			36 ± 3	/6,26,49/

- contd...

Table - 1 (contd..)

Reaction	Q-Value (a) (MeV)	Cross - section (mb)		
		Present work	Literature Values σ (n,p)	ref.
I	II	III	IV	V
^{52}Cr (n,p) ^{52}V	-3.19	88 ± 6	73 ± 5	/ 1/
			80 ± 6	/ 3/
			115 ± 15	/14/
			105 ± 11	/15/
			78 ± 11	/17/
			118 ± 16	/16/
			83 ± 6	/24/
			125 ± 15	/29/
			74 ± 10	/18/
			94 ± 10	/30/
			95 ± 10	/57-59/
^{56}Fe (n,p) ^{56}Mn	-2.92	100 ± 6	98 ± 7	/ 3/
			72 - 144	/35/
			90 ± 18	/36/
			82 ± 7	/18/
			109 ± 10	/44/
			103 ± 6	/31,60-67/
^{65}Cu (n,p) ^{65}Ni	-1.35	21 ± 2	18 ± 2	/ 1/
			25 - 29	/35/
			27 ± 23	/ 3/
			30 ± 6	/38/
			31 ± 13	/36/
			27 ± 11	/ 9/

- contd....

Table - 1 (contd..)

Reaction	Q-Value (a) (MeV)	Cross - Section (mb) Present work	Literature Values σ(n,p)	ref.
I	II	III	IV	V
^{65}Cu (n,p) ^{65}Ni			19 ± 4	/37/
			17 ± 4	/39/
			11 ± 1	/40/
			23 ± 3	/13, 15, 31, 68-71/
^{64}Zn (n,p) ^{64}Cu	+0.21	171 ± 13	205 ± 15	/ 1/
			160 ± 12	/ 3/
			154 - 284	/35/
			210 ± 20	/52/
			257 ± 51	/38/
			179 ± 18	/18/
			284 ± 20	/41/
			386 ± 60	/17/
			171 ± 18	/19/
			170 ± 15	/70, 72, 74-75 /
^{66}Zn (n,p) ^{66}Cu	-1.94	74 ± 6	62 ± 5	/ 1/
			72 ± 8	/ 3/
			60 - 78	/35/
			65 ± 6	/52/
			77 ± 10	/41/
			101 ± 17	/17/
			35 ± 4	/18/
			60 ± 6	/42/
			70 ± 7	/2, 70/

- contd....

Table - 1 (cont^d...)

Reaction	Q-Value (MeV) (a)	Cross - Section (mb)		
		Present work	Literature Values	
			σ (n,p)	ref
I	II	III	IV	V
^{75}As (n,n)^{75}Ge	-0.42	35 ± 3	42 ± 4	/ 1/
			29 ± 2.5	/ 3/
			12 - 35	/35/
			27 ± 5	/18/
			19 ± 2	/55/
			12 ± 2	/17/
			19 ± 3	/25,76/
			14.5 ± 1.3	/77/
^{88}Sr (n,p)^{88}Rb	-4.41	15 ± 2	9 ± 1	/ 1/
			13.5 ± 1.5	/ 3/
			30 ± 2	/56/
			16 ± 2	/73/
			20 ± 2	/33/
			13 ± 1	/55/
			18 ± 4	/17/
			≃ 17	/20/
^{109}Ag (n,p)^{109}Pd	-0.369	14 ± 2	7 ± 1	/ 1/
			12.5 ± 2	/46/
			10.5 ± 2	/47/
			15 ± 2	/6,15,76/
^{197}Au (n,p)^{197}Pt	+0.026	2 ± 1	2.4 ± 0.1	/75/

(a) Calculated from the binding energies given in ref. /78/.

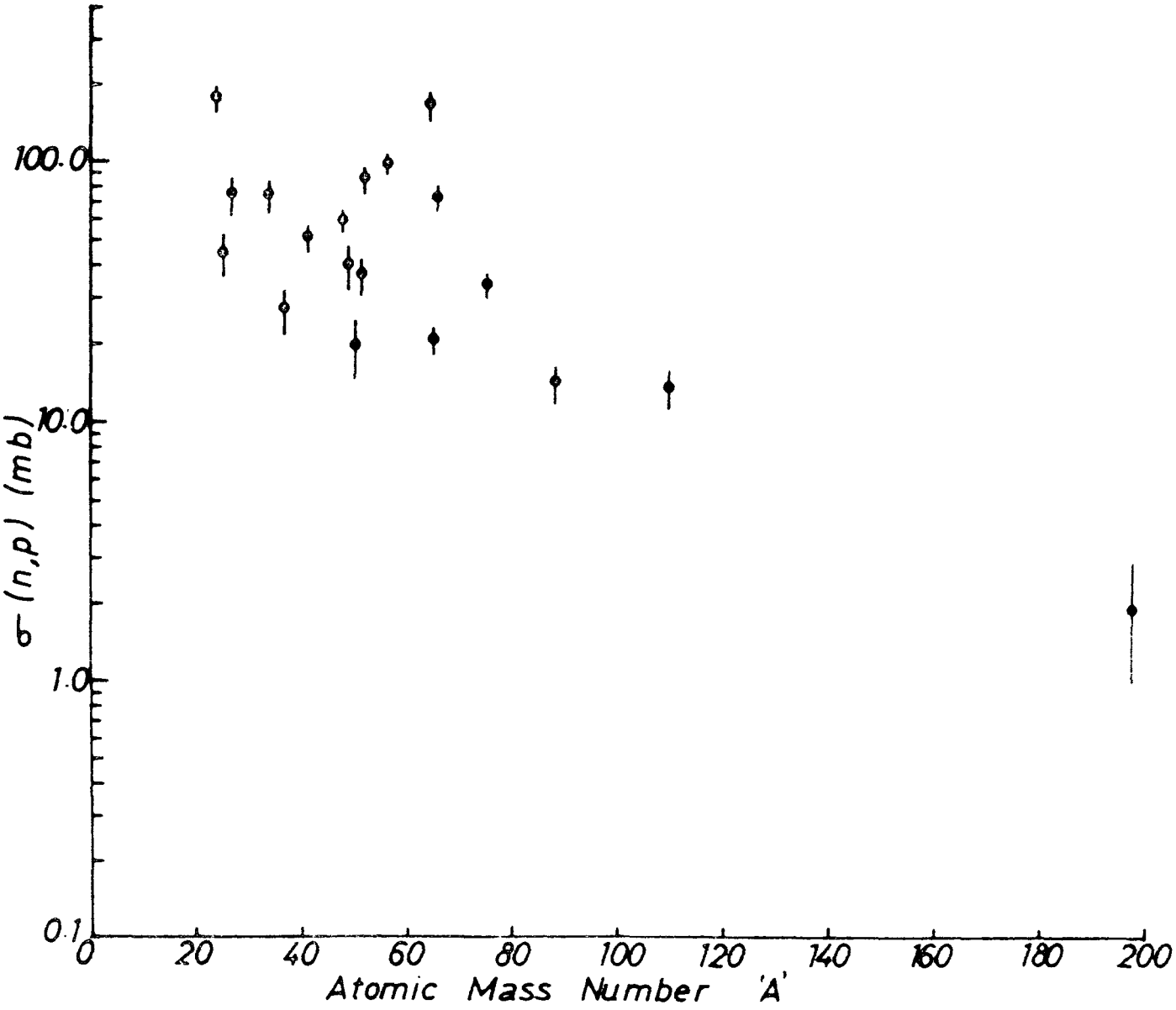

Fig 5.1 Measured cross-sections for (n,p) reactions Vs atomic mass number of the target nucleus

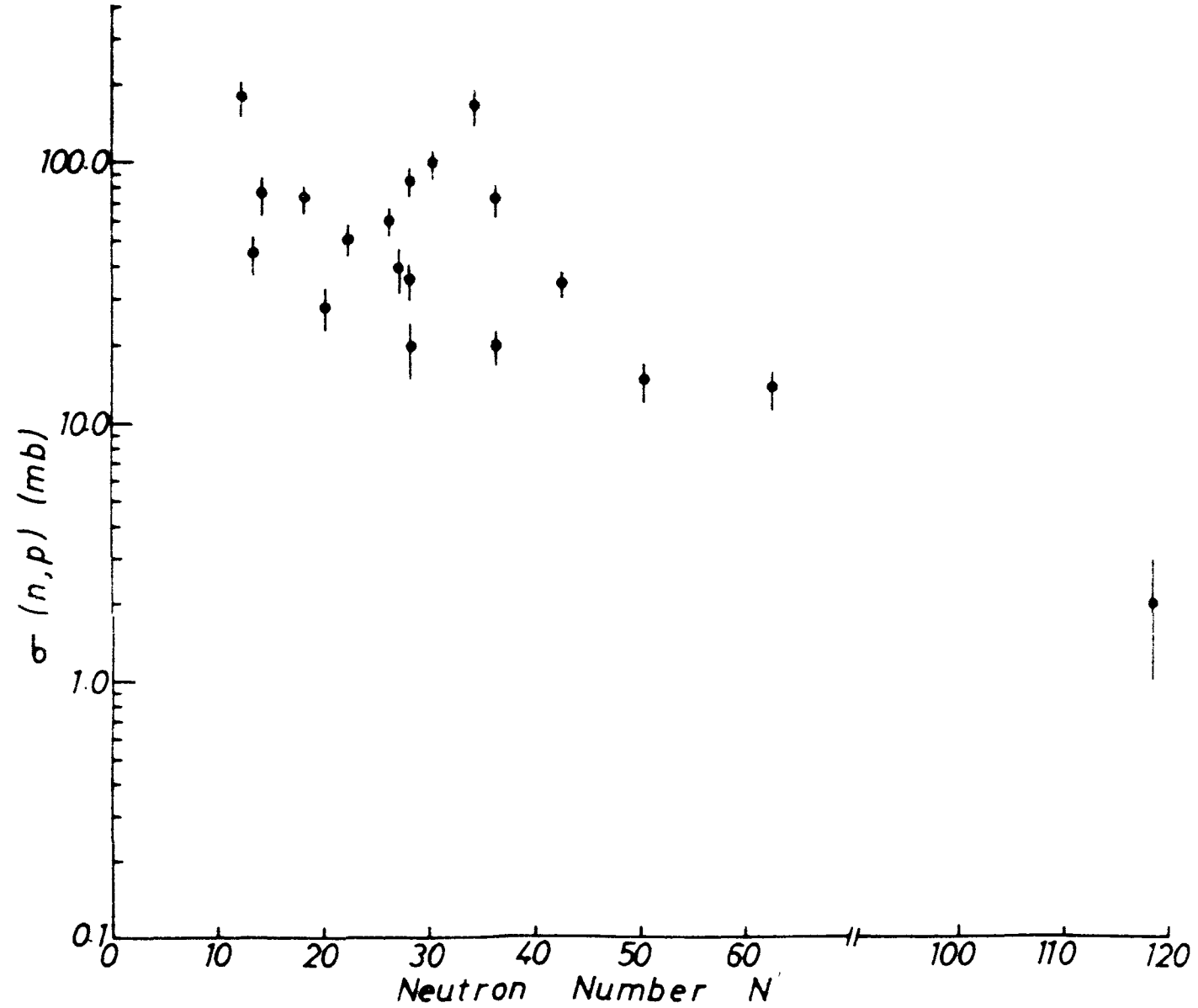

Fig. 5.2 Measured cross-sections for (n,p) reactions Vs neutron number of the target nucleus.

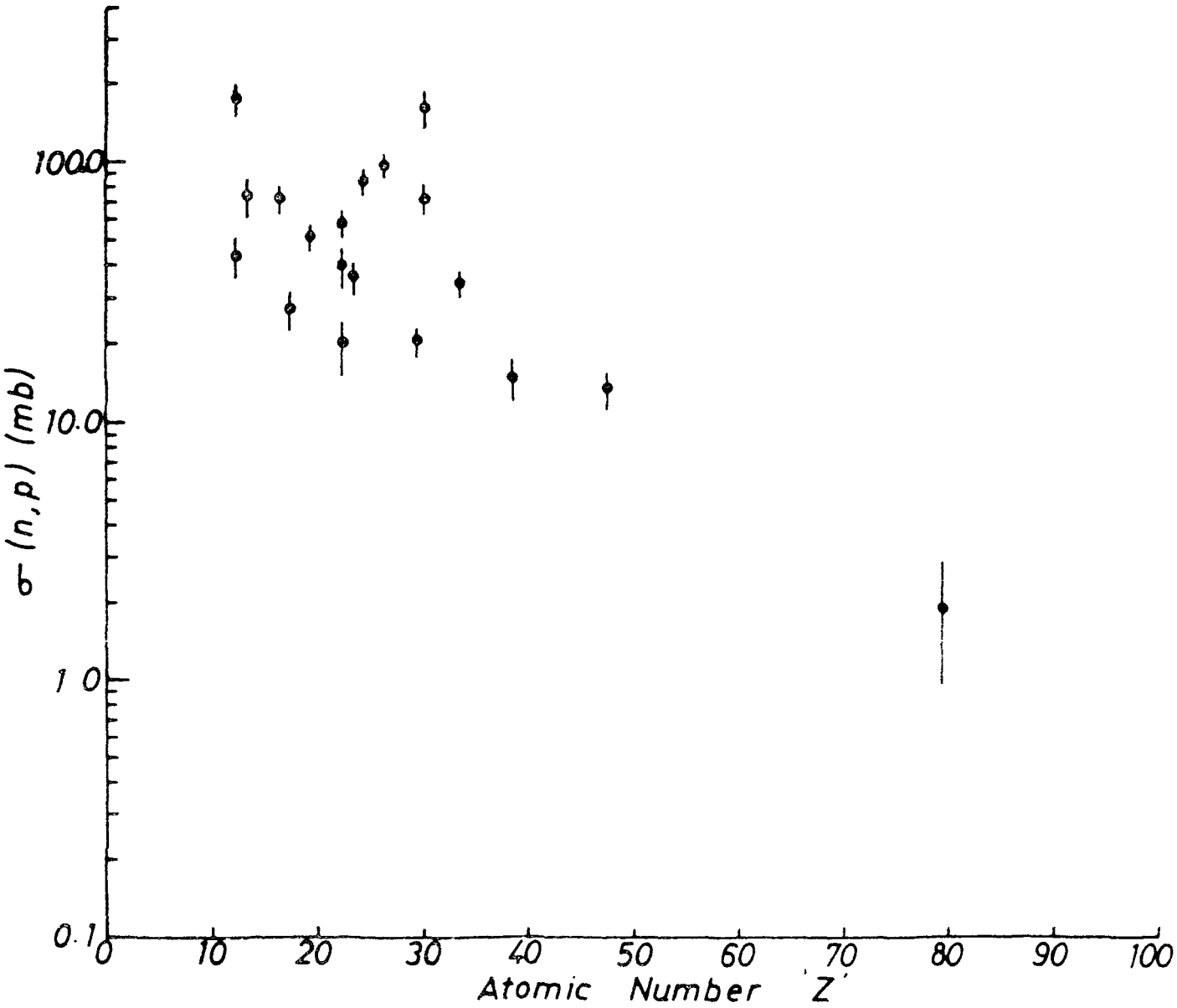

Fig. 5.3 Measured cross-sections for (n,p) reactions Vs the atomic number of the target nucleus

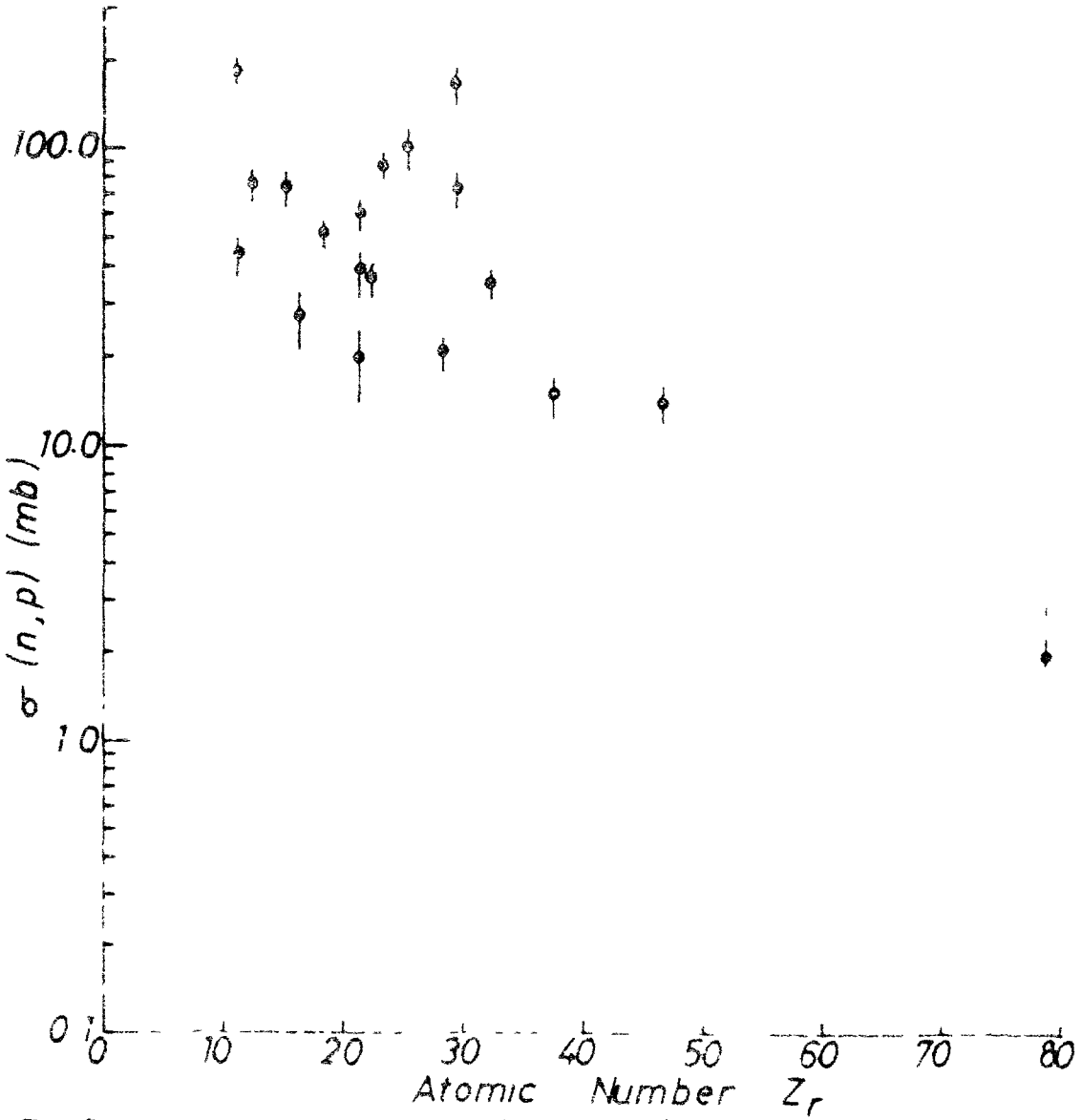

Fig 5.4 Measured cross-sections for (n,p) reactions vs the atomic number of the residual nucleus

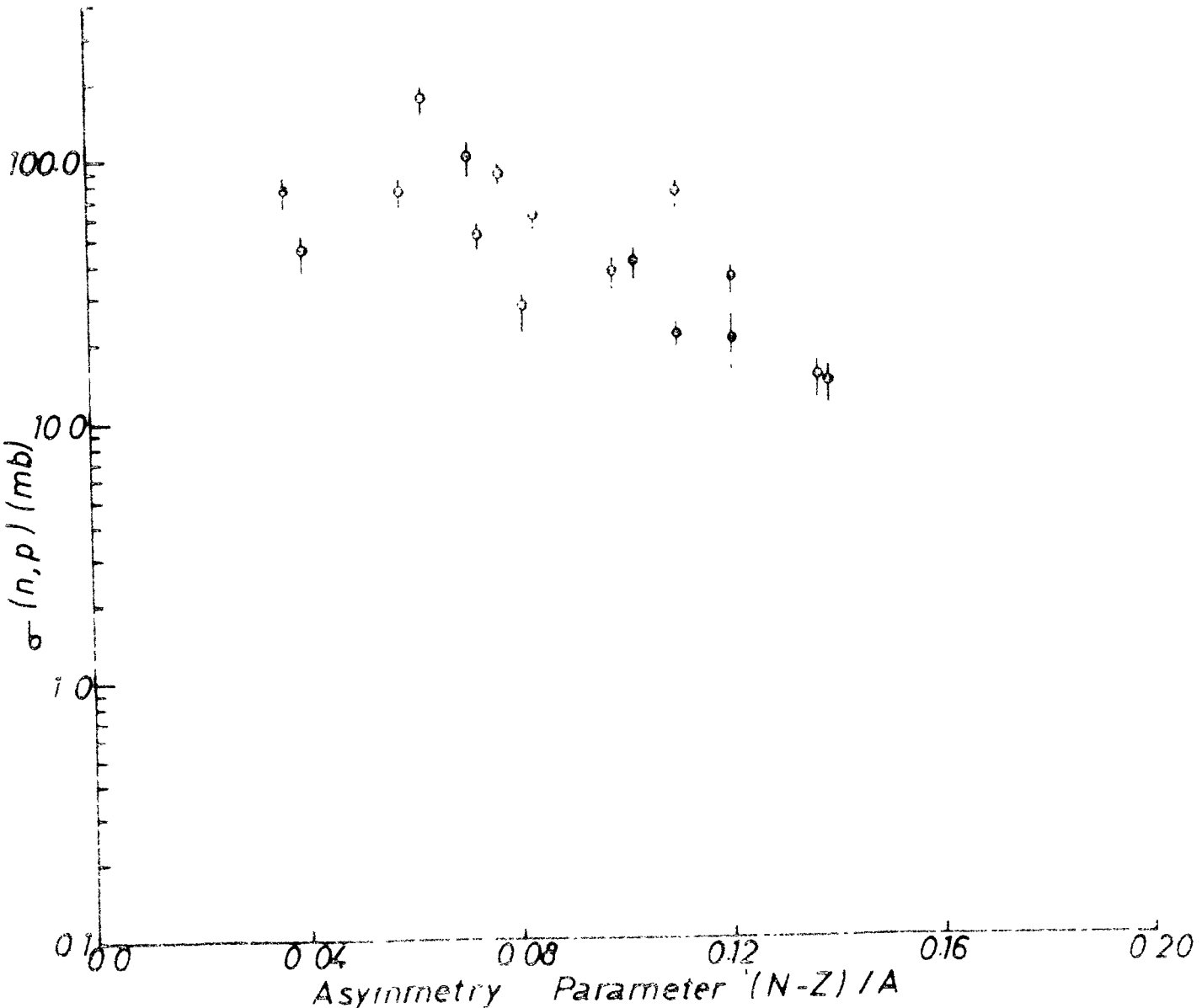

Fig 5 5 Systematics of (n,p) reaction cross-sections induced by 14 8 MeV neutrons

nuclear recoil or diffusion. In the present measurements care has been taken to minimise some of them (Chapter-II).

The measured activation cross-sections at 14.8± 0.5 MeV have been plotted against the atomic mass number 'A' of the target nucleus in figure (5.1). The general trend of the monotonic decrease in the (n,p) cross-section values can be seen from figure (5.1). This decrease of the σ(n,p) exhibits the effect of the Coulomb barrier, which increases with the Z-value of the target nucleus. The increasing Coulomb barrier reduces the probability of the proton emission and hence decreases the cross-section for (n, p) reactions. The (n, p) reaction cross-sections are also plotted against the neutron number 'N' of the target nucleus in figure (5.2). It may be observed that for the cases of magic neutron numbers i.e. ^{37}Cl (N=20), ^{50}Ti (N=28) & ^{88}Sr (N=50) the cross-section values are in general lower than the cross-section values for the neighbouring nuclei.

Measured (n, p) cross-section values are plotted against the proton number 'Z' and 'Zr' of the target and residual nuclei in figures (5.3 and 5.4) respectively. It can be seen from these figures that in general σ(n,p) decreases with 'Z' and 'Zr' for heavier elements, but in lower mass region there is no such definite variation.

Figure (5.5) shows a plot of cross-section data against the asymmetry parameter (N-Z)/A. Evidently, the data for the nuclei with very small asymmetry parameter (N-Z)/A (upto $\simeq$0.08) do not show any correlation, however, for medium and heavy mass nuclei, on the other hand, the (n, p) cross section decreases as a function of (N-Z)/A.

It appears to us, atleast quantitatively, that the proton binding energy for the target nucleus plays an important role. In general the proton binding energy decreases with the increase in the charge, mass and (N-Z)/A of different isotopes. Solely from the point of view of these studies, the (n, p) cross section should increase for the heavier elements with the increase of (N-Z)/A which is contrary to the trend seen in figure (5.5). It may be due to the following two reasons :-

(i) The Coulomb barrier increases with increasing charge of the target nucleus, retarding the probability of the proton emission.

(ii) Competition of neutron evaporation with proton emission, which increases with the increase of the neutron excess i.e. (N-Z)/A. Thus the decrease of the proton binding energy with (N-Z)/A in heavier elements is more than compensated by the increasing Coulomb barrier and the competition of neutron evaporation. As a net result σ(n, p) decreases with (N-Z)/A.

On the other hand for the different isotopes of the same element, the proton binding energy increases as a function of (N-Z)/A as may be seen from table-2. We have measured cross sections for the different isotopes of three elements ($^{24, 25, 26}$Mg, $^{48, 49, 50}$Ti and $^{64, 66}$Zn). The experimental (n, p) cross section in each case decreases with the increasing proton binding energy of the heavier isotopes.

Table - 2

Isotopes	Proton Binding energy (MeV)	σ(n,p) measured (mb)
^{24}Mg	2. 27	180 ± 20
^{25}Mg	6. 3	45 ± 8
^{48}Ti	6. 75	60 ± 5
^{49}Ti	7. 94	40 ± 7
^{50}Ti	8. 05	20 ± 5
^{64}Zn	3. 94	171 ± 13
^{66}Zn	5. 27	74 ± 6

Allen / 18 / indicated strong shell effects in systematics of (n, p) cross-sections at 14 MeV neutron energy. In a plot of experimental total (n,p) cross-section Vs the Z-value of the target nucleus, peaks at the magic proton numbers were observed indicating the shell dependence of the (n, p) cross-section. We, on the other hand, have not observed similar peaks at the closed proton shells. However, in the present measurements there are some indications that σ(n, p) decreases at closed neutron shells as can be seen from figure (5.2). Gardner and Rosenblum/82/ have sub-divided the shell effects into two :-

(1) The " True shell effect ", arising from the significant variation in a pertinent nuclear reaction parameter, such as level density or pairing energy around closed shells in the

daughter nucleus, from a general trend or average value.

(ii) The " Target effect ", the classical effect of closed shell on the abundance and beta stability of the target nuclei. The values of level density parameters 'a' and 'Δ' for residual nuclei of the (n, p) reactions in the targets : ^{34}S, ^{37}Cl, ^{41}K, ^{49}Ti, ^{50}Ti, ^{51}V, ^{75}As, ^{88}Sr and ^{109}Ag are given in table - 3, also given in this table are the Q-value for the (n, p) reactions.

Table - 3

Target Nucleus	Residual nucleus	Q-Value (MeV)	'a' (MeV^{-1})	'Δ' (MeV)
^{34}S	^{34}P	- 4.31	8. 35	-1.35
^{37}Cl (N=20)	^{37}S	- 4.087	8. 60	-0.10
^{41}K	^{41}Ar	- 1.74	5. 48	-0.49
^{49}Ti	^{49}Sc	- 1.23	6. 20	-2.35
^{50}Ti (N=28)	^{50}Sc	- 5.65	6. 10	-2.40
^{51}V	^{51}Ti	- 1.68	6. 82	+1.55
^{75}As	^{75}Ge	- 0.41	9. 14	-1.22
^{88}Sr (N=50)	^{88}Rb	- 4.41	9. 0	+0.88
^{109}Ag	^{109}Pd	- 0.369	15. 15	-0.52

It can be seen from table - 3 that for the magic neutron targets, (n, p) reaction Q- Values are unusually small (large -ve values) as compared to the other neighbouring nuclei. On the other hand the 'a' and 'Δ' values in the

residual nuclei do not show such an abrupt variation. Thus it may be concluded that the observed dip in σ(n,p) at magic neutron nucleus is purely Q-value effect. The (n, p) cross-sections for the cases presently measured have also been calculated theoretically using two options, (a) pure compound reaction mechanism (denoted by σcal. CN) and (b) with the Hybrid model of pre-equilibrium emission (denoted by σ cal. CN + Pre).

The pure compound calculations have been performed according to the statistical model of Hauser and Feshbach / 83 /. To perform the statistical model calculations, the transmission co-efficients, level density parameters and the discrete level information valid for each of the reaction studied are required. Transmission co-efficients for neutron, proton and alpha particles have been calculated using a computer code OPTIM / 84 / with the optical model parameters given by Bechetti & Greenlees / 85 /, Huizenga/86/ and from the Atomic and Nuclear data tables / 87 - 90 /. In few cases the optical model parameters for the nucleus of interest were not available in the literature. In such cases the values of these parameters have been taken equal to the values given for the nearest nucleus in the literature/85-90/. The parameters for the calculation of level density have been taken from the work of Dilg et al. / 91 /. The discrete level information has been taken from the table of isotopes compiled by Lederer and Shirley / 92 / and the separation energies have been taken from the work of the Wapstra / 93 /.

For the pre-equilibrium emission the Hybrid model / 94-95 /option has been chosen. Pre-equilibrium emission has been considered only in the first emission step where the excitation energy is sufficiently large. In these calculations

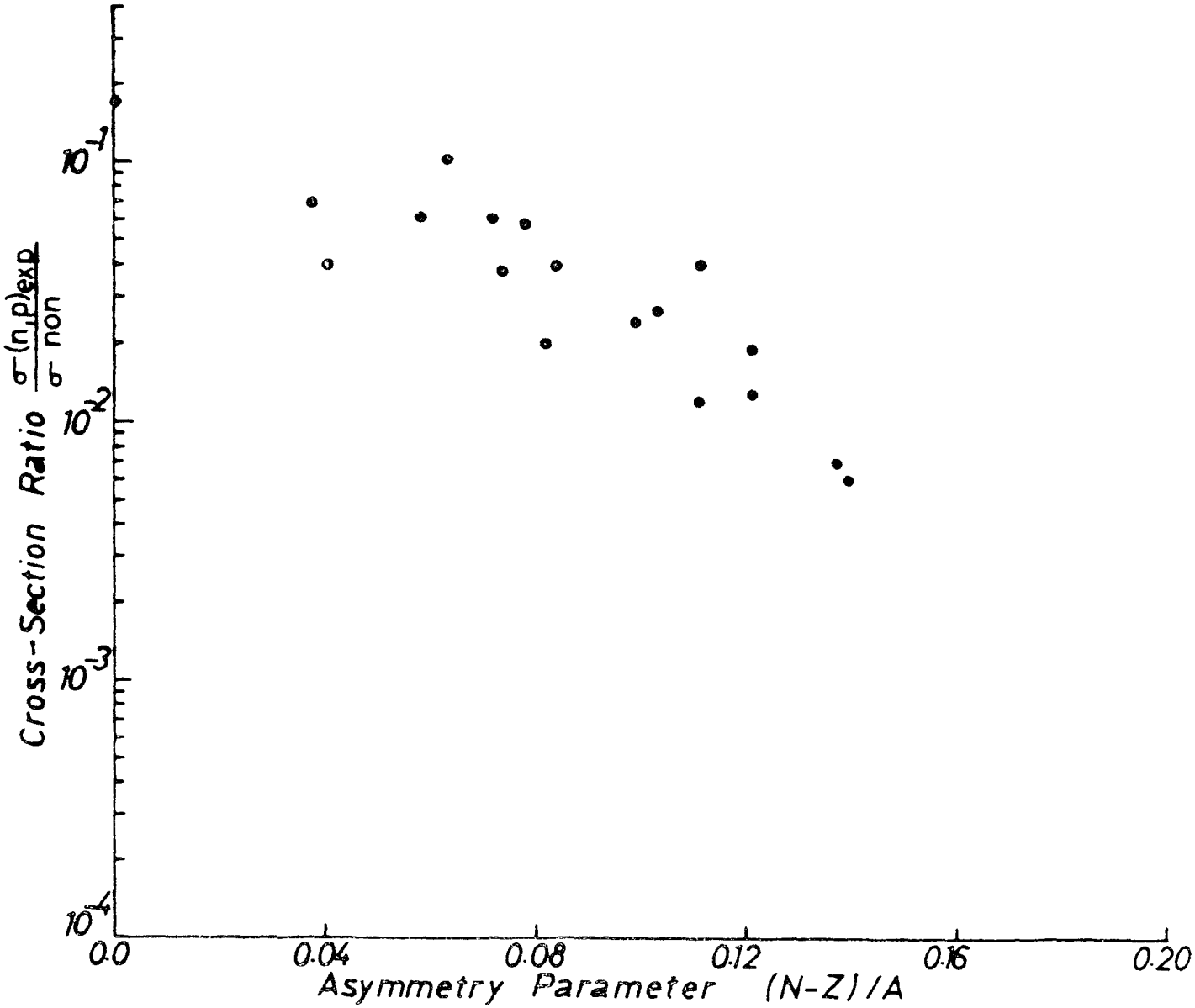

Fig. 5.6 Trend in the contribution of (n,p) reaction cross-section to the non-elastic cross-section of the target nucleus at 14.8 MeV

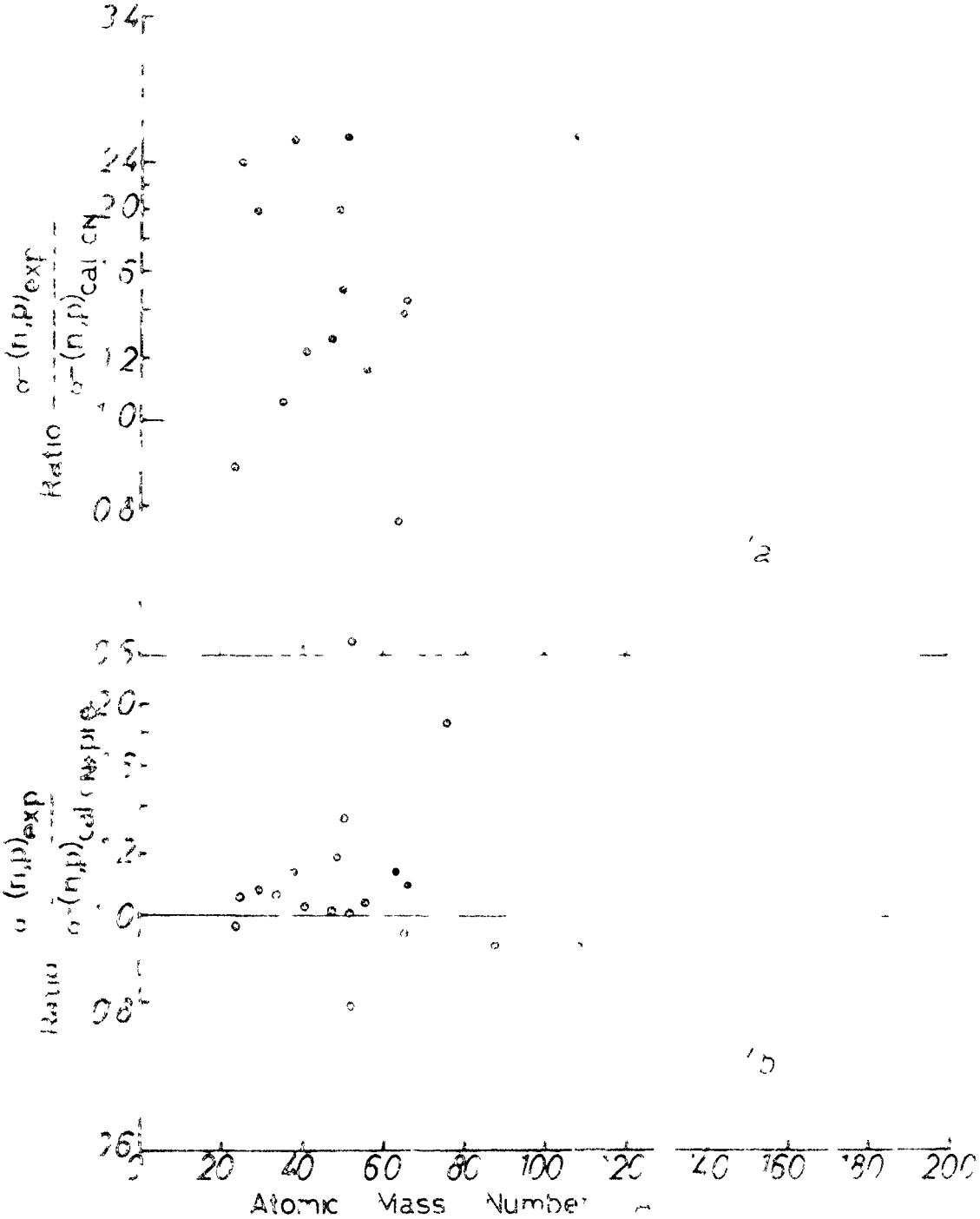

Fig 5.7 Comparison between experimental and calculated (n,p) reaction cross-sections vs atomic mass number of the target nucleus at 14.8 MeV (a) Calculations based on equilibrium statistical theory only (b) Calculations include pre-equilibrium emission

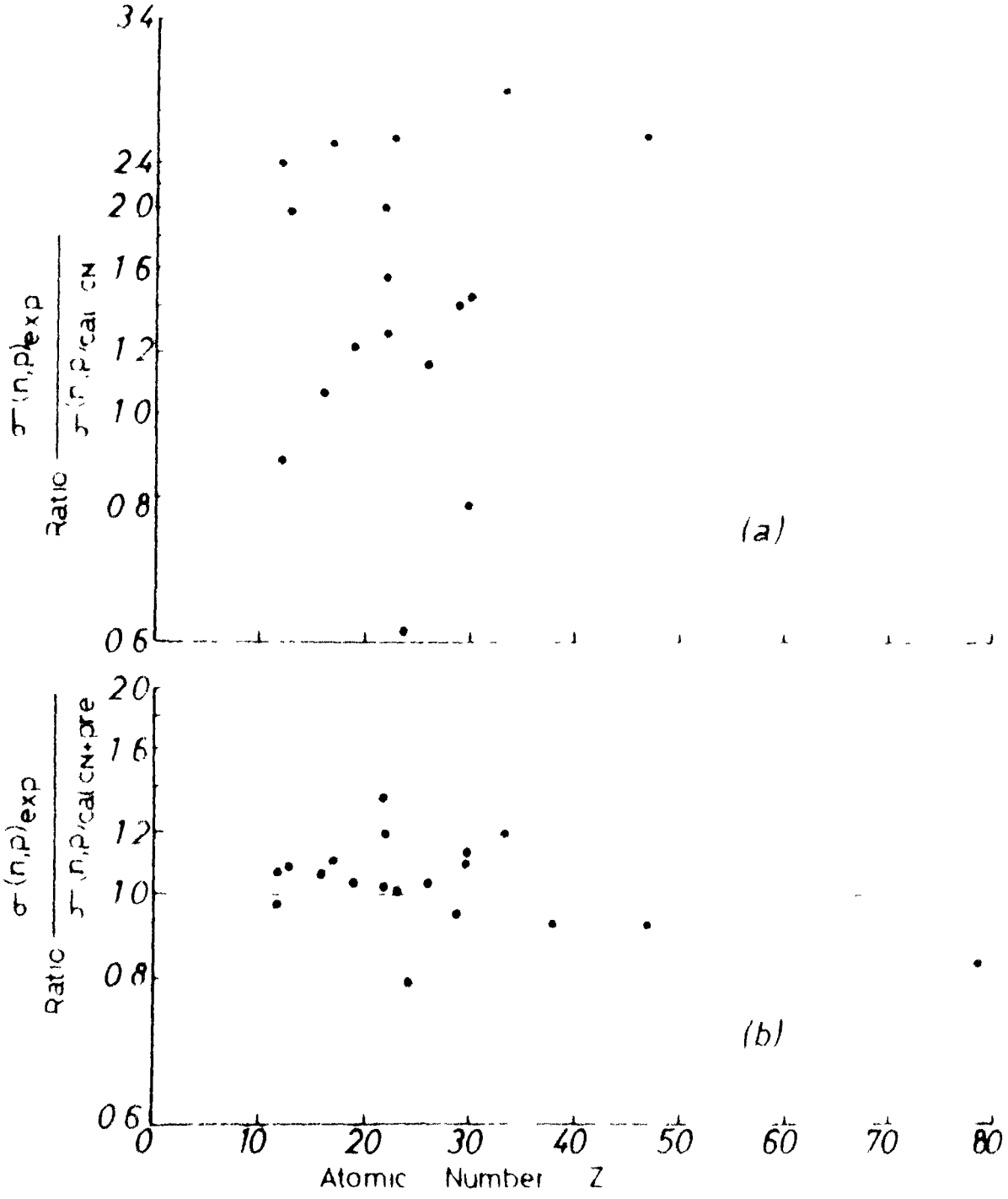

Fig 5.8 Comparison between experimental and calculated (n,p) reaction cross-sections vs atomic number of target nucleus at 14.8 MeV. (a) Calculations based on equilibrium statistical theory only. (b) Calculations include pre equilibrium emission

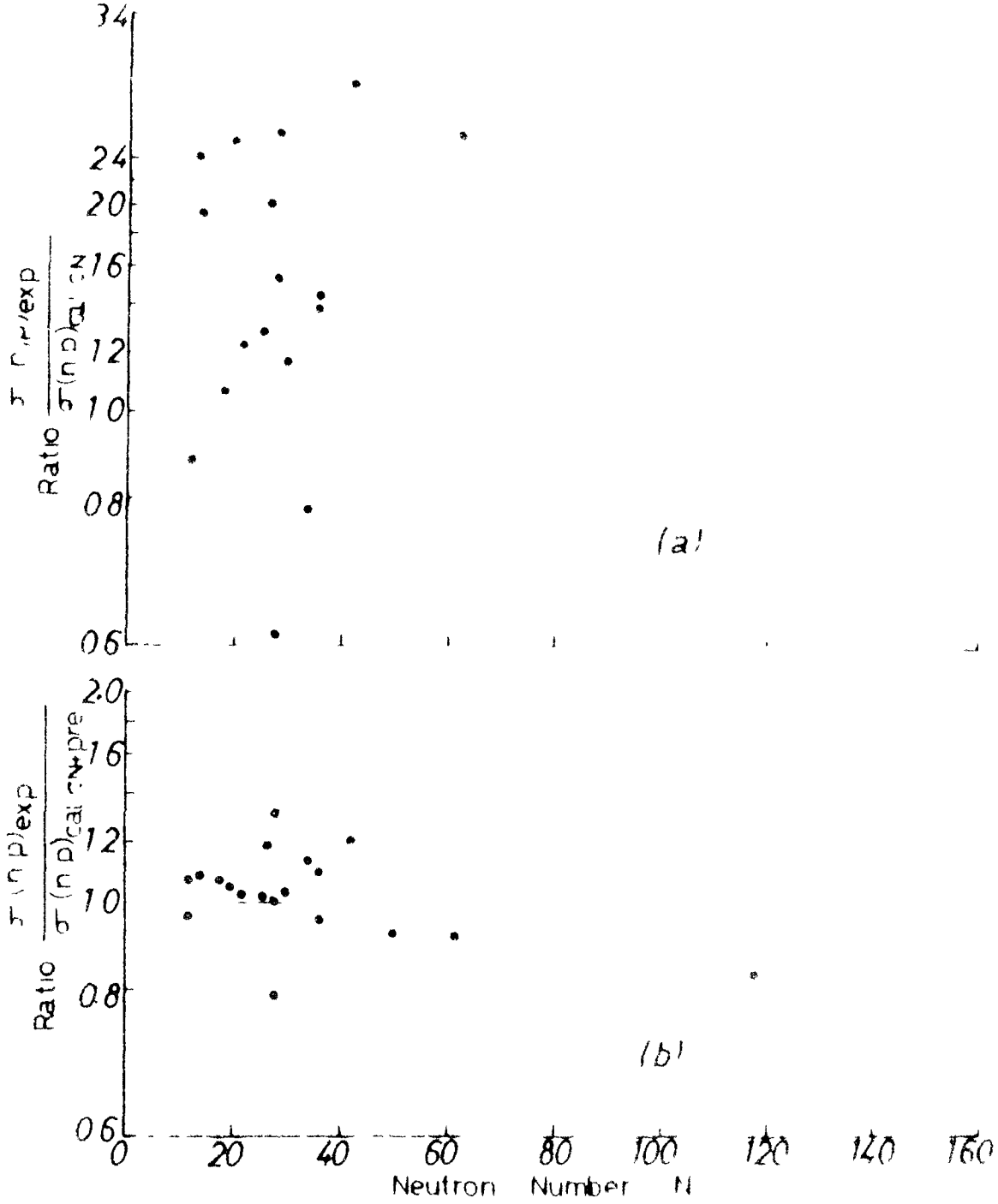

Fig. 5.9 Comparison between experimental and calculated (n,p) reaction cross-sections vs neutron number of target nucleus at 14.8 MeV (a) Calculations based on pre-equilibrium statistical theory only (b) Calculations including pre-equilibrium emission

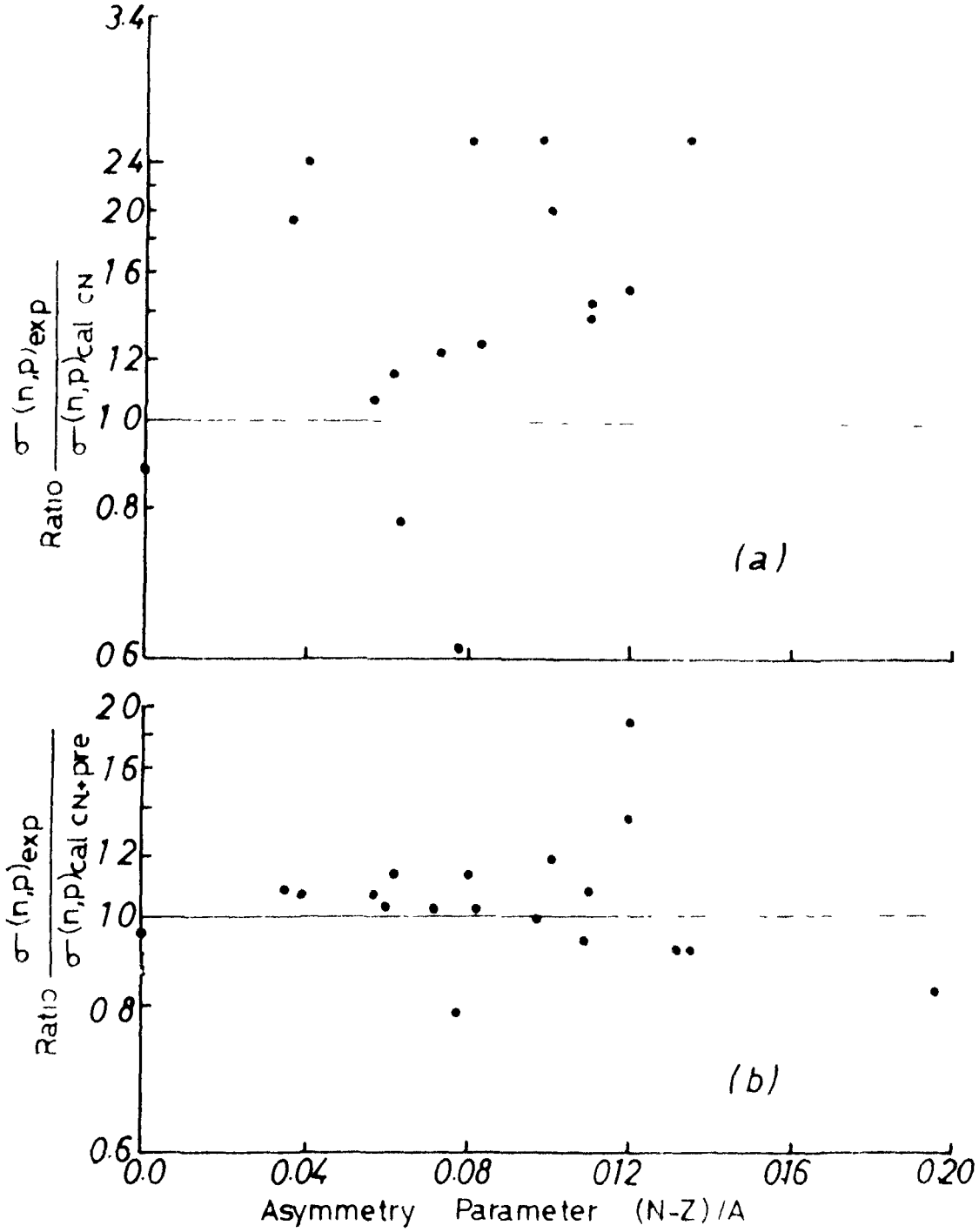

Fig 5.10 Comparison between experimental and calculated (n,p) reaction cross-sections vs asymmetry parameter of the target nucleus (a) Calculations based on equilibrium statistical theory only (b) Calculations include the pre-equilibrium emission E_N=14.8 MeV

conservation of the parity and angular momentum have explicitly been taken into account at each step of de-excitation.

In order to see the relative contribution of the (n, p) reaction to the total $\sigma_{non.}$ at 14.8 MeV, the ratio $\frac{\sigma(n,p)_{exp}}{\sigma_{non.}}$ for the measured cases has been plotted in fig. (5.6) against the asymmetry parameter (N - Z)/ A. The $\sigma_{non.}$ values at 14.8 MeV energy have been calculated with the optical model. It is evident from fig. (5.6) that in the lighter mass region the (n, p) reaction contributes significantly but the relative contribution does not exceed 10 % of the non-elastic cross-section. The contribution of the (n, p) reaction decreases constantly with increasing (N - Z)/ A so that for the heaviest mass nuclei ratio $\frac{\sigma(n,p)_{exp}}{\sigma_{non.}}$ is well below 1 %.

The ratios $\frac{\sigma(n,p)_{exp}}{\sigma_{cal.\ C\ N}}$ and $\frac{\sigma(n,p)_{exp}}{\sigma_{cal.CN+pre}}$ have been listed in table -4 and are plotted against atomic mass number 'A', atomic number 'Z' , neutron number 'N' and asymmetry parameter '(N-Z)/A' (figs. 5.7 to 5. 10). It is interesting to see from these figures, except for the cases of ^{24}Mg, ^{52}Cr and ^{64}Zn, measured cross-sections are higher than their values calculated without consideration of pre-equilibrium emission (upper part of the figs. 5.7 to 5. 10). The higher values of the ratio $\frac{\sigma(n,p)_{exp}}{\sigma_{cal.\ C\ N}}$ suggests the presence of some reaction mechanism, apart from the compound nucleus process, through which the emission of proton is

Table -4

Observed and Calculated Values of the (n, p) Reaction Cross-Section at 14.8 MeV.

Target Nucleus	Residual Nucleus	σ (n,p) exp. (mb)	Ratio $\frac{\sigma(n,p)_{exp.}}{\sigma_{non.}}$	σ cal.CN (mb)	Ratio $\frac{\sigma(n,p)_{exp.}}{\sigma_{cal.CN}}$	cal.CN +Pre (mb)	Ratio $\frac{\sigma(n,p)_{exp.}}{\sigma_{cal.CN+P}}$
$^{24}_{12}Mg$	$^{24}_{11}Na$	190 ± 20	0.17	205.0	0.93	180.0	0.95
$^{25}_{12}Mg$	$^{25}_{11}Na$	45 ± 8	0.04	18.7	2.41	42.6	1.07
$^{27}_{13}Al$	$^{27}_{12}Mg$	76 ± 12	0.07	39.3	1.96	70.0	1.08
$^{34}_{16}S$	$^{34}_{15}P$	75 ± 8	0.06	70.5	1.06	70.5	1.06
$^{37}_{17}Cl$	$^{37}_{16}S$	26 ± 5	0.02	11.4	2.45	24.4	1.15
$^{41}_{19}K$	$^{41}_{18}Ar$	53 ± 4	0.04	42.0	1.26	51.0	1.03

Table - 4 (contd..)

Target Nucleus	Residual Nucleus	σ (n,p) exp. (mb)	Ratio $\frac{\sigma (n,p)_{exp.}}{\sigma_{non.}}$	$\sigma_{cal.CN}$ (mb)	Ratio $\frac{\sigma (n,p)_{exp.}}{\sigma_{cal.CN}}$	$\sigma_{cal.CN+Pre}$ (mb)	Ratio $\frac{\sigma (n,p)_{exp.}}{\sigma_{cal.CN+Pre}}$
$^{48}_{22}Ti$	$^{48}_{21}Sc$	60 ± 5	0. 04	47. 0	1. 28	59. 0	1. 02
$^{49}_{22}Ti$	$^{49}_{21}Sc$	40 ± 7	0. 03	19. 5	2. 05	33. 5	1. 19
$^{50}_{22}Ti$	$^{50}_{21}Sc$	20 ± 5	0. 013	13. 0	1. 54	15. 0	1. 33
$^{51}_{23}V$	$^{51}_{22}Ti$	38 ± 4	0. 024	14. 5	2. 63	37. 0	1. 02
$^{52}_{24}Cr$	$^{52}_{23}V$	88 ± 6	0. 06	144. 0	0. 61	112. 0	0. 79
$^{56}_{26}Fe$	$^{56}_{25}Mn$	100 ± 6	0. 06	86. 0	1. 16	97. 0	1. 03
$^{65}_{29}Cu$	$^{65}_{28}Ni$	21 ± 2	0. 012	15. 0	1. 4	22. 2	0. 95

- contd...

Table - 4 (contd ..)

Target Nucleus	Residual Nucleus	σ(n,p)$_{exp.}$ (mb)	Ratio $\frac{\sigma(n,p)_{exp.}}{\sigma_{non.}}$	$\sigma_{cal.CN}$ (mb)	Ratio $\frac{\sigma(n,p)_{exp.}}{\sigma_{cal.CN}}$	$\sigma_{cal.CN+Pre}$ (mb)	Ratio $\frac{\sigma(n,p)_{exp.}}{\sigma_{cal.CN+Pre}}$
$^{64}_{30}Zn$	$^{64}_{29}Cu$	171 ± 13	0.102	220. 2	0. 78	151. 0	1. 13
$^{66}_{30}Zn$	$^{66}_{29}Cu$	74 ± 6	0.04	51. 0	1. 45	68. 0	1. 09
$^{75}_{33}As$	$^{75}_{32}Ge$	35 ± 3	0.02	12. 2	2. 86	29. 0	1. 20
$^{88}_{38}Sr$	$^{88}_{37}Rb$	15 ± 2	0.007	1. 1	13. 63	16. 3	0. 92
$^{109}_{47}Ag$	$^{109}_{46}Pd$	14 ± 2	0.006	5. 5	2. 54	15. 3	0. 92
$^{197}_{79}Au$	$^{197}_{78}Pt$	2 ± 1	0.0007	2.5×10^{-4}	8×10^{3}	2.4	0. 83

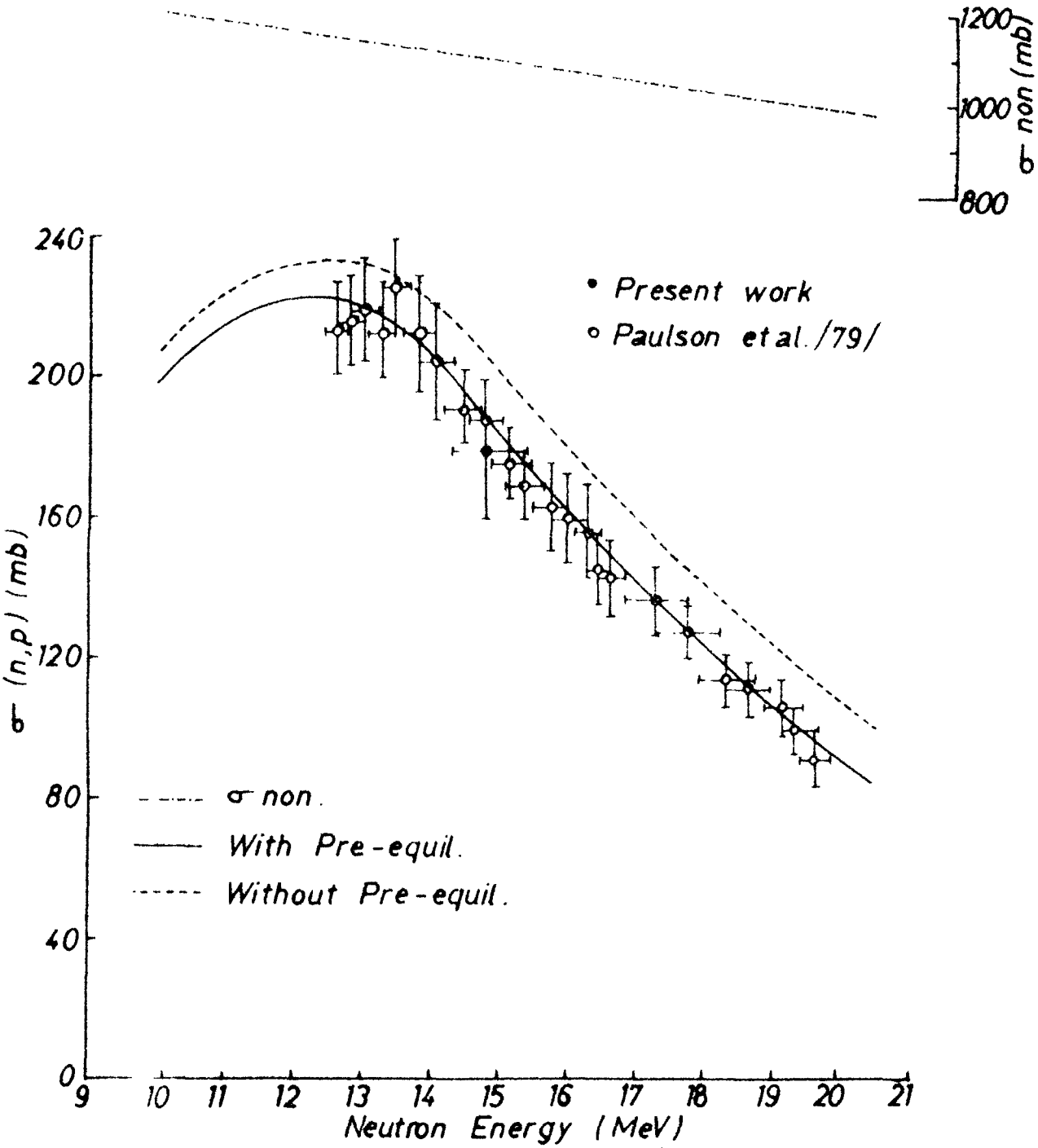

Fig 5.11 Experimental and calculated excitation functions for $^{24}Mg(n,p)^{24}Na$ reaction

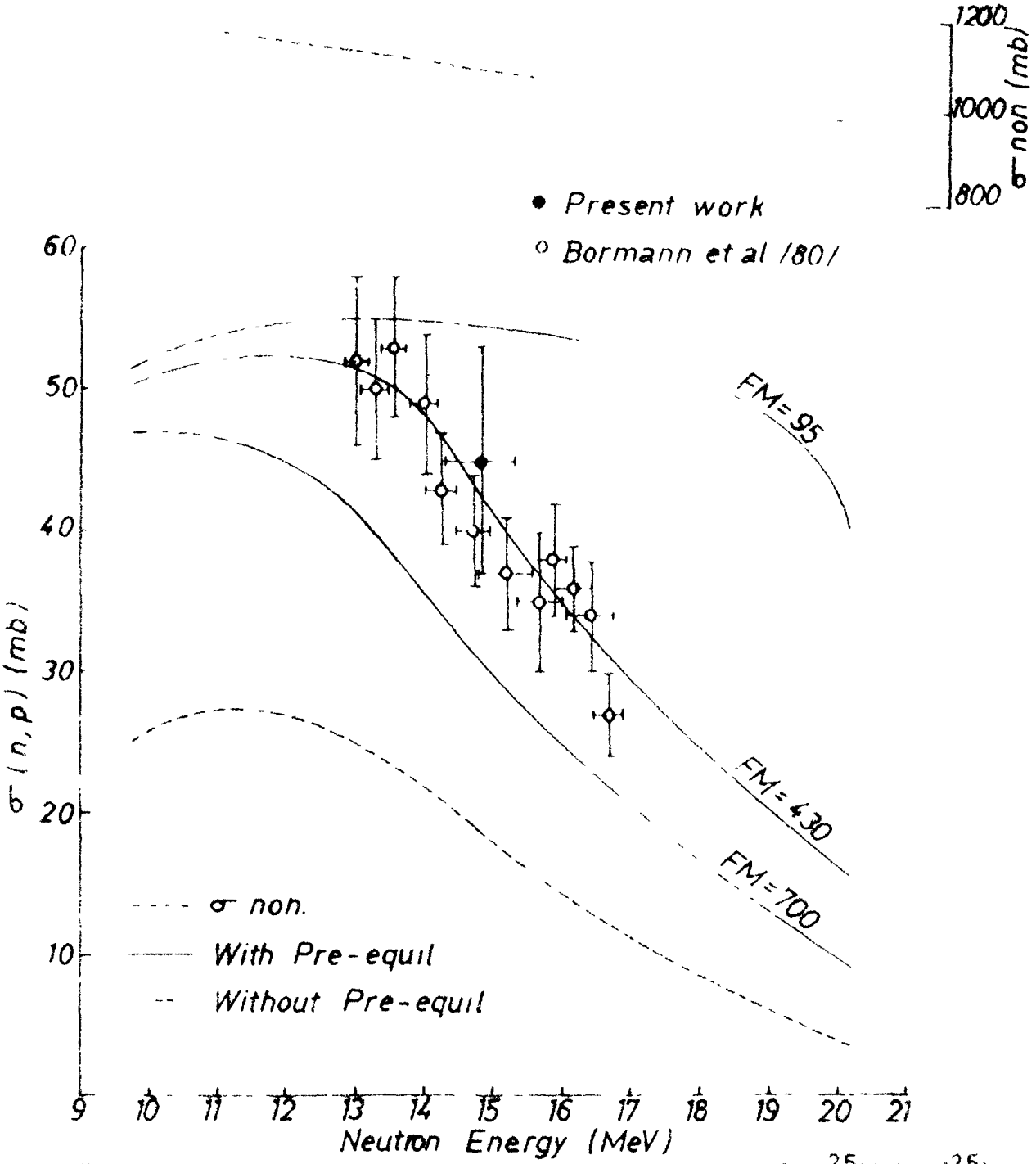

Fig 5.12 Experimental and calculated excitation functions for $^{25}Mg(n,p)^{25}Na$ reaction Calculated excitation functions with pre-equilibrium emission are obtained using FM = 95, 430, 700 MeV^3.

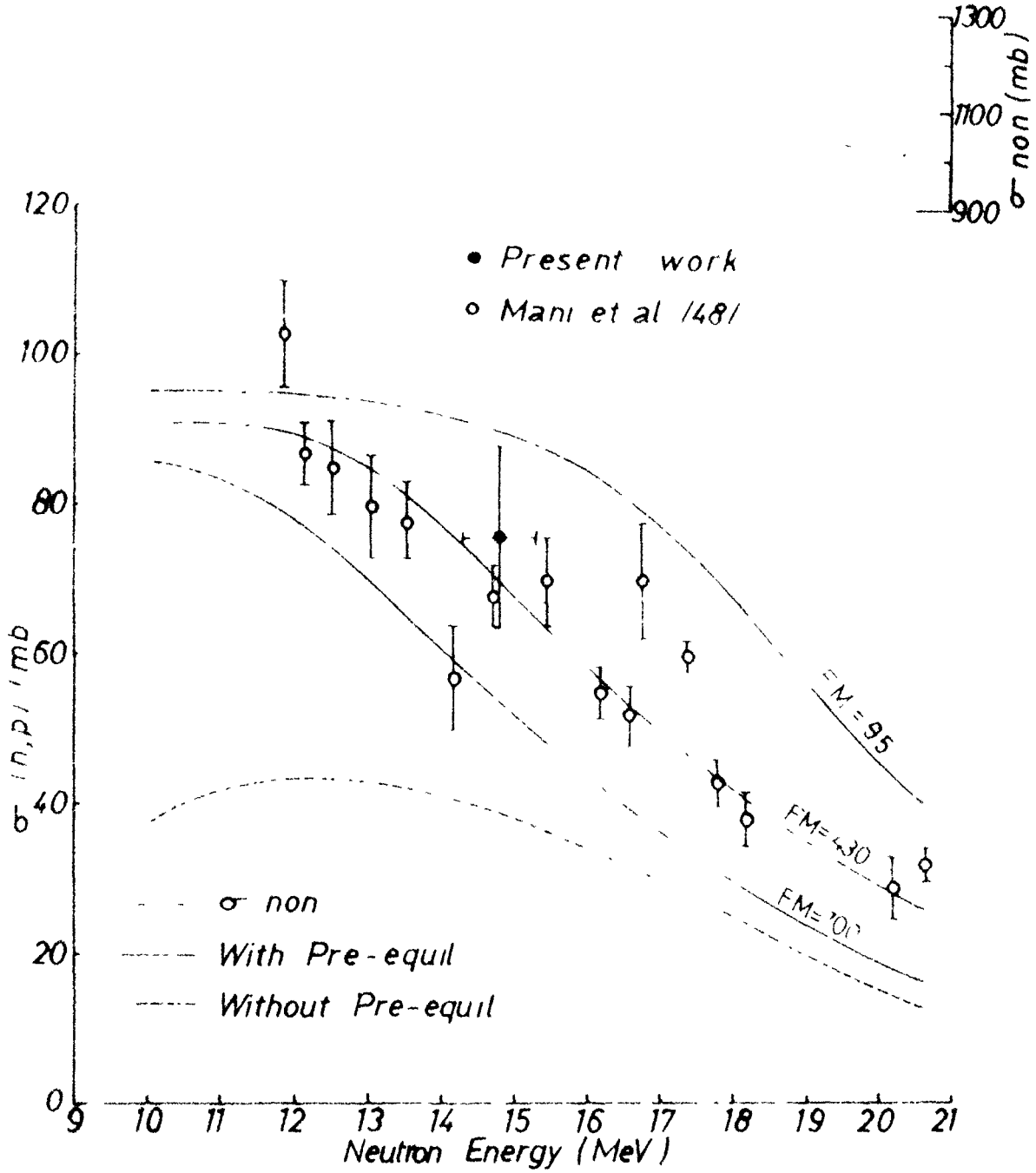

Fig 5 13 Experimental and calculated excitation functions for $^{27}Al(n,p)^{27}Mg$ reaction Calculated excitation functions with pre-equilibrium emission are obtained using FM=95, 430 & 700 MeV^3.

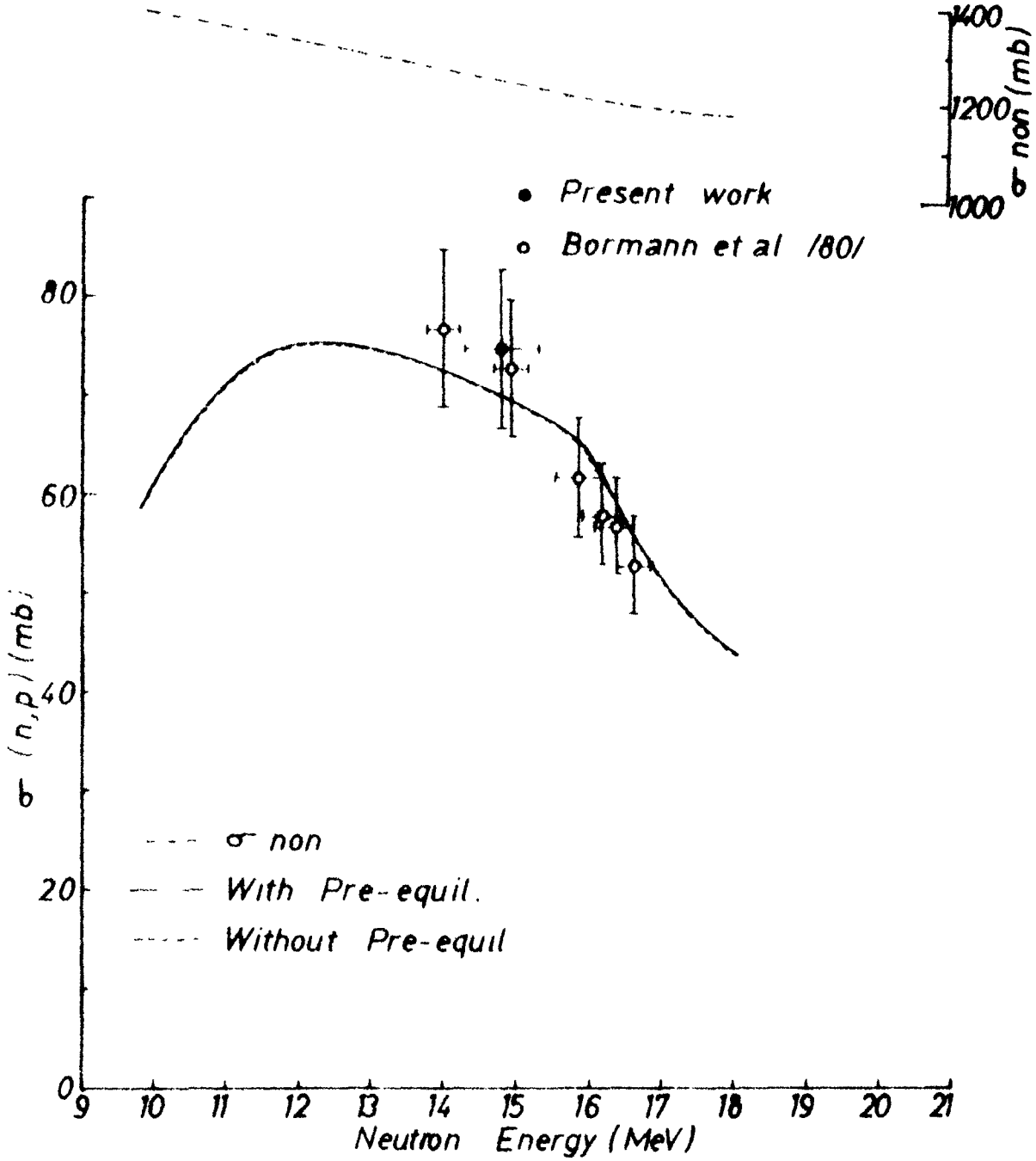

Fig 5.14 Experimental and calculated excitation functions for $^{34}S(n,p)^{34}P$ reaction

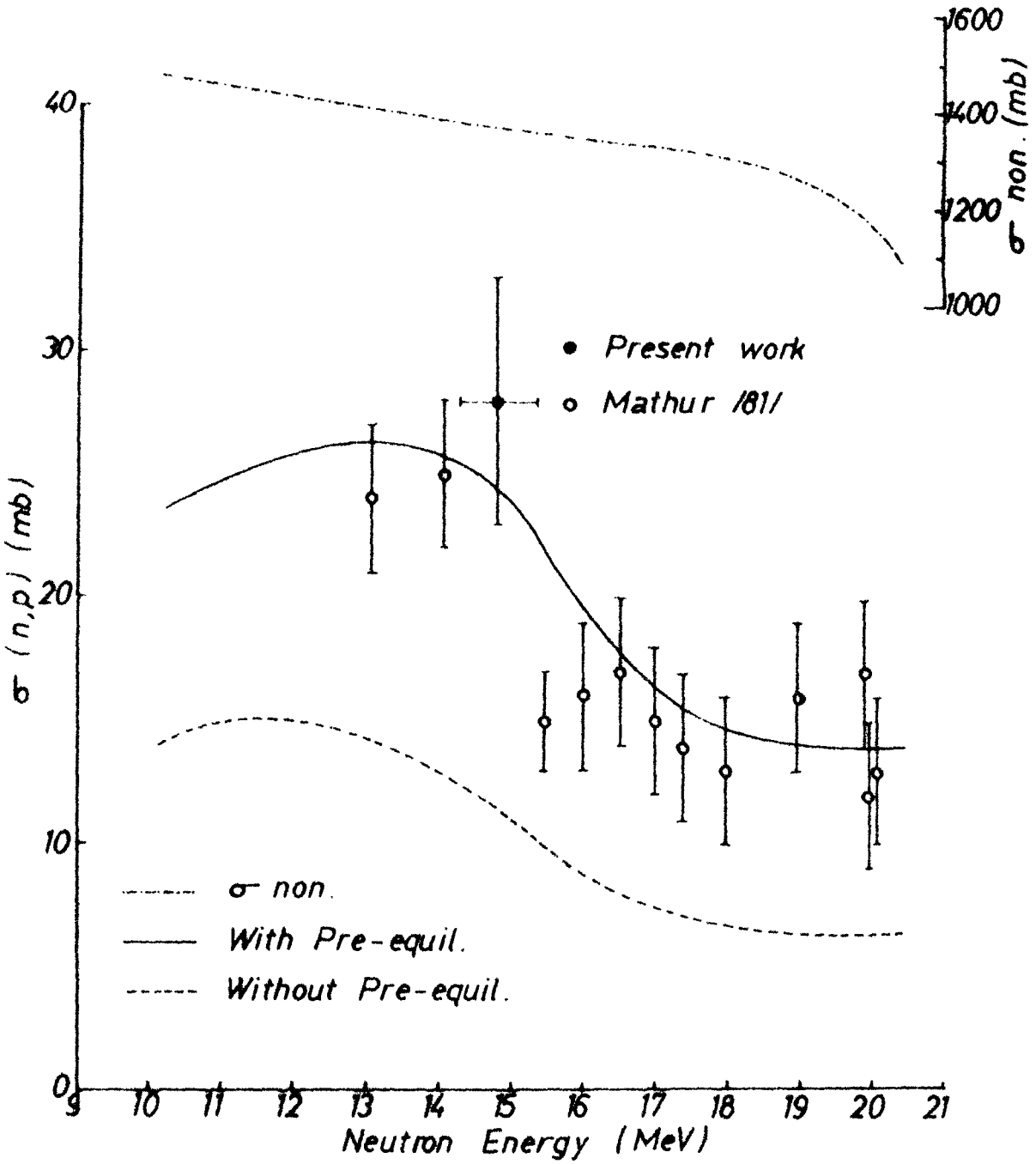

Fig. 5 15 Experimental and calculated excitation functions for $^{37}Cl(n,p)^{37}S$ reaction.

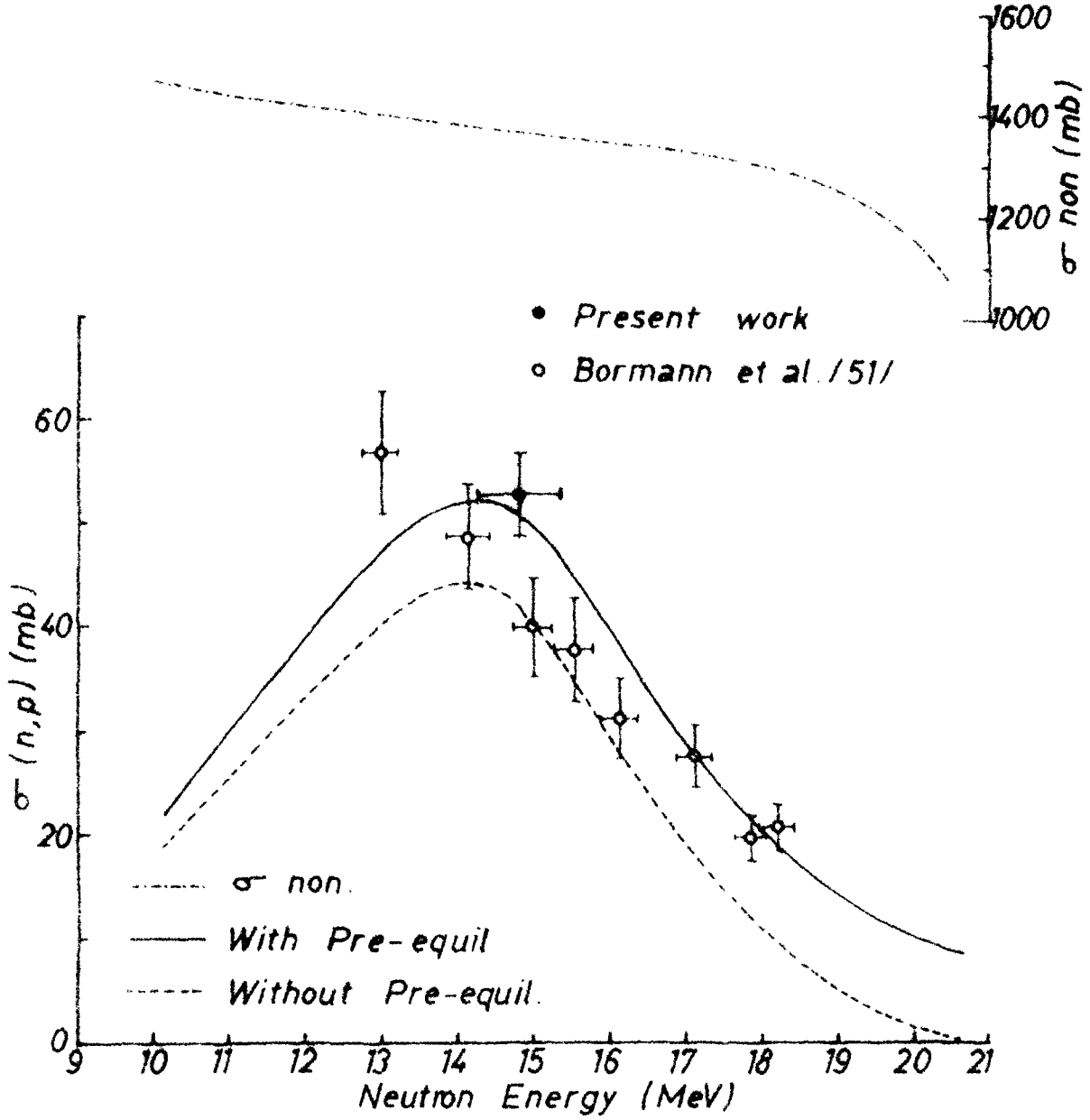

Fig 5.16 Experimental and calculated excitation functions for $^{41}K(n,p)^{41}Ar$ reaction.

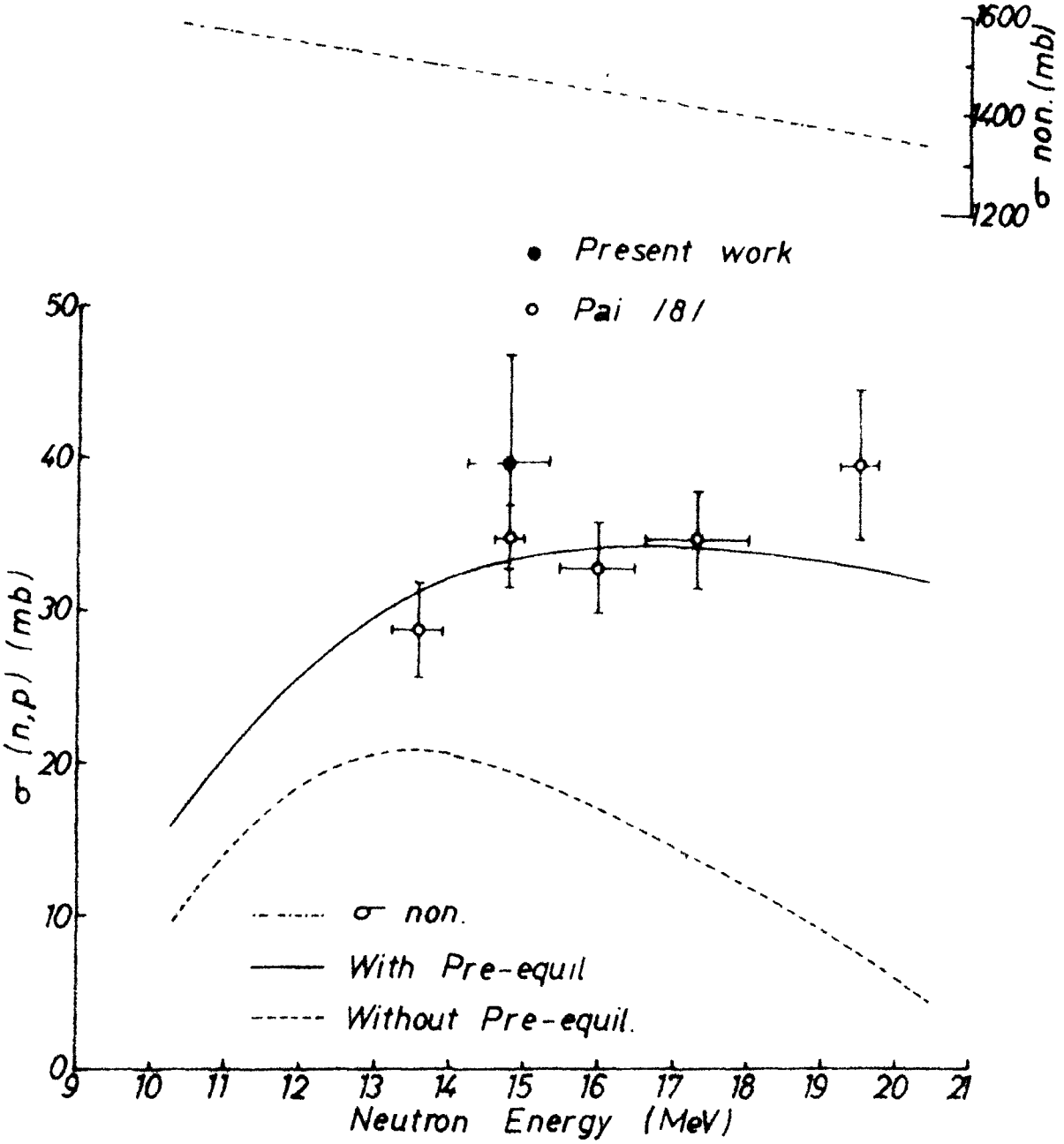

Fig 5.18 Experimental and calculated excitation functions for $^{49}Ti(n,p)^{49}Sc$ reaction

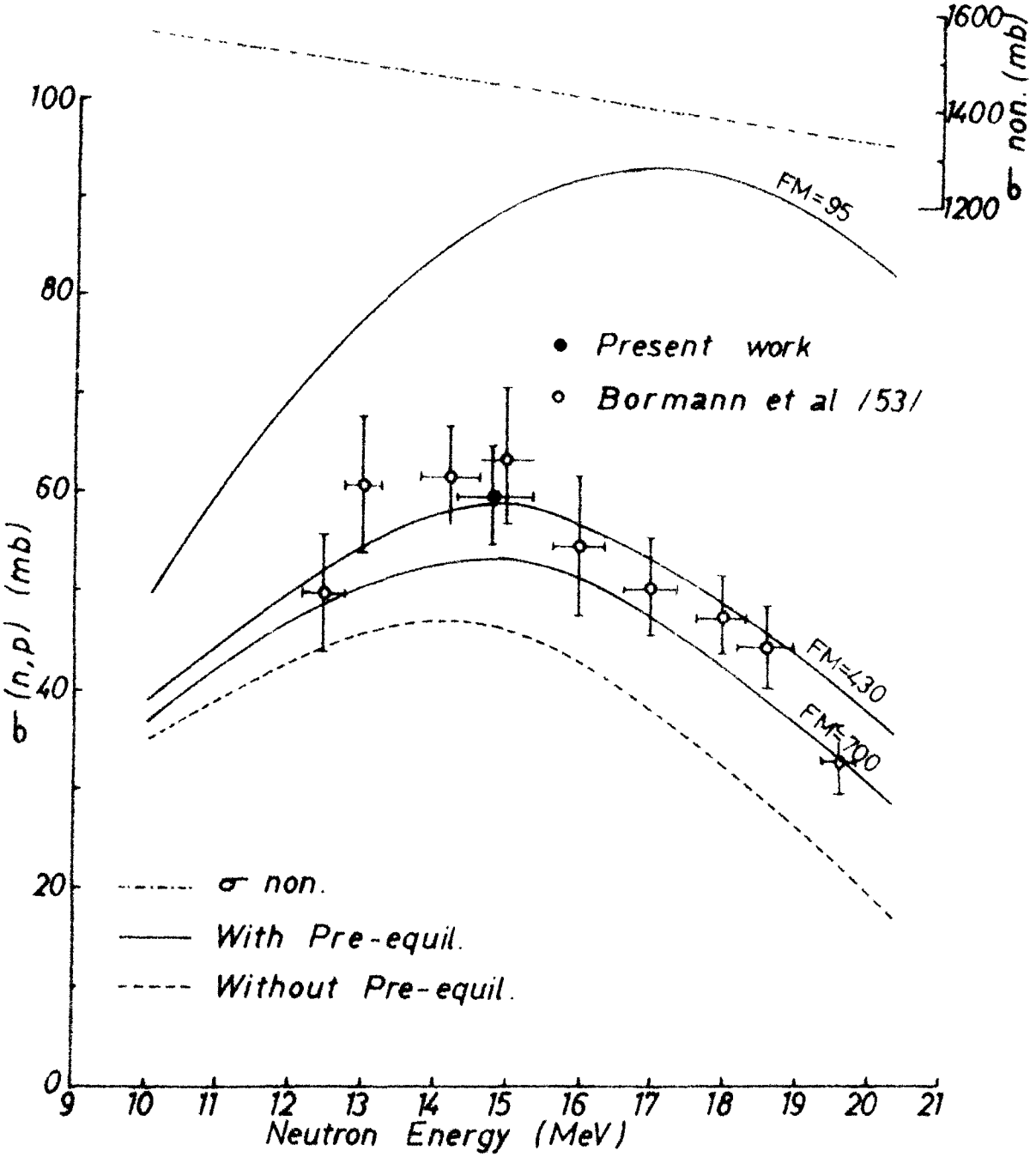

Fig 5.17 Experimental and calculated excitation functions for $^{48}Ti(n,p)^{48}Sc$ reaction. Calculated excitation functions with pre-equilibrium emission are obtained using FM=95,430 & 700 MeV^3

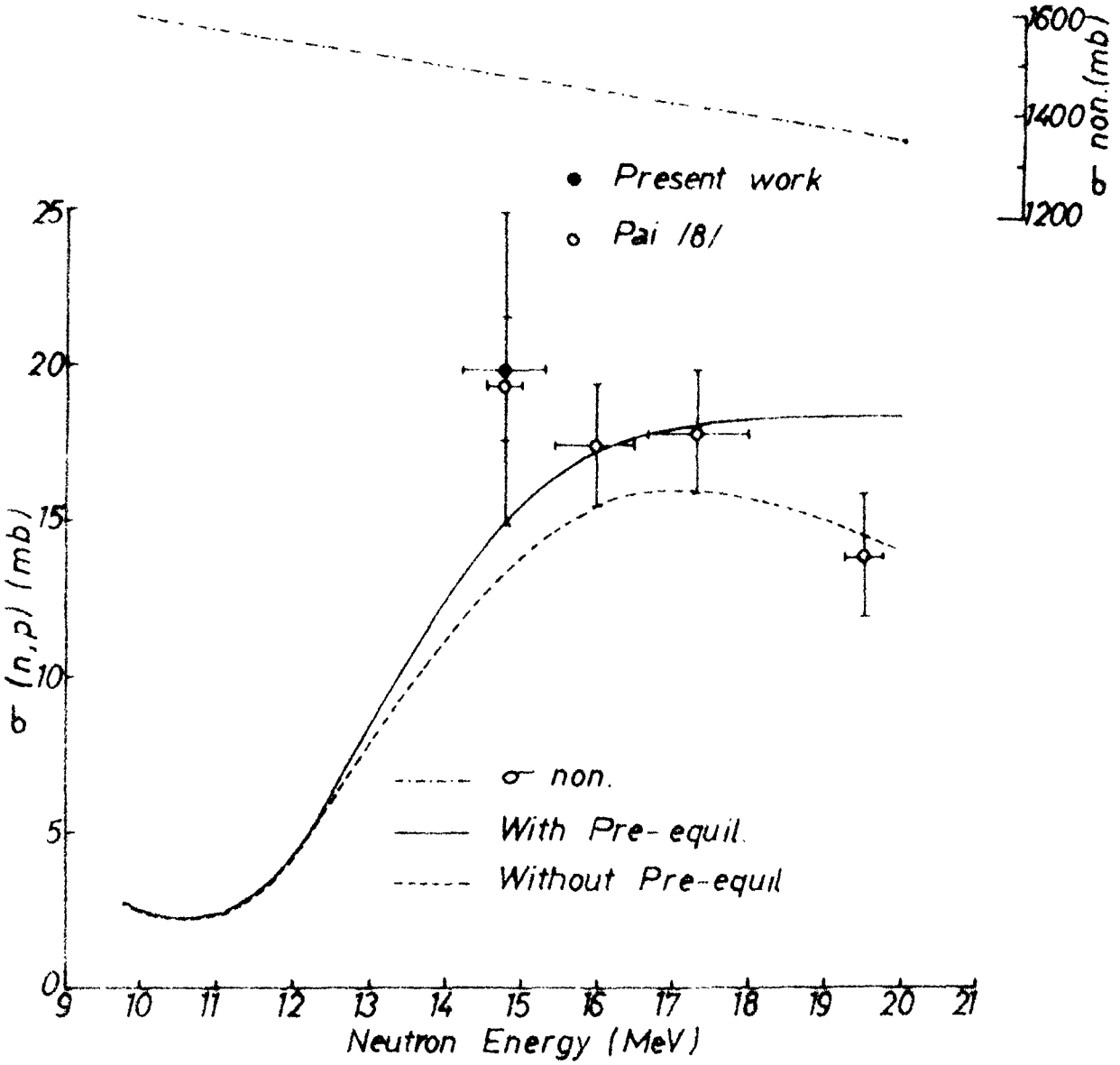

Fig 5.19 Experimental and calculated excitation functions for $^{50}Ti(n,p)^{50}Sc$ reaction

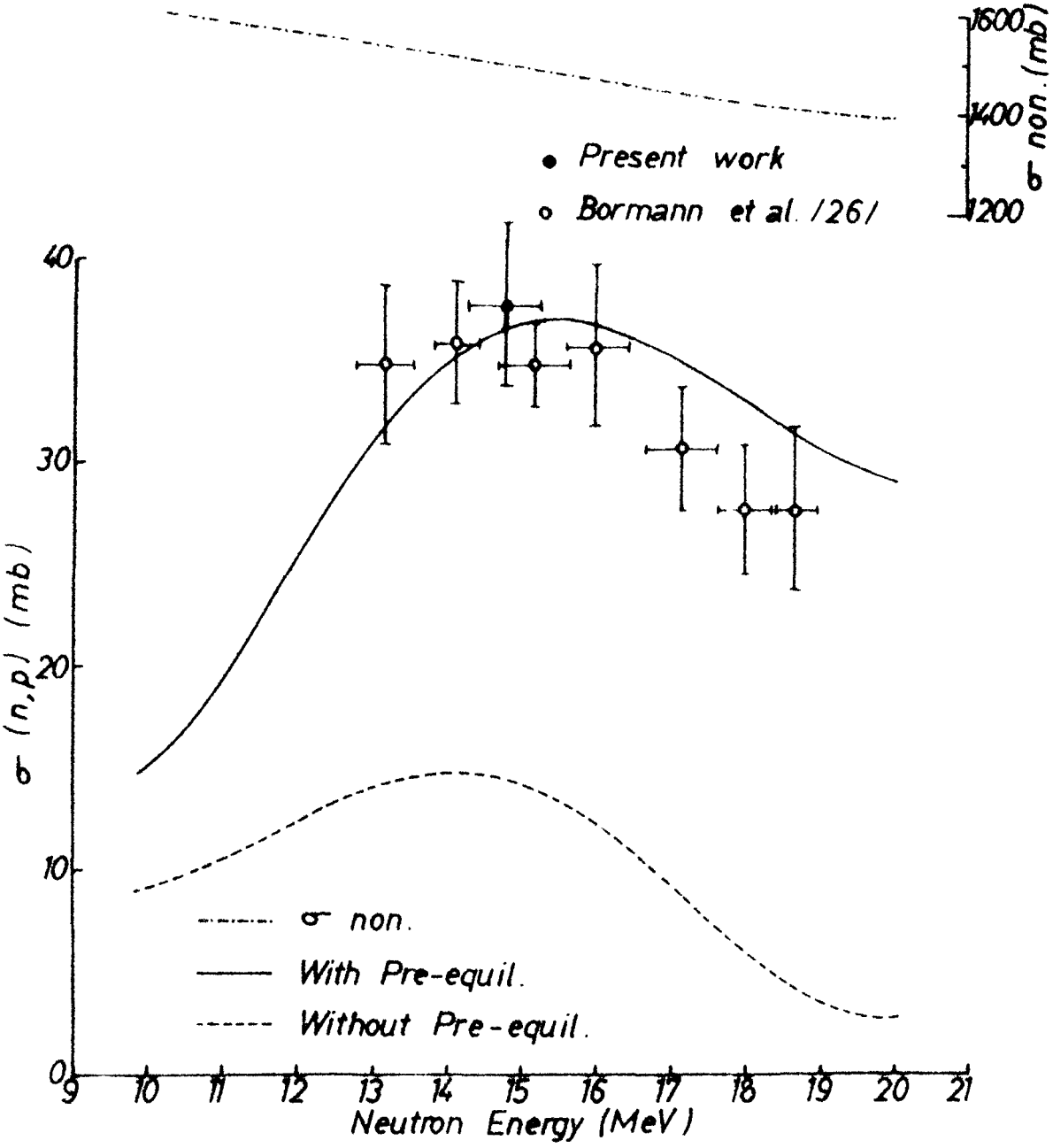

Fig.5.20 Experimental and calculated excitation functions for $^{51}V(n,p)^{51}Ti$ reaction

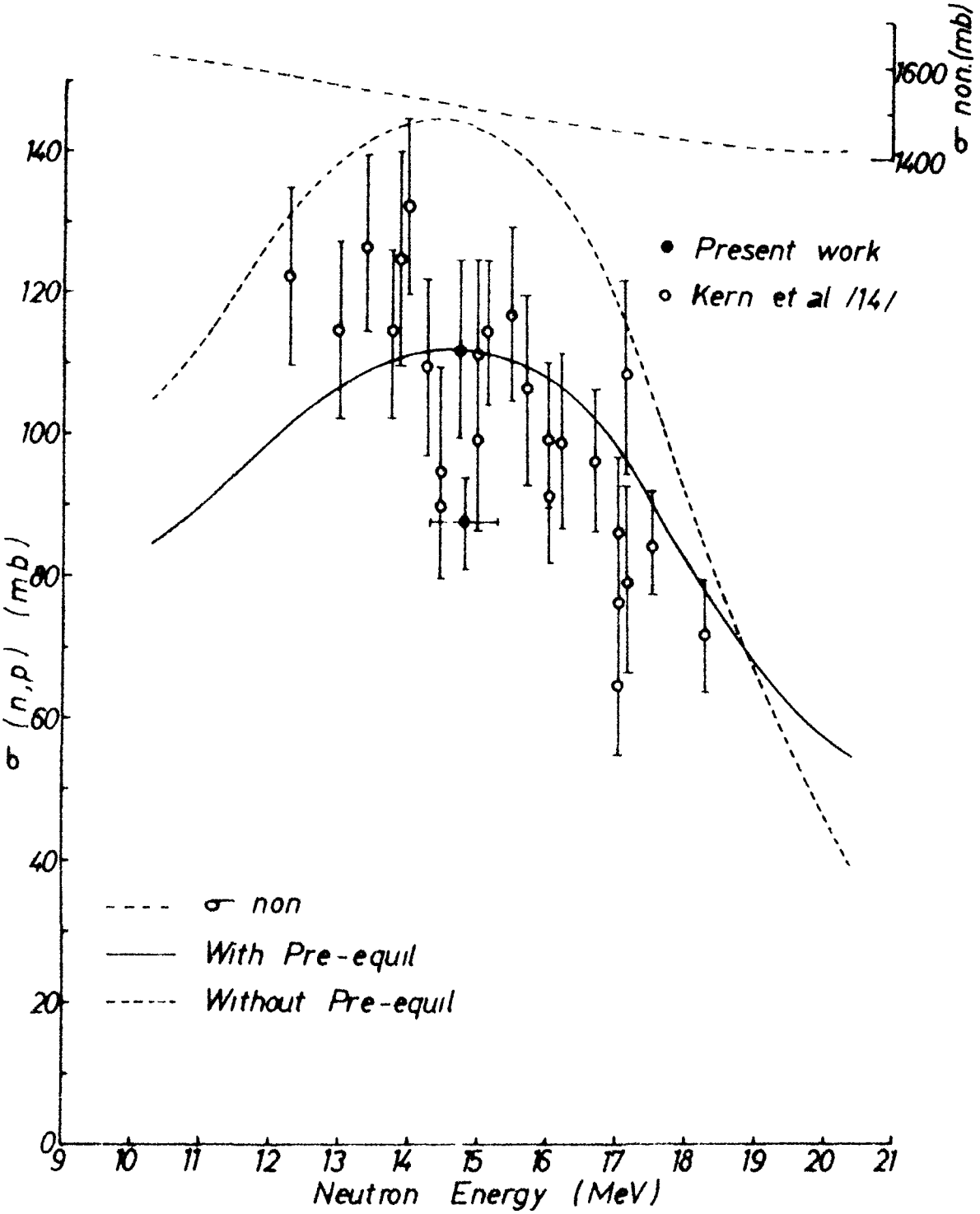

Fig 5 21 Experimental and calculated excitation functions for $^{52}Cr(n,p)^{52}V$ reaction

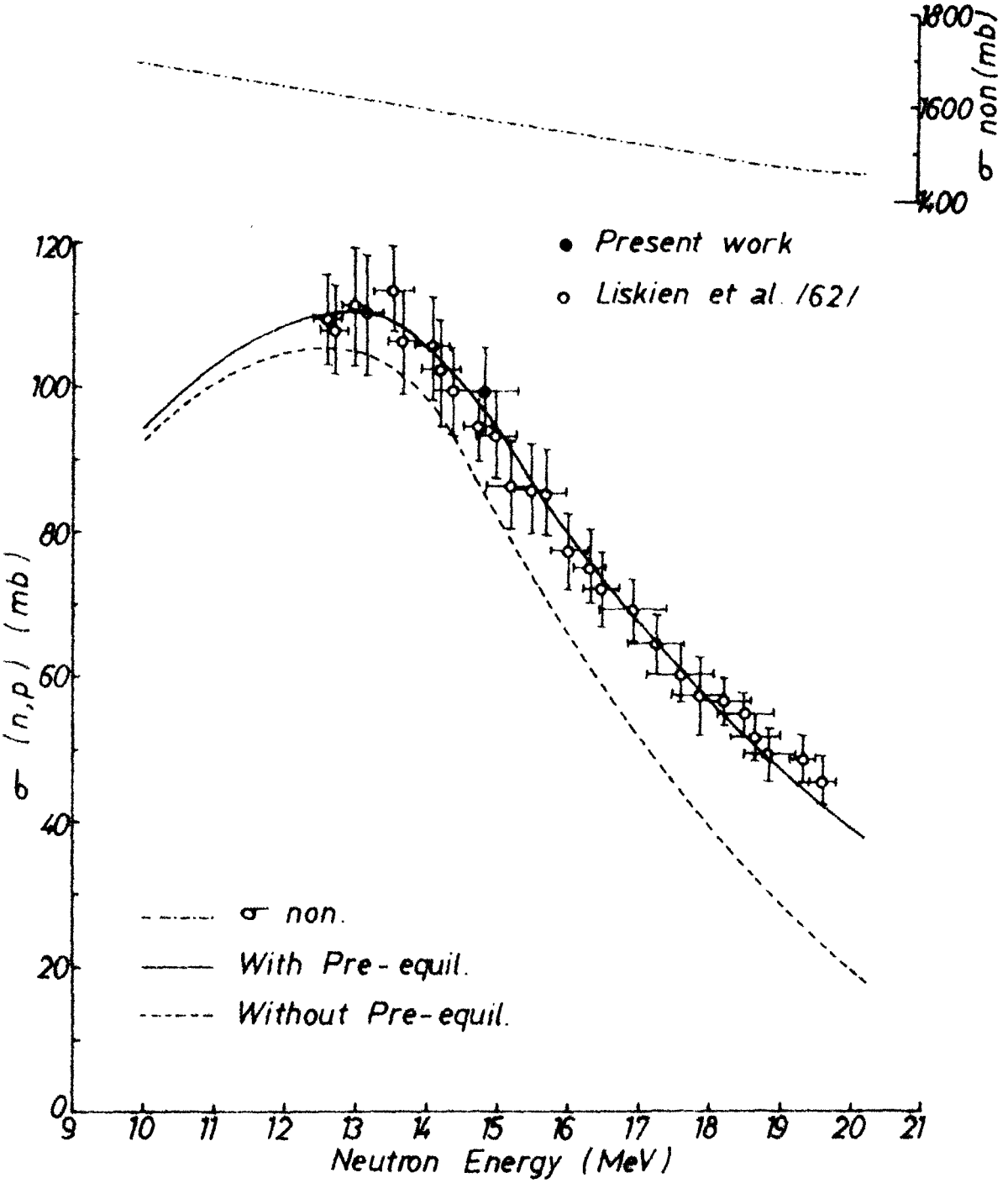

Fig 5 22 Experimental and calculated excitation functions for $^{56}Fe(n,p)^{56}Mn$ reaction.

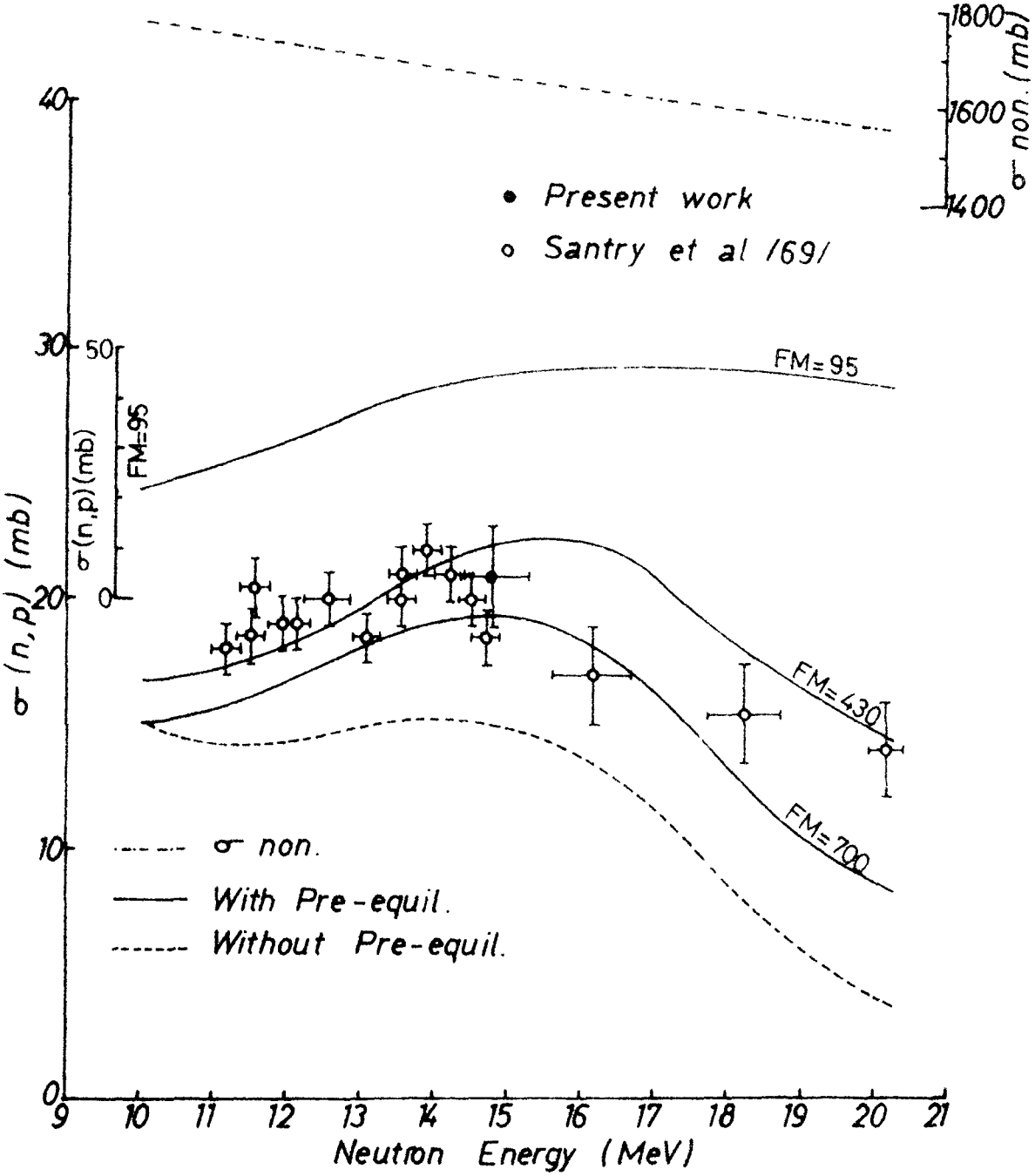

Fig. 5.23 Experimental and calculated excitation functions for $^{65}Cu(n,p)^{65}Ni$ reaction. Calculated excitation functions with pre-equilibrium emission are obtained using FM=95, 430 & 700 MeV[3]

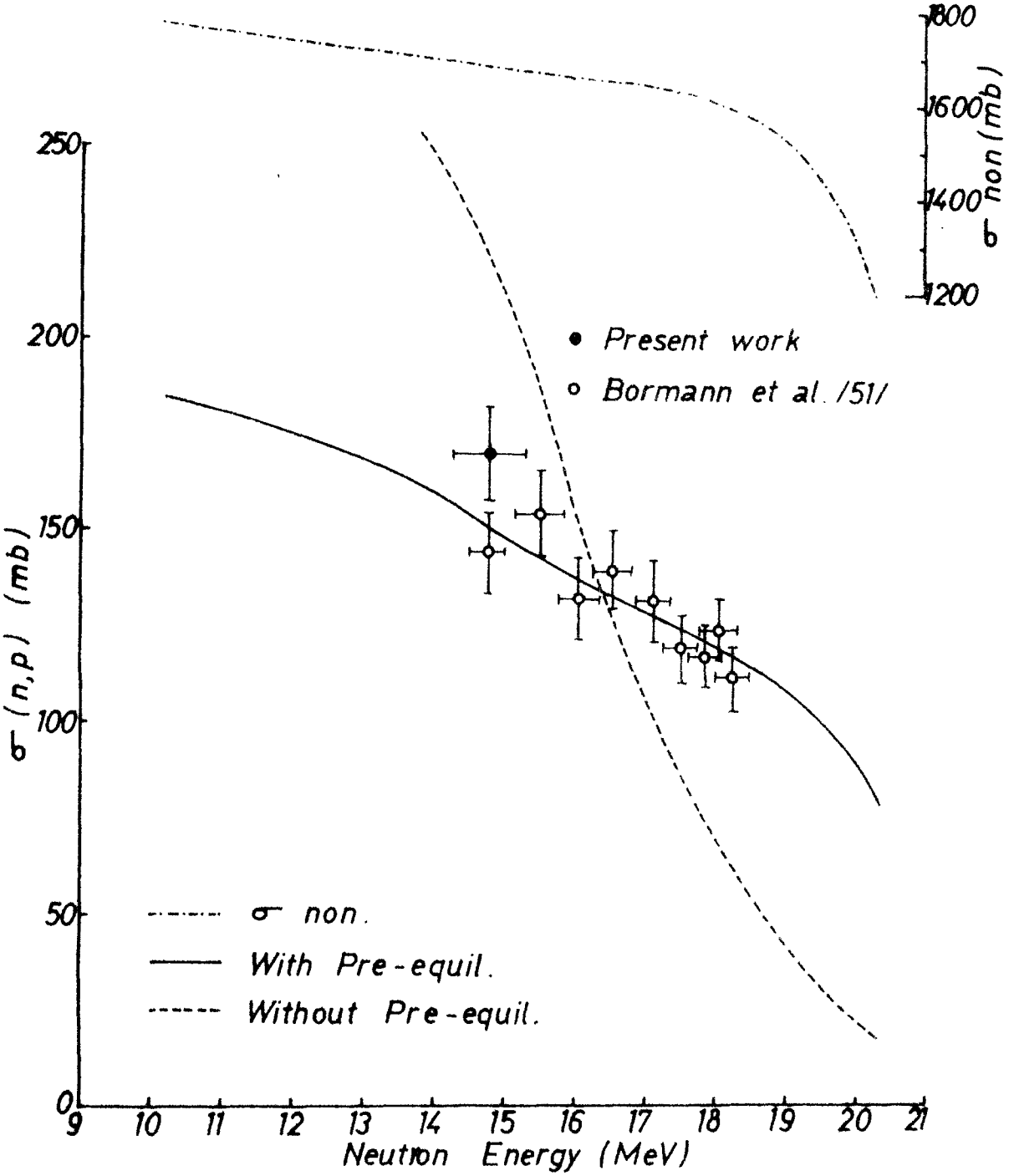

Fig.5.24 Experimental and calculated excitation functions for $^{64}Zn(n,p)^{64}Cu$ reaction

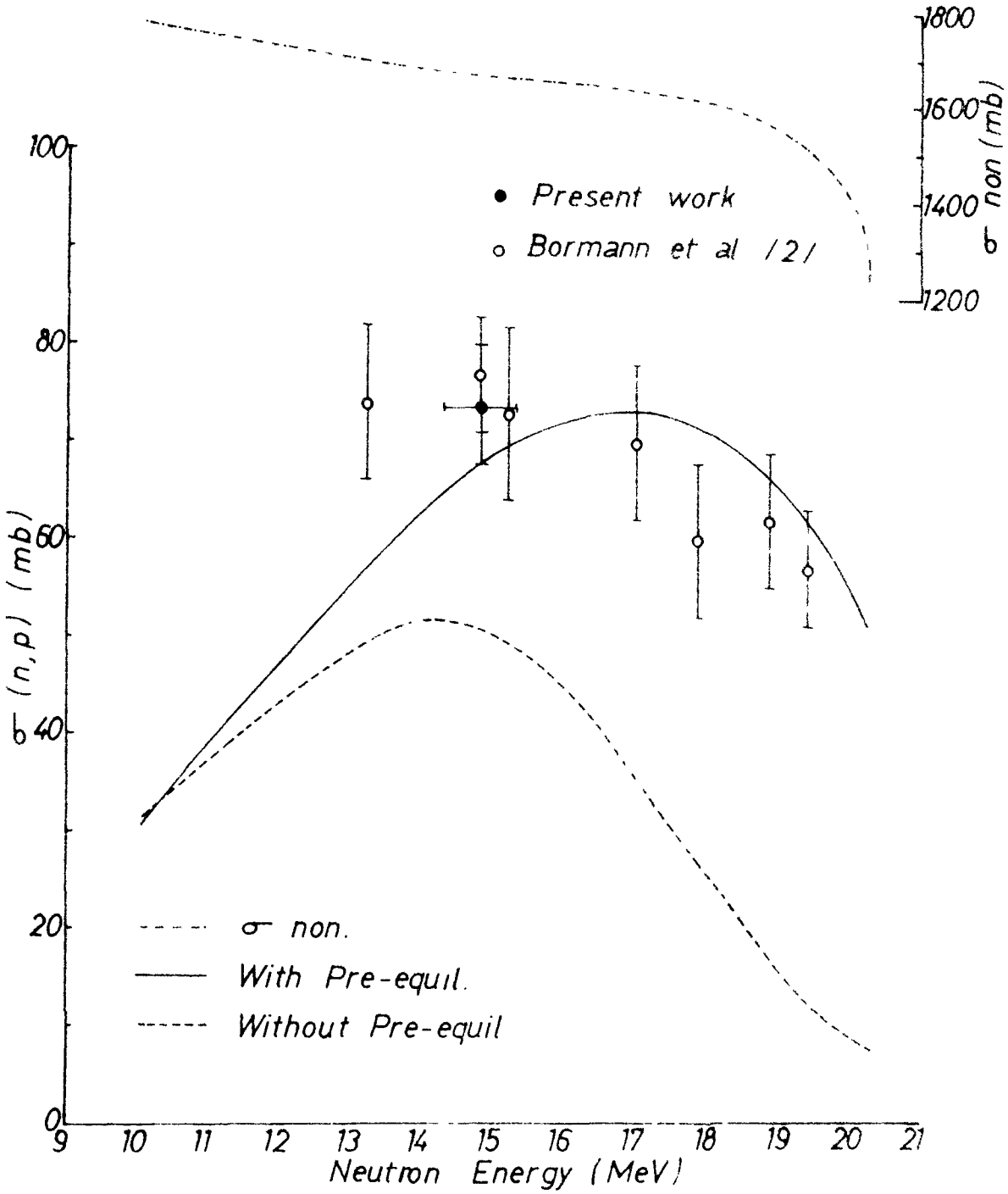

Fig 5 25 Experimental and calculated excitation functions for $^{66}Zn(n,p)^{66}Cu$ reaction

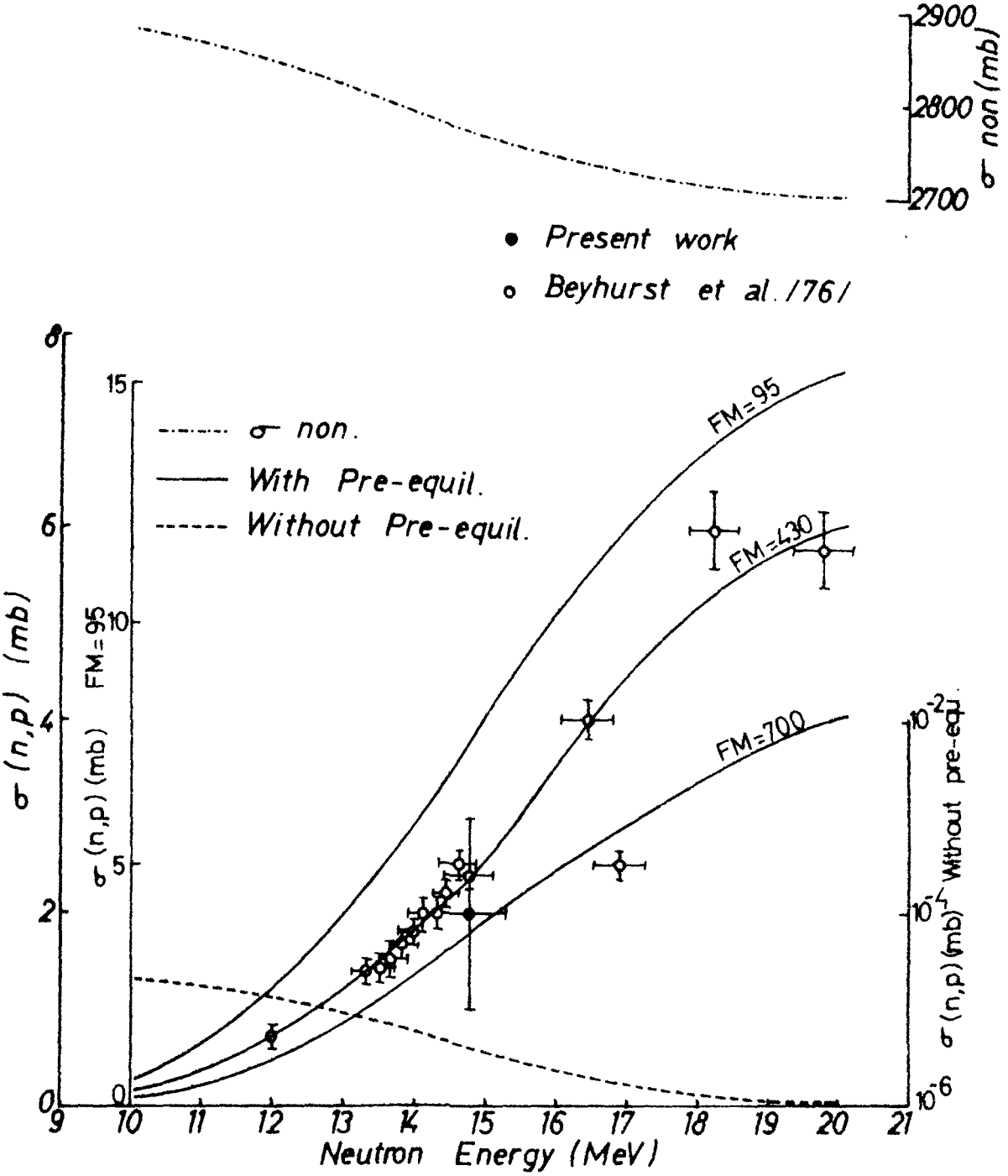

Fig. 5.29 Experimental and calculated excitation functions for $^{197}Au(n,p)^{197}Pt$ reaction. Calculated excitation functions with pre-equilibrium emission are obtained using FM=95,430&700 MeV[3].

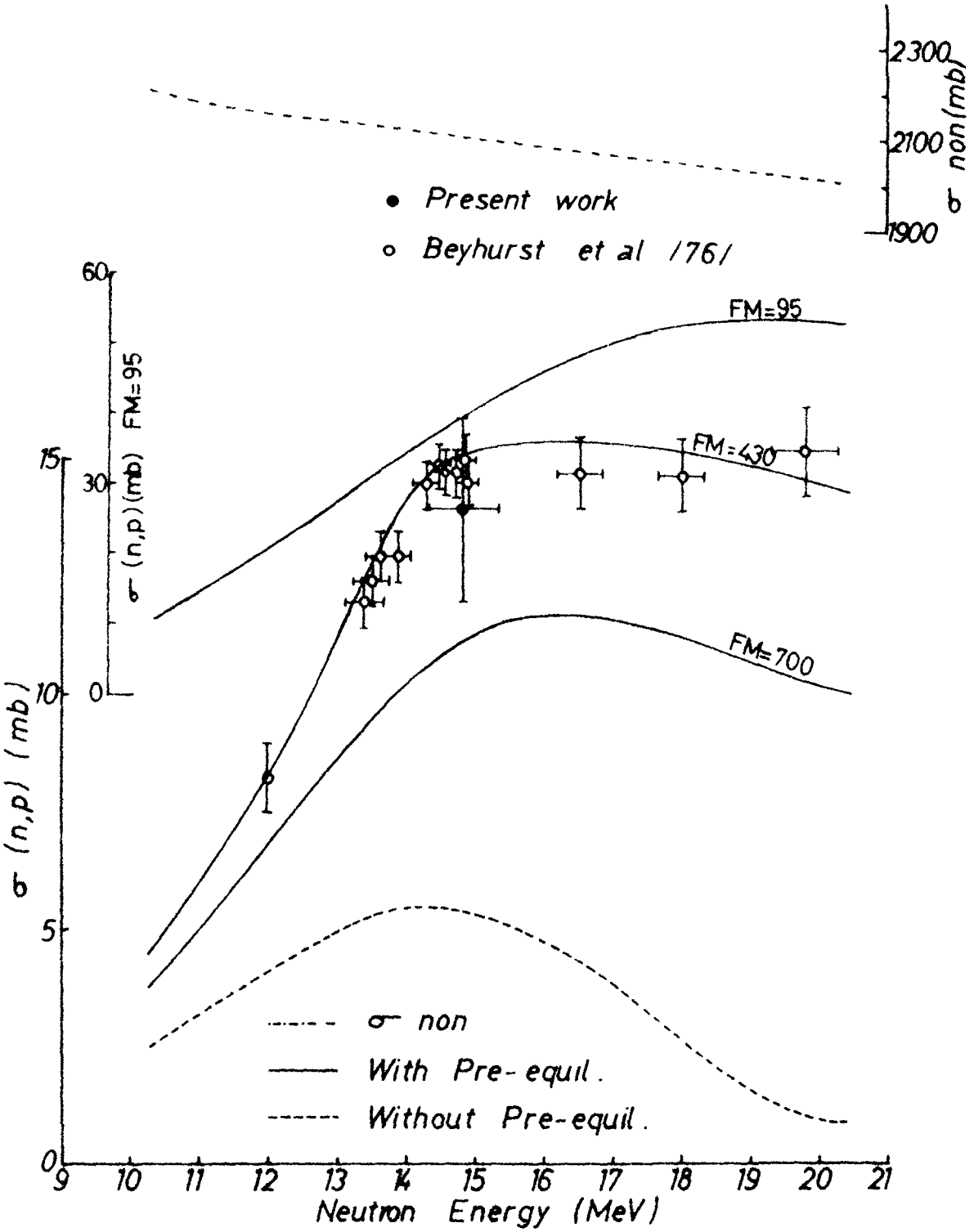

Fig 5.28 Experimental and calculated excitation functions for $^{109}Ag(n,p)^{109}Pd$ reaction Calculated excitation functions with pre-equilibrium emission are obtained using FM=95,430&700MeV^3.

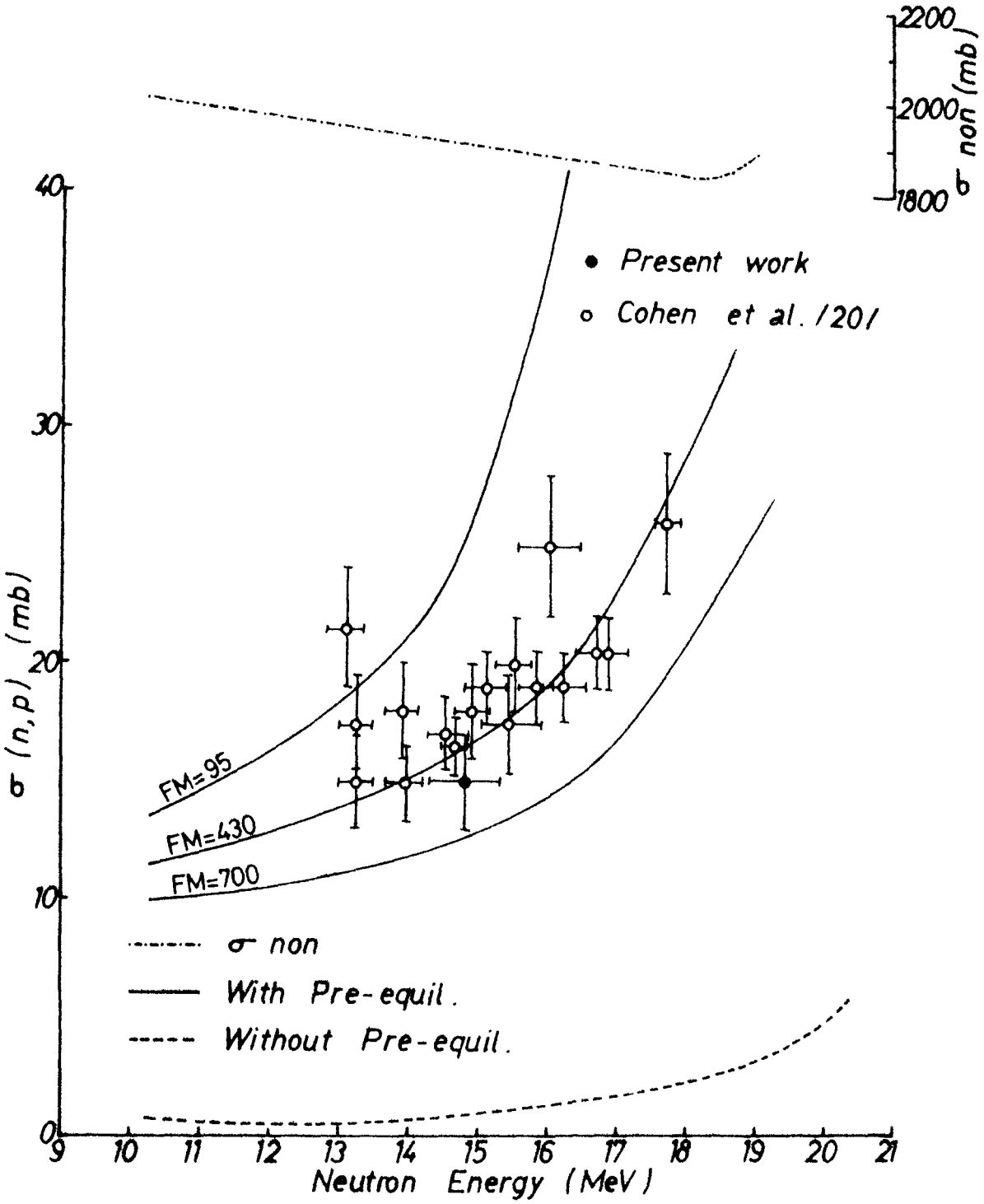

Fig 5.27 Experimental and calculated excitation functions for $^{88}Sr(n,p)^{88}Rb$ reaction. Calculated excitation functions with pre-equilibrium emission are obtained using FM=95,430&700 MeV[3].

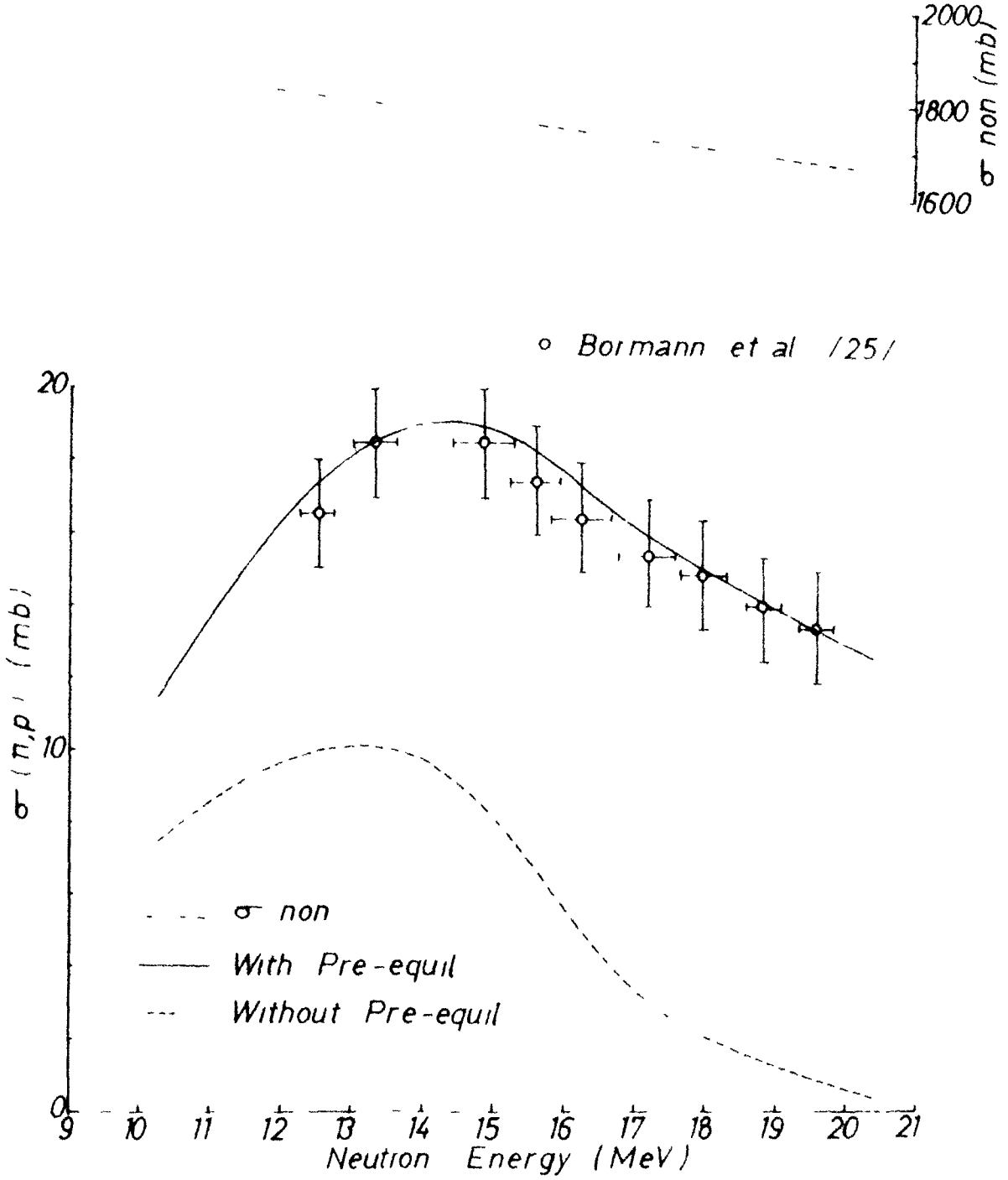

Fig 5 26 Experimental and calculated excitation functions for $^{75}As(n,p)^{75g}Ge$ reaction

taking place. The ratio $\frac{\sigma(n, p)_{exp}}{\sigma_{cal.\ CN + pre}}$ is also plotted in figs. (5.7 to 5.10) against A, Z, N and (N-Z)/A (lower part of figs. 5.7 to 5.10). As can be seen now the points in these figures lie quite close to unity. This better agreement between the experimental and calculated cross-section values in the later case strengthen the presence of pre-equilibrium emission process.

(5.2) EXCITATION FUNCTIONS IN THE ENERGY RANGE 10 MeV to 20 MeV -

Literature values of the (n,p) cross-sections in the energy range 10 MeV to 20 MeV have been compiled to study the excitation functions for $^{24, 25}Mg$ (n, p) $^{24,25}Na$, ^{27}Al (n, p) ^{27}Mg, ^{34}S (n, p) ^{34}P, ^{37}Cl (n,p) ^{37}S, ^{41}K (n, p) ^{41}Ar, $^{48, 49, 50}Ti$ (n, p) $^{48, 49, 50}Sc$, ^{51}V (n, p) ^{51}Ti, ^{52}Cr (n, p) ^{52}V, ^{56}Fe (n,p) ^{56}Mn, ^{65}Cu (n,p) ^{65}Ni, $^{64, 66}Zn$ (n, p) $^{64,66}Cu$, ^{75}As (n,p) ^{75g}Ge, ^{88}Sr (n,p)^{88}Rb, ^{109}Ag (n, p) ^{109}Pd and ^{197}Au(n,p) ^{197}Pt reactions. These excitation functions are shown in fign. (5.11 to 5.29). Also shown in these figures are the presently measured cross-section values at 14.8 $\pm$ 0.5 MeV and $\sigma_{non.}$ (non-elastic cross-section). Excitation functions in this energy range have also been calculated using pure compound mechanism and a combination of compound and pre-compound emission decay. The pure compound mechanism calculations have been done according to Hauser-Feshbach formalism. A computer code ACT (Chapter- IV) has been used for the calculations which takes into account the particles

which are emitted during the equilibration of the excited composite system alongwith the usually statistically emitted particles.

The results of calculations depend on many parameters. In the pure compound calculations which have been done according to Hauser-Feshbach statistical model, the values of level density parameter 'a' and the fictive ground state energy 'Δ' for all nuclei have been taken consistently equal to that given by Dilg et al. / 91 /. The calculated excitation functions are shown in figures (5.11 to 5.29) by dashed line. It has been observed that the calculated excitation functions, without consideration of the pre-equilibrium emission, fail to reproduce the experimental excitation functions. In general, it may be seen that the excitation functions calculated with pure compound mechanism lie below the experimental ones except for the three cases of ^{24}Mg (n, p) ^{24}Na, ^{52}Cr (n,p) ^{52}V and ^{64}Zn (n, p) ^{64}Cu. In case of ^{24}Mg (n, p) ^{24}Na reaction, the excitation function without consideration of pre-equilibrium emission lies above the experimental excitation function in the whole energy (10 - 20 MeV) range (as in fig .(5.11)). However, in the two cases of ^{52}Cr (n,p) ^{52}V and ^{64}Zn(n,p) ^{64}Cu, a different trend has been observed, as can be seen from figures (5.21) and (5.24), the excitation functions calculated with pure compound mechanism lie below the experimental ones in the higher energy range (above 16 MeV), but above them in the lower energy range. It is obvious from the inspection of these figures (5.11 to 5.29) that the agreement between the pure compound and experimental excitation functions

is very poor. As such there is need to include some other reaction mechanism for a better agreement in the theoretical and experimental excitation functions. Pre-equilibrium emission process is then added to compound nucleus process to calculate the excitation functions. For these calculations Hybrid model / 94 -95 / has been chosen. In the pre-compound calculations, three parameters are required (1) The initial exciton number 'n', (2) the probability of exciting a preformed α-particle ' ϕ ' and (3) the average squared matrix element ' $|M|^2$ ' for two body residual interaction. The values of all common input parameters for both compound and pre-compound calculations have been kept same through out these calculations. The initial exciton number for (n,p) reactions is generally / 96 / taken to be n = 3 (n = p + h, p = 2, h = 1 where p and h stand for the numbers of the excited particles and hole degrees of freedom). The probability of exciting a pre-formed α-particle ' ϕ ' has been taken to be 0.2 / 97 /. Since the value of average squared matrix element $|M|^2$, required to reproduce the experimental results, depends sensitively on details of the employed model, as for instance, the expressions for emission rates and the single particle state density 'g', the choice of this parameter is important.

For the pre-compound calculations internal transition decay rates are required. The internal transition decay rates can be calculated at low excitation energy where the average squared matrix element $|M|^2$, can be considered approximately energy independent / 98 /, by means of first order perturbation theory / 99 /. The expression : -

$$|M|^2 = FM_0 A^{-3} E^{-1} \quad .. \quad ... \quad .... \quad (5.1)$$

proposed by Cline / 100 / for the dependence of squared matrix element $|M|^2$ on the atomic mass number 'A' and excitation energy ' E ' of the excited nucleus has been used. Here 'FM' is the constant (in MeV^3) , considered as an adjustable parameter which by equ. (5.1) defines the matrix element for internal transitions competing with pre-equilibrium decay. It has been observed that the calculated excitation functions depend both on the choice of FM and level density parameters.

In the present calculations FM has been kept as an adjustable parameter to get better agreement between the calculated excitation functions with the experimental ones. For FM, values in the range 95 MeV^3 to 700 MeV^3 have been proposed / 100 - 105 /. By keeping the values of the level density parameters ('a' and 'Δ') for all nuclei consistently equal to that given by Dilg etal. / 91 /, calculations have been done using several values of FM in the range 95 MeV^3 to 700 MeV^3 for all reactions studied. In general, it has been observed that the best agreement between experimental and calculated excitation functions can be obtained with FM $\simeq$ 130 MeV^3. To show this, excitation functions with FM = 95 MeV^3 and 700 MeV^3 for seven selected cases are shown in figures 5.12, 5.13, 5.17, 5.23, 5.27 to 5.29). From these figures it may be seen that for FM = 95 MeV^3 the maxima of the calculated excitation functions, which generally occurs around 14 MeV in the experimental excitation functions, shifts towards the higher energy side and the excitation fuentions lie above the experimental ones. While for FM = 700 MeV^3 the maxima of the calculated excitation functions shifts to the lower energy side and the calculated excitation functions go below the experimental functions. As such the best $\int^{ne}$ production of the position

of the matrix as well as the total excitation function has been obtained with $PM = 430\ MeV^3$.

Once the value of PM has been so fixed, it has been required in some cases to change the level density parameter 'a' slightly (< 10 %) from the values given by the Gilbert et al., for a better agreement between the experimental and calculated excitation functions. The effect of the variation of the level density parameters 'a' for all residual nuclei corresponding to the various reaction channels (n, n'), (n, p), (n, α) etc. have also been studied. It has been observed that the excitation functions are only slightly affected in the lower energy region (below 14 MeV) with the variation of 'a' of the residual nucleus of (n, n') channel. However, there has been negligible effect with the variation of level density parameter 'a' for the residual nucleus of (n, α) channel. On varying the value of initial exciton number 'n' from n = 3 to n = 7, it has been observed that the excitation functions remain unaltered, while the variation in the value of 'β' i.e. the probability of exciting pre-formed α-particle from $\beta = 0.1$ to $\beta = 0.5$, slightly affects (within 3 %) the calculated excitation functions. Since a large atomic mass range has been observed (A = 24 to A = 197) in these calculations and a good agreement is found between the experimental and calculated excitation functions, therefore, it may be concluded that the present choice of the parameters is valid for all (n,p) reactions.

To have a quantitative estimate of the contribution of pre-equilibrium emission to the total cross section for the neutron induced reactions in this energy range, the fraction of the pre-equilibrium emission decay (q_{pre}) defined as :

$$q_{pre} = 1 - \frac{\sum_{k=0}^{K} \sum_{n} b^{(k)}(n) \lambda^{0}(n)}{\lambda(n)} \quad \ldots (5.2)$$

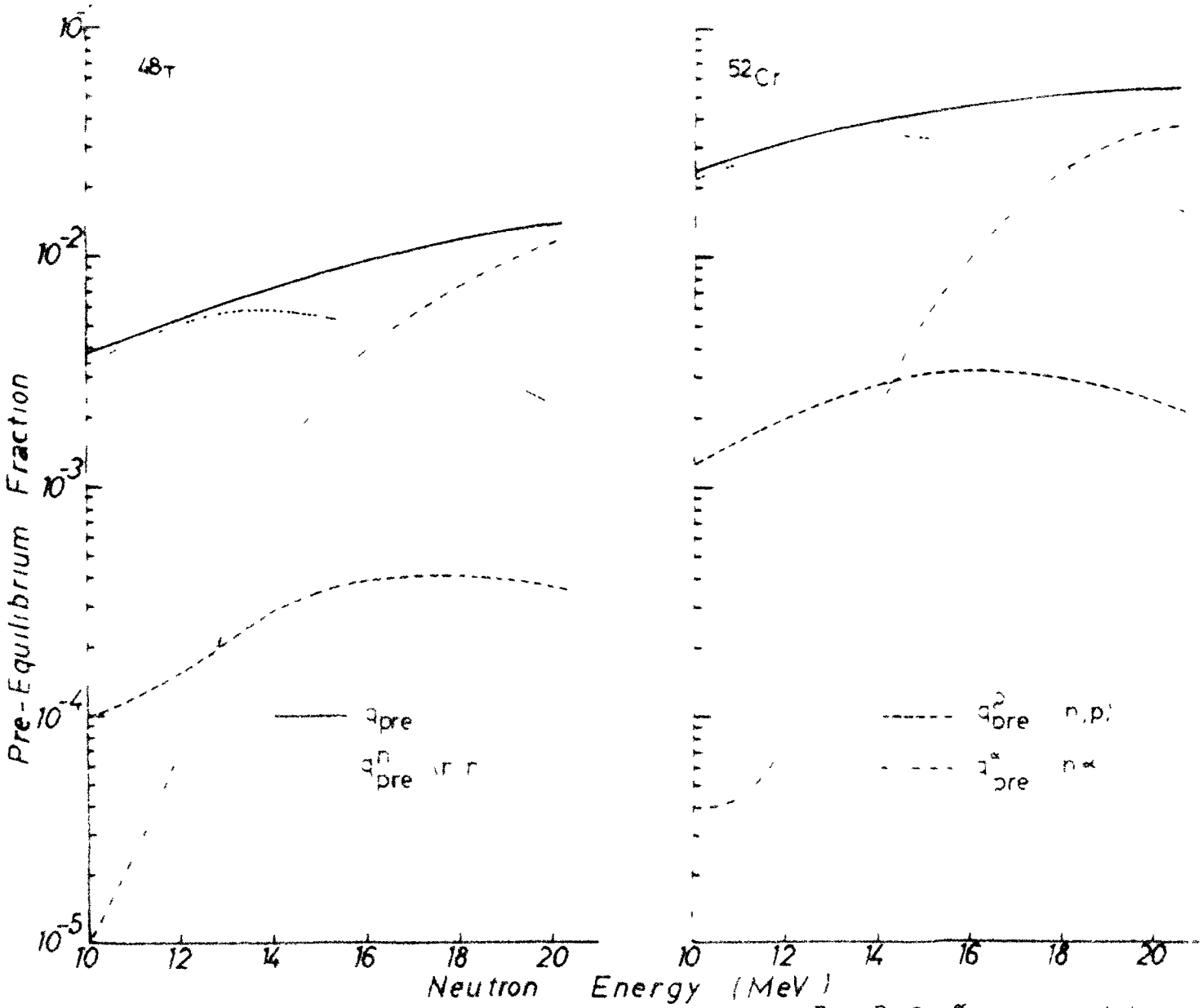

Fig 5.32 Relative pre-equilibrium emission contributions q^{n}_{pre}, q^{p}_{pre} & q^{α}_{pre} for (n,n'), (n,p) and (n,α) reactions on ^{48}Ti and ^{52}Cr target nuclei

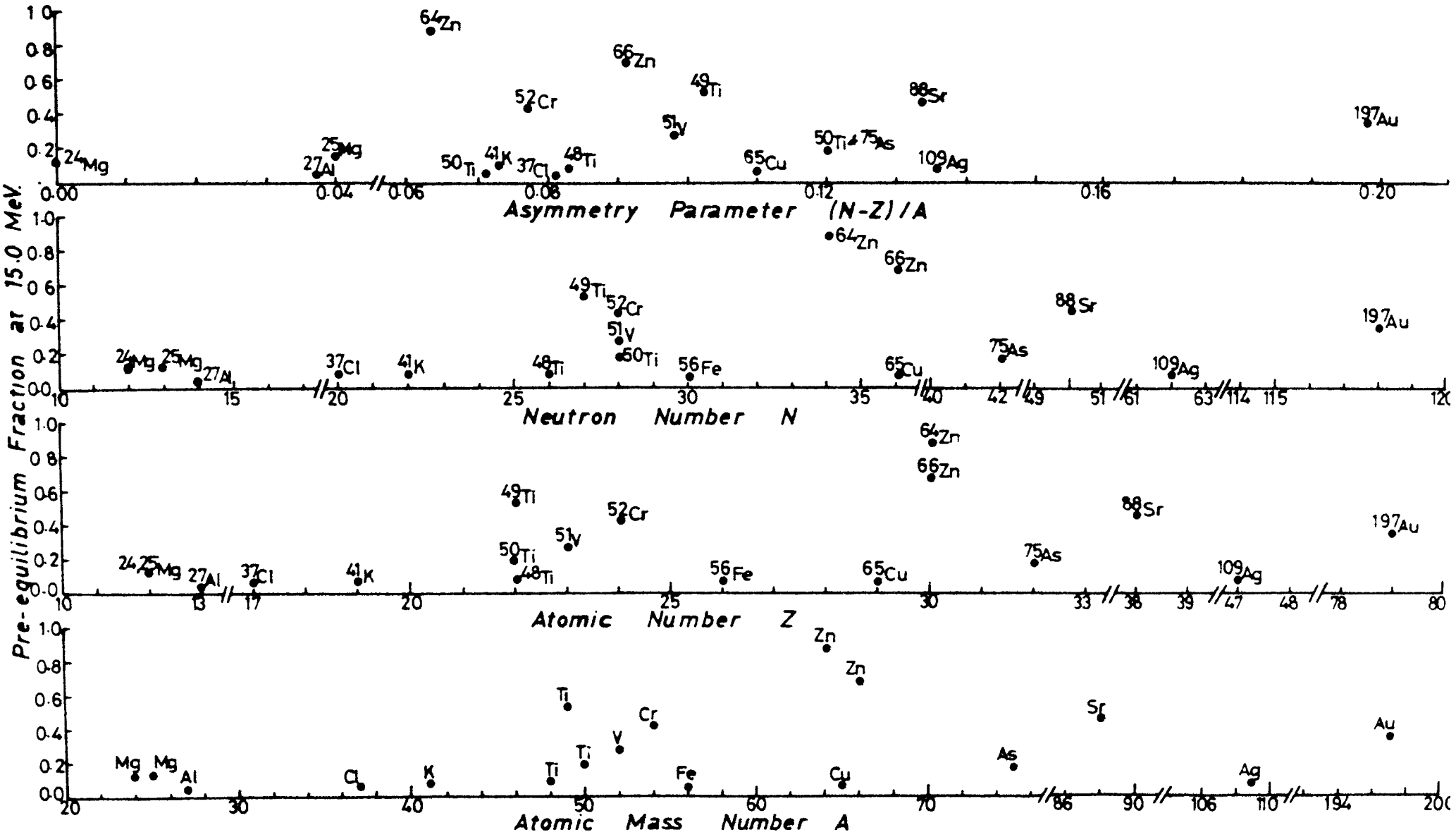

Fig. 5.31 Variation of pre-eqilibrium fraction 'q_{pre}' with atomic mass number 'A', atomic number 'Z', neutron number 'N' and asymmetry parameter '(N-Z)/A' of the target nucleus at 15.0 MeV.

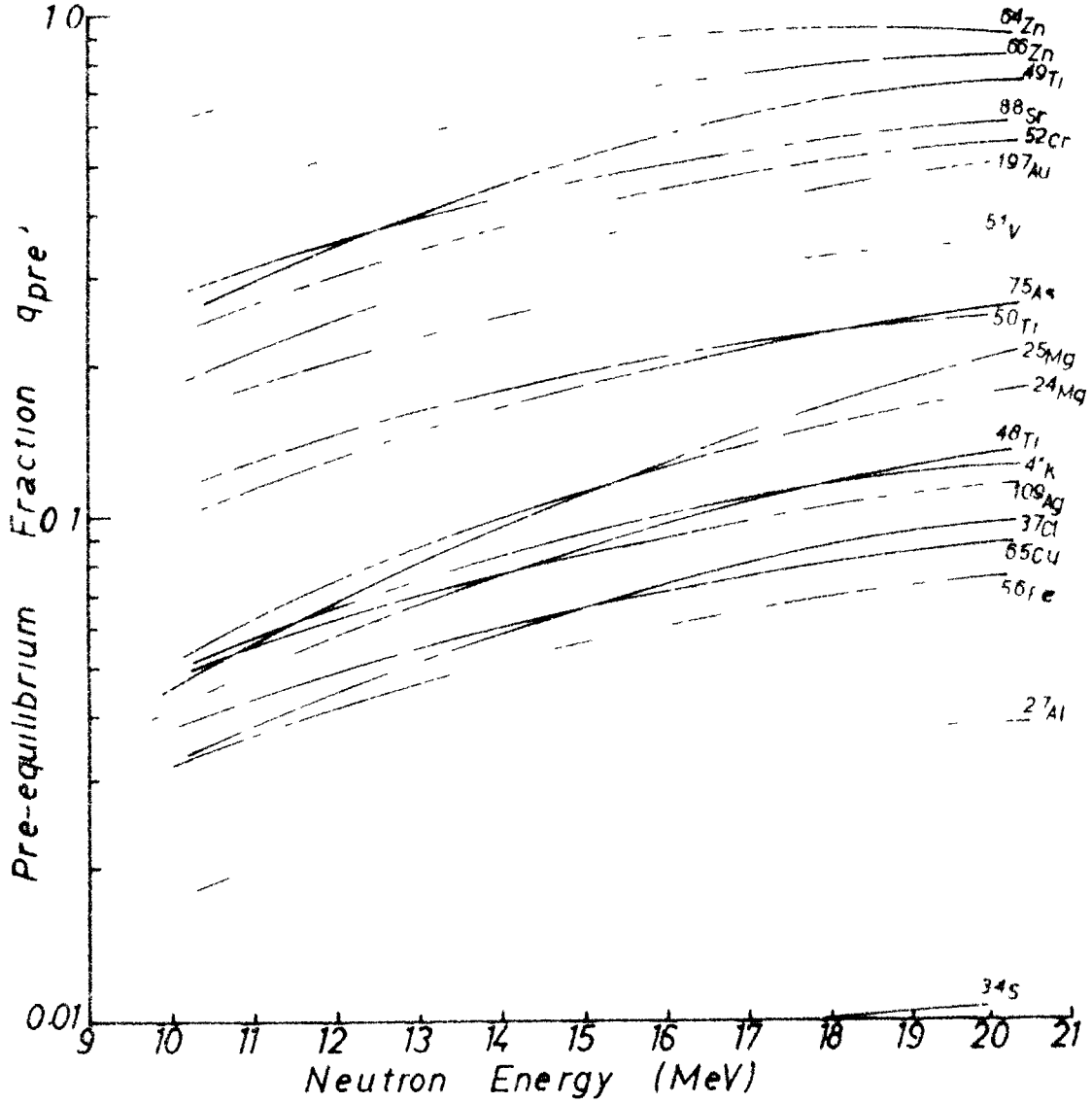

Fig 5 30 Variation of pre-equilibrium fraction 'q_{pre}' as a function of neutron energy

has been calculated (Chapter - IV). It is plotted as a function of the neutron energy in fig. (5.30). This figure shows that in all cases there is considerable contribution of pre-equilibrium emission, and that the q_{pre} increases almost linearly with the increasing excitation energy of the composite system. It may be observed from fig. (5.30) that the pre-equilibrium contribution is present even at 10 MeV neutron energy except for the ^{34}S target nucleus. However, q_{pre} varies from reaction to reaction. In some cases like ^{49}Ti, ^{52}Cr, $^{64,66}Zn$ and ^{88}Sr, target nuclei the contribution of q_{pre} is about 50% or more in the higher energy region, while in the other cases, its contribution is within 4 % to 30%. It may be observed that there is no regular variation of q_{pre} with the atomic mass number 'A' of the target nucleus (fig. 5.30). It is because, q_{pre} depends on many parameters in a complicated way (Chapter-IV). The q_{pre} at a fixed energy of 15 MeV for all the target nuclei has also been calculated and has been plotted against atomic mass number A, atomic number Z, neutron number N and asymmetry parameter $(N-Z)/A$ of the target nucleus in fig. (5.31). It may be observed from this figure that there is no regular dependence of q_{pre} on these parameters also.

To study in more explicit way, how the fraction of the pre-equilibrium emission is distributed in the individual reactions (n, p), (n, α) and (n, n'), the relative pre-equilibrium emission contributions q^{p}_{pre}, q^{α}_{pre} and $q^{n'}_{pre}$ for the respective reactions have been calculated for the two cases of ^{40}Ti and ^{52}Cr target nuclei and are plotted against the neutron energy in fig (5.32). It may be seen from this figure that $q^{n'}_{pre}$ has the maximum relative contribution in lower energy region and it decreases with the increase of

the pre-equilibrium emission constants q^{p}_{pre} and q^{α}_{pre} have lower values in lower energy region and these increase with neutron energy. The rise of q^{α}_{pre} with neutron energy is much faster as compared to that of q^{p}_{pre}. This behaviour of the relative pre-equilibrium emission constants can be understood in terms of the competition between (n, p), (n, α) and (n, n') reactions. It may, therefore, be concluded that the compound nuclear reaction is a dominant reaction process in the lower range of excitation energies of the composite system. The pre-equilibrium process also plays an important role in neutron induced reactions, its contribution increases with increasing excitation energy. The excitation functions for (n, p) reactions for a number of nuclei in the mass region $A = 24$ to $A = 197$ could be well reproduced in a consistent way using the Hauser-Feshbach evaporation model and the pre-compound hybrid model in its closed form. The best fit values of calculated excitation functions for all the reactions can be obtained with the parameters $PM = 430$ MeV^3, $\beta = 0.2$ and $n = 3$. Varying the value of the level density parameter 'a' for residual nucleus of the (n, p) channel, appreciably changes the excitation function while similar variations for other channels do not have such an effect. The present analysis shows that the dominant transition rate λ^{+}, used in the pre-equilibrium hybrid model, does not exhibit any structure effect of its own (except those due to the variation of the level density parameter 'a'), λ^{+} remains nearly constant (for a given exciton number 'n' and excitation energy 'E') throughout the studied mass region $A = 24$ to $A = 197$. The results of calculations are sensitive to the quantities as level densities, level schemes and gamma ray strength

functions. Their effect on the cross-section differs from reaction to reaction depending on the uncertainties in these quantities. In some cases inaccurate results may be obtained even if the reaction is adequately described by the model employed. Therefore, the accuracy of the result has to be investigated in each case individually. Quite generally, the accuracy for a particular case can be further improved by fitting as much experimental data for competing reactions as is available with one set of values for the above mentioned quantities.

Recently the effects of the nuclear density distribution in the preEquilibrium emission have been considered by Blann / 106 - 107 /. A modification of the Hybrid model referred to as the Geometry-dependent Hybrid (GDH) model, has been proposed by Blann / 106 - 107 / to describe processes mainly occuring at the nuclear surface. In some recent findings effect of this kind has been observed in case of some (p, p') reactions / 107- 108 /. However, we have not used GDH model for the present calculations as the errors of experimental measurements are far too large for testing such a model.

****

References

/ 1/ R. Prasad and B.C. Sarkar; Il Nuovo Cim. 3A (1971)467.

/ 2/ M. Borrmann, E.Fretwurst, K. Schehka, G.Kreye, H.Buttner, A. Lindner and P. Meléner ; Nucl.Phys. 63 (1965) 438.

/ 3/ B.I. Noble and S.M. Qaim; Nucl. Phys. A283 (1977) 269.

/ 4/ D.R. Koehler and W.L.Alford ; J.Nucl.Energy A/B 18 (1964) 81.

/ 5/ D. Crumpton ; J.Inorg.Nucl.Chem. 31 (1969) 3727.

/ 6/ V.N. Levkovskii, G.P. Vinitskaya and V.K. Stepanov ; Soc.J.Nucl.Phys. 10 (1969) 25.

/ 7/ F. Gabbard and B.D. Kern ; Phys.Rev. 128 (1962) 1276.

/ 8/ H.L. Pai; Can.J. Phys. 44 (1966) 2337.

/ 9/ A. Poularikas and R.D. Fink; Phys.Rev. 115 (1959)989.

/10/ M. Hillman ; Nulc. Phys. 37 (1962) 78.

/11/ C.S. Khurana and H.C. Hans; Nucl.Phys. 13 (1959) 88.

/12/ J. Janczyszyn and L.Gorski ; J. Radio.Analyt. Chem. 14 (1973) 201.

/13/ E.T. Bramlitt. and R.D. Fink ; Phys.Rev. 131 (1963)2649.

/14/ B.D. Kern, W.E. Thompson and J.M. Ferguson ; Nucl.Phys. 40 (1959) 226.

/15/ S.K. Mukherjee, A.K. Ganguly and N.K. Majumder; Proc. Phys. Soc. A77 (1961) 500.

/16/ C.S. Khurana and I.M. Govil ; Nucl.Phys. 62 (1965) 153.

/17/ E.B. Paul and R.L. Clarke; Can.J.Phys. 31 (1953) 267.

/18/ D.L. Allan; Nucl. Phys. 24 (1961) 274.
; Proc.Phys. Soc.B70 (1957) 195.

/19/ J.M. Ferguson et al. ; UCN RDL-TR 269 (1958).

/20/ A.V. Cohen and P.H. White ; Nucl. Phys. 1, (1956) 73.

/21/ M.J. Murmis and R.D. Fink ; Nucl.Phys. 8 (1958) 139.

/22/ M. Cevolani and S. Petralia ; Nuovo.Cim. 26 (1962)1328.

/23/ J. Picard and C.F. Williamson; Nucl.Phys. 63 (1965)673.

/24/ B. Mitra and A.M. Ghose; Nucl.Phys. 83 (1966) 157.

/25/ M. Bormann, I. Nichle and F. Meyer, Nucl. Data for Reactors, IAEA, 223 (1967).

/26/ M. Bormann, G. Clerjeaks, H. Fastrarat, K.J. Ciacchio, H. Bevaart and H. Pellehny E. Physik 174 (1963) 1.

/27/ A. Pasquarelli, Nucl. Phys. A91 (1967) 210.

/28/ N. Prasad, D.C. Sarkar and C.S. Khurana, Nucl. Phys. 89 (1966) 369.

/29/ L. Hussain and P.K. Kuroda, J. Inorg. Nucl. Chem. 29 (1967) 2665.

/30/ P. Kolmberg, R. Diegge, J.K. Kalmman and K. Valkonen, J. Inorg. Nucl. Chem. 36 (1974) 715.

/31/ C.C. Bonazzola, P. Brunetto, E. Chiavassa, E. Spinnglio and A. Pasquarelli, Nucl. Phys. 51 (1964) 337.

/32/ O.M. Hudson and L.L. Morgan, Bull. Am. Phys. Soc. II 4 (1959) 97.

/33/ L. Husain, A. Kori and P.K. Kuroda, Phys. Rev. 10 (1970) 1239.

/34/ J. Roncolo and D.C. Santroy, Nucl. Phys. 38 (1962) 353.

/35/ P. Cuzzocrea, E. Perillo and S. Catarrigo, Nuovo. Cim. 6A (1971) 251.

/36/ R.S. Scalan and R.W. Finky, Nucl. Phys. 9 (1958) 324.

/37/ S.C. Forbes, Phys. Rev. 88 (1952) 1309.

/38/ R.S. Story, W. Jack and A. Ward, Proc. Phys. Soc. A75 (1960) 526.

/39/ H. Pollehn and H. Beuerle, Z. Natural 16a (1961) 227.

/40/ J.P. Butler and D.C. Santry, Bull. Am. Phys. Soc. 6(1961)250.

/41/ J.L. Preiss and R.W. Finky, Nucl. Phys. 15 (1960) 326.

/42/ S. Yamni, J. Phys. Soc. Japan 12 (1957) 443.

/43/ P. Avignon and L. Rosiery Compt. Rend 247 (1958) 1040.

/44/ W.C. Dyer and J.H. Hamilton, J. Inorg. Nucl. Chem. 34 (1972) 1119.

/45/ W.L. Alford and D.R. Kochler, Phys. Rev. 122 (1963) 703.

/46/ R.F. Coleman et al., Proc. Phys. Soc. 73 (1959) 215.

/47/ D.G. Ozanliev et al., Sov. Phys. 3 (1957) 135.

/48/ E.S. Hand, C.J. Mccallum and A.T.G. Ferguson, Nucl. Phys. 19 (1960) 539.

/49/ A. Poularikas et al., J. Inorg. Nucl. Chem. 13 (1960) 196.

/50/ J.E. Strain and W.J. Ross, Report ORNL 3672 (1965).

/51/ M. Hormann and J. Lamers ; Nucl. Phys. A130(1969) 195.

/52/ [illegible] Kondaiah and K.K. Link; Nucl. Phys. A122 (1969) 679.

/53/ M. Hormann, L. Schehka, F. Krayer and J. Pretwurst; [illegible] (E) 57 "U" 17 (1965)

/54/ [illegible] and [illegible] Kern; Phys. Rev. 128 (1962) 1276.

/55/ [illegible] Venkatopalan Rao, K.L. Wood, J.M. Palmos and R.K. Link; Phys. Rev. C3 (1971) 629.

/56/ [illegible] Strohal, L. Cindro and B. Zeman; Nucl. Phys. 30 (1962) 49.

/57/ D.M. Whittenden and [illegible] Gardner; Ann. Prog. Rep. Nucl. Chem. (1961).

/58/ [illegible] Finetti and A. Pasquarelli; Nuovo. Cim. 44B (1966) 5336.

/59/ J.R. Ferguson, W.L. Thompson and [illegible] Kern; Nucl. Phys. 2 (1962) 373.

/60/ [illegible] Worrall, M. Silvergold and [illegible] Gardner; Nucl. Phys. A138 (196) 397.

/61/ W.[illegible] Gross and W.L. Clarke, Prog. Re t. A [illegible] 1542 (1962).

/62/ H. Liskien and A. Paulsen; J. Nucl. Energy vol19 (1965) 73.

/63/ [illegible] Wain, [illegible] Wolfle and [illegible] Stocklin; Preprint Canterbury (1971).

/64/ [illegible] Gentry and J.K. Butler; Can. J. Phys. 42 (1964) 1130.

/65/ J. Terrel and J.R. Holm, Phys. Rev. 109 (1958) 2031.

/66/ J.[illegible] Cunningham, [illegible] James, L.B. Martin and G.[illegible] Martin; Proc. Roy. Soc. A292 (1966) 180.

/67/ M. Hormann, [illegible] Pretwurst and [illegible] Wrege; Report [illegible] 325(1969).

/68/ M.J. Depraz, [illegible] Legros and M. Salin; J. Phys. Rad. 21 (1960) 377.

/69/ D.G. Gentry and J.K. Butler, Can. J. Phys. 44 (1966) 1103.

/70/ L.I. Vinitskaya, V.E. Mavkovskii, V.V. Sokolskif and I.[illegible] Lazachevskij; Nov. J. Nucl. Phys. 5 (1967) 630.

/71/ [illegible] Preiss, [illegible] -ink, and [illegible] Gardner; Ann. Prog. Rep. Nucl. Chem (1960).

/72/ [illegible] Rybakov; Bull. Ac. Phys. Soc. 6 (1961) 462.

/73/ V.[illegible] Levkovskii, G.L. Lovelskaya, G.P. Vinitaskaya, V.[illegible] Stepanov and V.V. Sokolskii; Nov. J. Nucl. Phys. 2 (1965) 4.

/74/ [illegible] Seigold and [illegible] Glover; Nucl. Phys. 32 (1962) 196.

/75/ [illegible] Jelberg, [illegible] Pappas and [illegible] Steinnes; Radio Chem. Act. 5 (19 6) 28.

/76/ B.P. Bayhurst and R.J. Prestwood; J. Inorg.Nucl.Chem 23 (1961)173.

/77/ C. Abele, M. Bormann and W.Carstens; E A N D C (E) 76 "U" (1967) 51.

/78/ C.M. Lederer, J.M. Holtander and I.Perlman ; Table of Isotopes Wiley, New York (1967).

/79/ A. Paulsen and H. Liskien; J.Nucl.En. AB19 (1965)907.

/80/ M. Bormann, F.Dreyer and V. Zielinski; E A N D C (E) 66 "U" (1966) 42.

/81/ S.C. Mathur and I.L. Morgan; Nucl.Phys. 75 (1966)561.

/82/ E.G. Gardner and Rosenblum; Nucl.Phys. A96 (1967)121.

/83/ W. Hauser and H.F. Feshbach; Phys. Rev. 87 (1952)366.

/84/ H. Vonach ; Private Communication.

/85/ F.D. Becchetti Jr and G.W. Greenlees; Phys.Rev.182(1969)1190.

/86/ J.R. Huizenga and G.Igo; Nucl.Phys. 29 (1962) 462.

/87/ Atomic Data and Nuclear Data Tables 9A(1971).

/88/ Atomic Data and Nuclear Data Table 10 (1971)539.

/89/ Atomic Data and Nuclear Data Table 17 (1976)1 .

/90/ Atomic Data and Nuclear Data Table 26 (1981)19.

/91/ W. Dilg, W. Schantl, H. Vonach and M. Uhl; Nucl Phys. A217 (1973) 269.

/92/ C.M. Lederer and V.S. Shirley; Table of Isotopes 7th Edition New York (1978).

/93/ A.H. Wapstra and K. Bos ; Atomic Data and Nuclear Data Table 19 (1977) 215.

/94/ M. Blann; Phys. Rev. Lett. 27 (1971) 337.
/ errata 27 (1971) 1550.

/95/ M. Blann and A. Mignerey; Nucl Phys. A186 (1972)245.

/96/ M. Uhl and B. Strohmaier; Private communication.

/97/ L. Milazzo -Colli and G.M. Braga Marcazzan; Nucl. Phy. A210 (1973) 297.

/ 98/ E. Gadoili, E. Gadioli erba and P.G. Sona; Nucl. Phys. A217 (1973) 589.

/ 99/ J.J. Griffin, Phys. Rev. Lett. 17 (1966) 478.

/100/ C.K. Cline ; Nucl Phys. A210 (1973) 590.

/101/ G.M. Braga Marcazzan, E. Gadioli erba, L.Milazzocolli and P.G. Sona, Phys. Rev. C6 (1972) 1398.

/102/ H. Harmsdorf, A. Meister, S. Sessonov, D.Seeliger, and K. Seidel ; Nuclear Theory in Neutron Date Evaluation, Vol. II I.A.E.A. -190 (1976).

/103/ J.M. Akkermans; Phys. Lett. B82 (1979) 20.
; Z. Physik A292 (1979) 57.

/104/ C. Kalbach ; Z. Physik A283 (1977) 401.

/105/ E. Holub, D. Pocanic, R. Caplar and N. Cindro; Z. Physik A286 (1980) 341.

/106/ M. Blann; Phys. Rev. Lett. 28 (1972) 757.

/107/ M. Blann; Nuclear Phys. A213 (1973) 570.

/108/ W. Scobel et al. ; Proc. of the Int. Workshop on Reaction Models for continuous spectra of light particles, Bad Honnef Institute für strahlen- und Kern Physik der Universitat Bonn (1978).

****

NUCLEAR PHYSICS
AND
SOLID STATE PHYSICS
SYMPOSIUM

PROGRAMME & ABSTRACTS

BHABHA ATOMIC RESEARCH CENTRE
TROMBAY, BOMBAY-85
FEBRUARY 1-4, 1972

ORGANISED BY
THE PHYSICS COMMITTEE OF THE
DEPARTMENT OF ATOMIC ENERGY
GOVERNMENT OF INDIA

*N7 ON THE SHELL EFFECT IN (n, 2n) REACTION CROSS SECTIONS AT 14.8 MeV. J.P. GUPTA, RAJ KUMAR AND R. PRASAD, Department of Physics, Aligarh Muslim University, Aligarh.

Presence of shell effects in (n, 2n) reactions at 14.8MeV have been indicated by various workers. Hille and Dilg et al., however, have recently shown the lack of evidence of shell effects by plotting literature values of (n, 2n) reaction cross sections against the asymmetry parameter (n - z)/A. In a programme of cross section measurements, (n, 2n) reaction cross sections for some forty four cases have been measured. Measured cross sections are compared with the cross sections calculated from the empirical formula given by Barr et al. The ratio $\sigma_{exp}/\sigma_{cal}$, when plotted against the proton number 'Z', indicates the presence of shell effect.

*N8 MEASUREMENT OF NON-ELASTIC CROSS SECTION AT 14.2 MEV. Bharati Pal, Arun Chatterjee and A.M. Ghose, Nuclear Physics Laboratory, Bose Institute, Calcutta.

Measurement of non-elastic cross section of several nuclei for 14.2 MeV neutron by the multibias neutron counting method developed by us will be presented.

N9 STATISTICAL EMISSION OF ALPHA PARTICLES FROM 14 MEV NEUTRON INTERACTIONS WITH NICKEL. S. ROYCHOWDHURY AND O.N. KAUL, Physics Department, Government Engineering College, Bilaspur (M.P.).

A study of alpha particles emitted as a result of 14 Mev neutron interactions with nickel was under taken by the emulsion technique. Angular and energy distributions of α-particles were measured. The Angular distributions are roughly symmetrical about 90° and convave upwards, but are sharply peaked in the forward directions. Energy distribution of alphas are analysed in the frame work of statistical theory in order to determine the level density parameter. Anamolies in the behaviour of evaporation mechanism are attributed to precompound process. Total cross section is estimated to be 80 mb ± 10%.

N10 DETERMINATION OF (n,X) CROSS SECTION ON THE [illegible] LABORATORY. S. ROY CHOUDHURY AND O.N. KAUL, Physics Department, Govt. Engg. College, Bilaspur (M.P.).

Experimental values of ( ) cross sections in the case of 14-15 Mev neutron induced reactions show that the reactions cross sections decrease monotonically with increasing asymmetry factor $(N-Z)/Z$, and show no deviations from this behaviour in the magic regions. Plotted against neutron excess, it is observed that the cross section decreases rapidly for lighter elements and some what slowly for heaviour elements. It is found that the observations reported here agree well with the predicted behaviour that with increase of Z-value the tendency towards symmetry decreases. Further, it is found that our observations are well in line with that of Levkovskii's experimental results for ( ) reactions.

7th Conference on the Application of accelerators in Research and Industry, North Texas State University, Denton, Texas, USA (1982)

A STUDY OF PRE-COMPOUND EMISSION IN (n,p) REACTIONS INDUCED BY NEUTRONS OF 10 TO 20 MeV.

J.P.Gupta and R.Prasad
Department of Physics
Aligarh Muslim University, Aligarh, India

Summary

Cross sections for some (n,p) reactions have been measured by the activation technique at 14.8±0.5MeV neutron energy. Literature values of these cross-sections have also been compiled in the energy range 10 to 20 MeV. Excitation functions in this energy range have been calculated using a combination of compound and pre-compound emission decay. In these calculations, back-shifted Fermi level density parameters have been used and correction for the width fluctuation and Pauli-exclusion principle have been applied. The experimental and theoretical excitation functions have been matched by varying the exciton model parameters. Variation of the pre-compound part with the excitation energy has been studied.

Introduction

Many workers[1-10] have measured the cross-sections for neutron induced reactions at about 14 MeV, attempts are made to study the trend in cross-section values. The problem with such investigation is the existence of large discrepancy between the cross-section values of same reaction reported by different groups of workers. These discrepancies may be partly due to the different techniques and experimental set-ups employed by different workers[1-10].

A small difference in the mean energy of the incident neutrons can change the cross-section values by a large amount in some cases. Another problem is the absolute calibration of incident neutrons flux. Most of the measurements have been done by the activation technique. In this method the neutron flux is generally calibrated through some other standard reaction. Different standard reactions used for flux caliberation may also introduced systematic errors. The experimental results of the cross-sections measurement for (n,p) reactions show that the statistical theory of compound nucleus formation can not fully account for the observed values. The calculated cross-sections are smaller than experimental one by a factor varying from 10 to 10^3 at the increase of target nucleus mass[11].

For the study of trend in nuclear reactions, it, therefore, is necessary to measure the cross-sections for a large number of target nuclei using the same technique and the standard reaction. A programme of cross-section measurements at 14.8 MeV neutron energy by the activation technique has been undertaken with this view. Cockcroft-Walton accelerator of this laboratory supplied fast neutrons. Cross-sections for some selected (n,p) reactions have been measured at 14.8±0.5 MeV. Literature values of the cross-sections at other energies have been compiled. The experimental cross-section values have been compared with the cross-section values calculated by the statistical theory. Pre-compound emission of particles has also been taken into account using the Hybrid model[12]. A computer code ACT has been developed for this purpose.

Measurements

Neutrons of energy 14.8 MeV have been produced by means of the $^3H(d,n)^4He$ reaction using 130 keV deuteron beam of the Cockcroft-Walton accelerator of this laboratory. Spectroscopically pure substances of chemical purity better than 99.9% have been used in preparing samples for irradiation. The samples have been made by uniformly spreading the powdered substance or thin metal foils in thin perspex rings of inner diameter 1.3 cm. sandwiched between two cellulose tapes. Irradiations have been carried out at the outer side of the brass backing to whose other side the tritium target was fixed. The neutron yield at the place of irradiation have been of the order of 10^9 neutron/Sec. Irradiation times have been decided by half-life of the residual nuclei and controlled by the electro-static deflection of the deuteron beam. Cross-sections have been measured with respect to the $^{56}Fe(n,p)^{56}Mn$ reaction. The activities have been studied with the end-window β-counter of 2.5mg/cm^2 window thickness and or the γ-ray scintillation spectrometer.

Results and Discussion

The measured values of (n,p) reaction cross-sections at 14.8 MeV in $^{45,49,50}Ti$, ^{51}V, ^{52}Cr, ^{65}Cu and $^{64,66}Zn$ targets and the literature values of (n,p) reaction cross-sections in the energy range 10 to 20 MeV for the same cases are given in figure 1 to 10. Excitation functions in this energy range have been calculated using a combination of compound and pre-compound emission decay. A computer code ACT[13] has been used, that takes into account the particles which are emitted during the equilibriation of the excited composite system along with the usually statistically emitted particles. Hybrid model frame work has been used for treating the pre-compound emission. Pre-compound emission is considered only in the first emission step where the excitation energy is sufficiently large. After the first step of de-excitation the excitation energy of the still excited residual nucleus is considerably lowered, hence the probability of pre-compound emission is negligible. In these calculations conservation of the parity and angular momentum are also explicitly taken into account at each step of de-excitation. For the calculations level density parameter, the effective moment of inertia and fictive ground state position have been taken from ref.14. Transmission coefficients for neutrons, protons and α-particles have been calculated with another computer code OPTIM using optical model

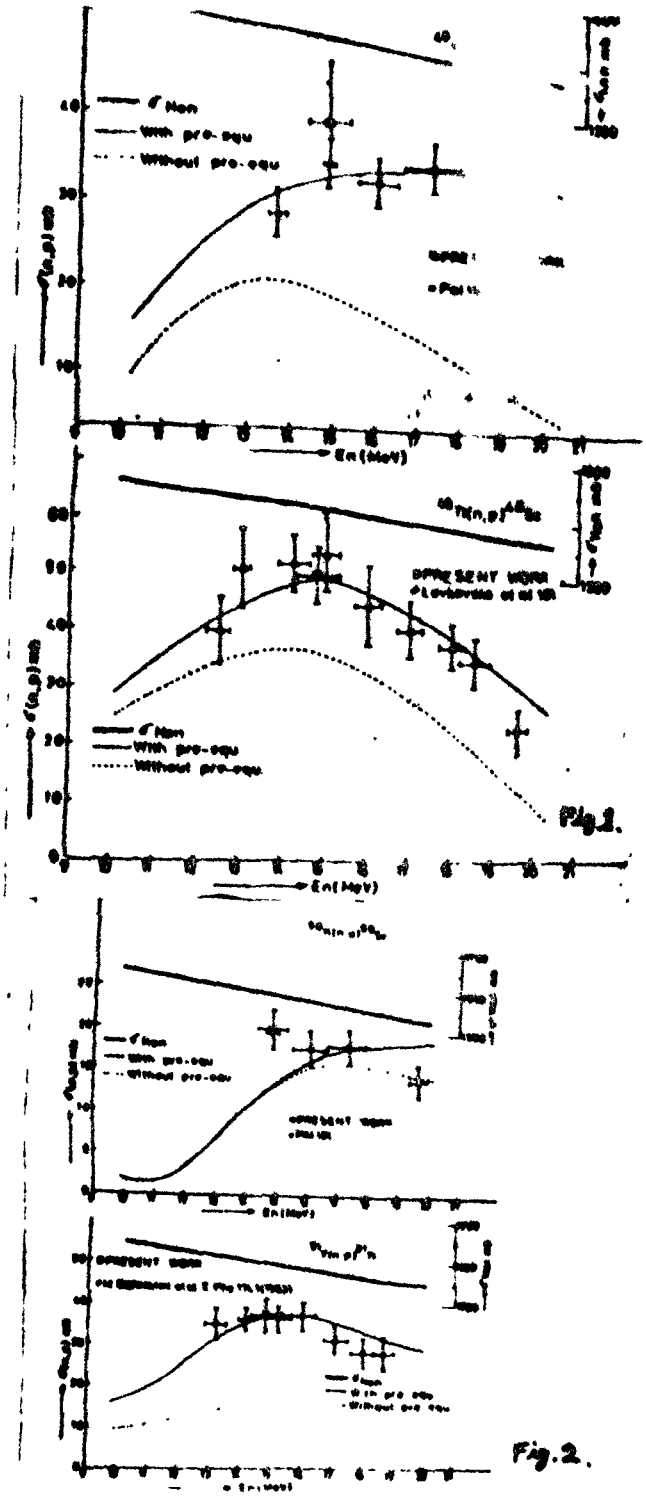

Fig. 1-4 Experimental data and results for calculations for the $^{48,49,50}Ti, ^{51}V(n,p)^{51}Ti, ^{52}Cr(n,p)^{52}V, ^{63}Cu(n,p)^{63}Ni$ and $^{64,66}Zn$ $(n,p)^{66}Cu$ activation cross-sections. σ non is also shown.

parameters from nuclear data tables(1970-1980).It has been seen that thetheoretical results depend strongly on the level density parameter.On varying the values of this parameter given in ref.14 with in 4%to 8 % the theoretical excitation fupctions for the $^{48,49,50}Ti, ^{51}V, ^{52}Cr, ^{63}Cu$ and $^{64,66}Zn(n,p)$ reactions have been matched with the excitation functions experimentally measured as shown in Fig.1 to 4, as can be seen from fig. 1 to 4 the calculations without consideration of pre-equilibrium emission obviously fails to re-produce the experimental excitation function for high incident energy (10 to 20 MeV). Good agreement with the data is achieved by taking into account pre-equilibrium emission with the following values for the parameters : p =2, h=1 and FM =4%, where p and n stands for the particles number and the number of holes of the initial state respectively.FM is the constant (MeV^3) which by the following equation :

$|M|^2 = FM.A^{-3}.B^{-1}$

defines the matrix element for internal transition competing with pre-equilibrium decay [2]. The variation of the pre-equilibrium fraction with the excitation energy is shown in Fig.5. The fraction of the pre-equilibrium emission increases for each case with increasing incident neutron energy. The slope 'm' of this variation has also been plotted against mass number A, atomic number Z, neutron number N and asymmetry parameter (N-Z)/A for these cases. The trend of these shown in fig.6 which indicates that the

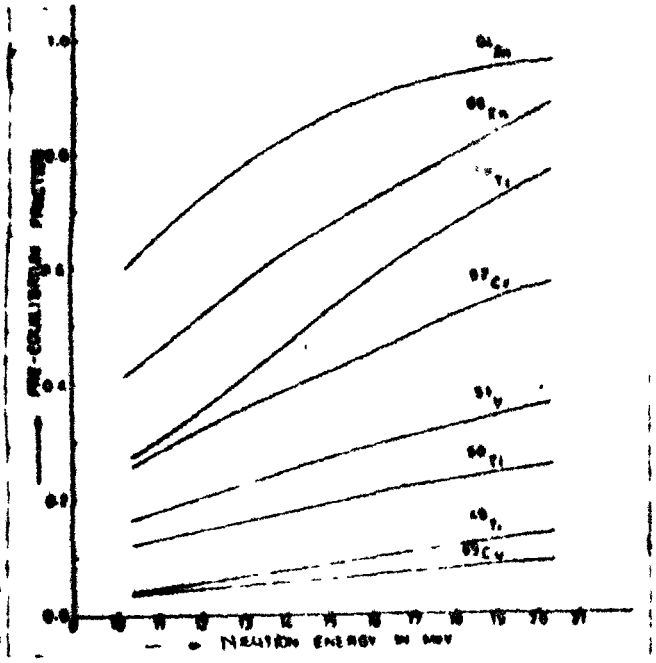

Figure 5. Variation of Pre-equilibrium fraction as a funotion of incident neutron energy for various nuclei.

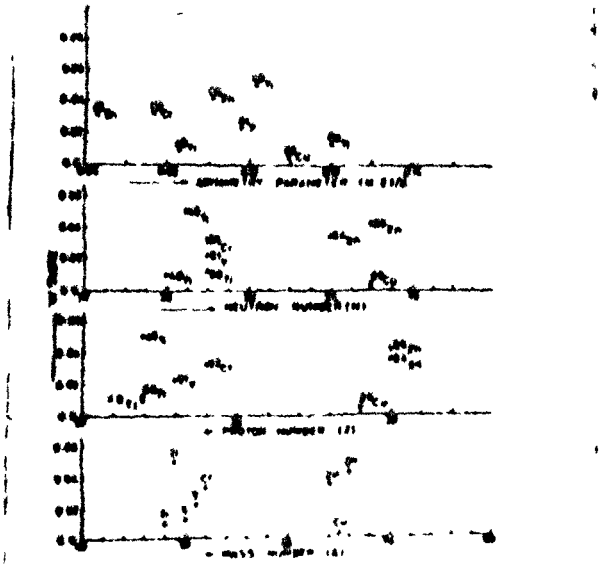

Figure 6. Variation of 'm' the slope of pre-equilibrium fraction with asymmetry parameter, neutron number, proton number and mass number of the target nuclei.

slope 'm' increases in all cases regularly except for ^{65}Cu and ^{47}Ti with increasing mass number, atomic number and neutron number, but with asymmetry factor variation of 'm' is not so regular.

Acknowledgement

The authors are grateful to Prof. M.Z.K. Khan, Chairman of the Physics Department for providing the facilities to carry out this work and appreciate the assistance of I. Sulim in preparation of the manuscript.

References

1. J.Csikai, M.Buczko, Z.Rody and A.Demany Nuclear data for neutron activation analysis. Atomic Energy Review 7, 3 (1969).
2. E.T.Jolla and S. [illegible], A systematic study of (n,p) reactions [illegible] MeV. Nucl. Phy. A293, 269 (1977).
3. G.F. Bruno-Ranieri, B. Cadioli [illegible], B. Millazzo colli and P.G. Sona, Analysis of the total (n,p) cross-section around 14 MeV with the pre-equilibrium exciton model. Phys. Rev. 26, 1 [illegible] (1972).
4. R. Prasad and A.C. Sarkar, [illegible] reaction cross-section and [illegible] predicted value [illegible] Nuovo Cim-1A, 467 (1971).
5. M.L. Pal, The (n,p) cross-section of Titanium isotopes for neutron [illegible] between 13.6 MeV and 14.7 MeV. Phys. 44, 2537 (1966).
6. M. Bormann and H. Lange, [illegible] functions of (n,p) and (n,2n) reactions for some isotopes of A, Ni, and Cu. Nucl. Phys. 130, 195 (1969).
7. D.C. Santry and J.D. Butler, [illegible] curves for the ^{65}Cu(n,2n), (n,p) and (n,na) reactions of ^{65}Cu. Can. J. [illegible] (1966).
8. M. Bormann, E. Fretwurst, [illegible] and W. Wrege, [illegible] excitation functions of neutron induced reactions [illegible] from 12.6 to 19.6 MeV. Nucl. Phys. [illegible].
9. V.N. Levkovskii, G.E. Vinitskaya, [illegible] skaya and V.I. Strizhov, [illegible] for (n,p) and (n,α) reactions [illegible] MeV neutrons. Sov. J. Nucl. [illegible] (1970).
10. B.D. Kern, W.E. Thompson, [illegible] Cross-section [illegible] reactions. Nucl. [illegible].
11. L. Milazzo-Colli, [illegible] Pre-equilibrium emission [illegible] (n,α) reactions on Cu, [illegible] 47 (1971).
12. M. Blann and A. [illegible], Pre-equilibrium decay at moderate excitation and the Hybrid model. Nucl. [illegible] (1972).
13. J.P. Gupta, [illegible] Aligarh India to be published.
14. W. Gil[illegible], [illegible] Level density parameters for [illegible] shifted [illegible] in the mass range 40<A<250. Nucl. [illegible] (1973).
15. J.K. Dickens, [illegible] for pre-equilibrium calculations. Nucl. Phys. A [illegible] (1977).

B.A.R.C.-1183

B.A.R.C.-1183

भारत सरकार
GOVERNMENT OF INDIA
परमाणु ऊर्जा आयोग
ATOMIC ENERGY COMMISSION
भाभा परमाणु अनुसंधान केन्द्र

PROGRESS REPORT ON NUCLEAR DATA ACTIVITIES IN INDIA

for the period from July 1981 to December 1982

Compiled by
R. P. Anand
Nuclear Physics Division

BHABHA ATOMIC RESEARCH CENTRE
बंबई, भारत
BOMBAY, INDIA
1982

A STUDY OF PRE-EQUILIBRIUM EMISSION IN (n,p) REACTIONS BETWEEN 10-20 MeV

J.P. Gupta and R. Prasad
Physics Department
Aligarh Muslim University, Aligarh 202 001.

A computer code ACT has been used to calculate the excitation functions for $^{48,49,50}Ti$, ^{51}V, ^{52}Cr, ^{65}Cu, and $^{64,66}Zn(n,p)$ reactions in the energy range 10 to 20 MeV/1/. Hybrid model /2/ frame work has been used for treating the pre-equilibrium emission. Pre-equilibrium emission is considered only in the first step of de-excitation where the excitation energy is sufficiently large. In these calculations conservation of the parity and angular momentum have been taken into account at each step of de-excitation. Back-shifted Fermi level density parameters have been used, Pauli exclusion principle and width fluctuation correction can also be incorporated optionally. For all calculations level density parameter, the effective moment of inertia and fictive ground state position have been taken from ref./3/. The following values for the other parameters have been used in these calculations : p=2, h=1 and FM=430, where p and h stands respectively for the particles number and the hole degrees of freedom of the initial state. FM is the constant (MeV^3) which defines /4/ the matrix element for internal transitions competing with pre-equilibrium decay. As can be seen from Fig.1 the function of the pre-equilibrium emission increases for each case with increasing excitation energy /1/. At 15.0 MeV excitation energy the pre-equilibrium fraction for $^{48,49,50}Ti$, ^{51}V, ^{52}Cr, ^{65}Cu and $^{64,66}Zn$ target nuclei have been plotted in Fig.2 as a function of atomic mass number A, proton number Z, neutron number N and asymmetry parameter (N-Z)/A. It can be seen from fig.2 that the pre-equilibrium fraction at this energy varies linearly with mass number, proton number and neutron number in general, except for ^{49}Ti, ^{65}Cu and ^{64}Zn target nuclei. However, no regular variation of the pre-equilibrium fraction has been observed as a function of asymmetry parameter (N-Z)/A. Further investigations are in progress to [illegible]

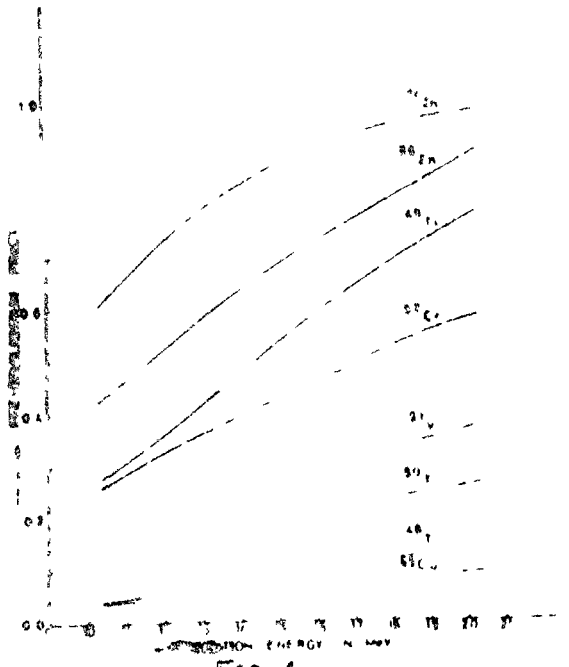

FIG. 1

this trend in other nuclei also.

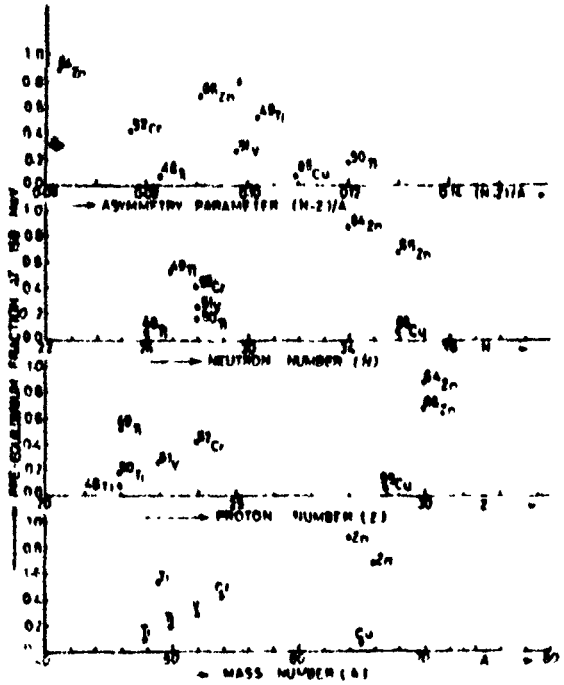

FIG. 2

/1/ J.P. Gupta and R. Prasad, Proceeding of 7th conference on the application of accelerator in research and industry, North Texas state university, Texas, USA (1982) To be published)

/2/ M. Blann and A.Mignery, Nucl.Phys.A186, 245 (1972).

/3/ W.Dilg, W.Schantl, H.Vonach and M.Uhl, Nucl.Phys.217A, 269 (1973).

/4/ C.K. Cline, Nucl.Phys.A210, 590 (1973).